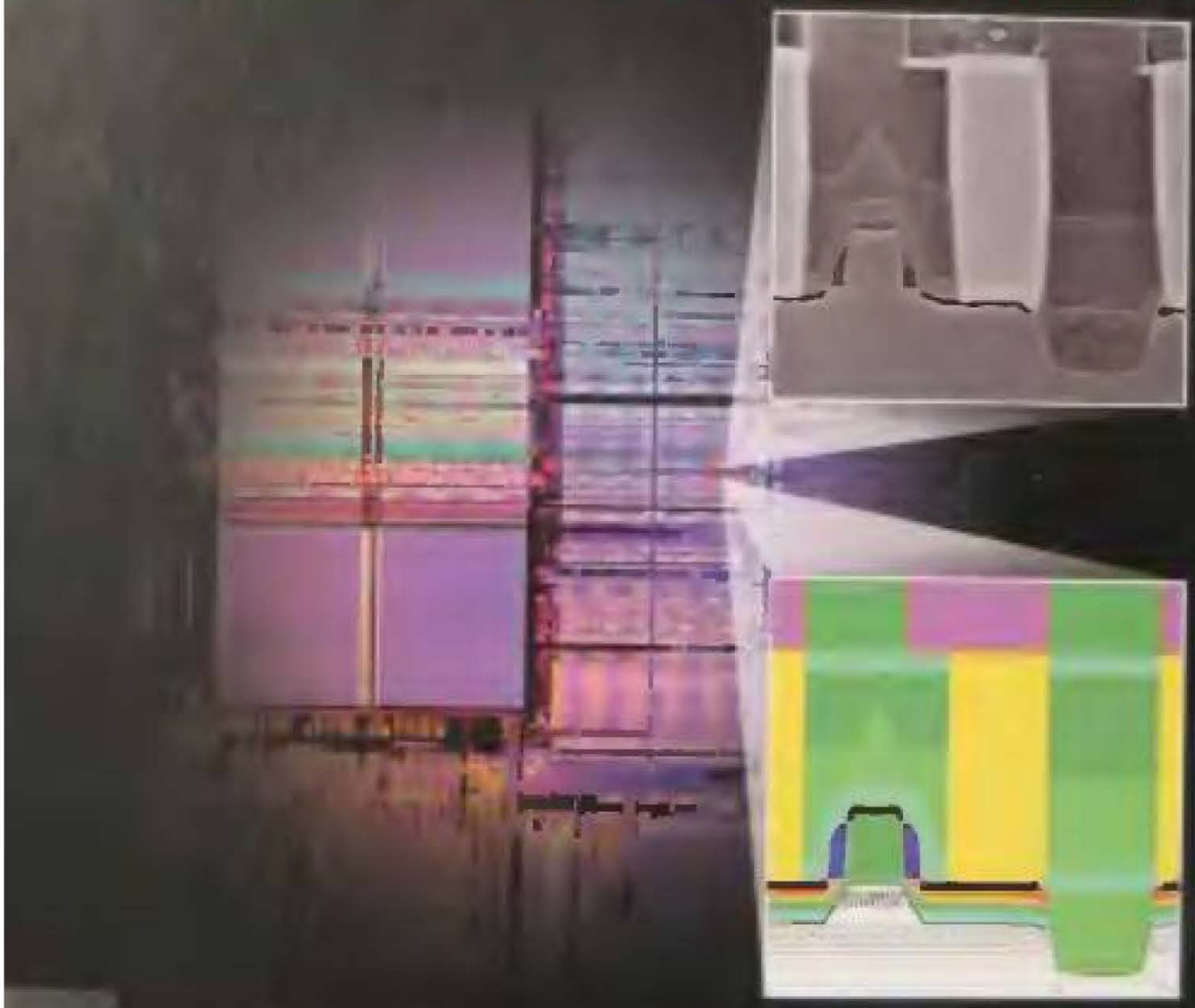
SILICON VLSI TECHNOLOGY

Fundamentals, Practice and Modeling



James D. Plummer • Michael D. Deal • Peter B. Griffin

Prentice Hall Electronics and VLSI Series—Charles Sodini, Series Editor

Micron Ex. 1022, p. 1
Micron v. YMTC
IPR2025-00294

Library of Congress Cataloging-in-Publication Data
Silicon VLSI technology
p. cm.
ISBN 0-13-085037-3
1. Integrated circuits—Very large scale integration—Design and construction. 2. Silicon. 3. Silicon oxide films. 4. Metal oxide semiconductors. 5. Silicon technology.
TK7874.75.S54 2000 99-42745
621.39'5—dc21 CIP

Publisher: Tom Robbins
Associate Editor: Alice Dworkin
Editorial/Production Supervision: Rose Kernan
Vice President and Editorial Director, ECS: Marcia Horton
Vice President of Production and Manufacturing: David W. Riccardi
Executive Managing Editor: Vince O'Brien
Marketing Manager: Danny Hoyt
Managing Editor: David A. George
Manufacturing Buyer: Pat Brown
Manufacturing Manager: Trudy Pisciotti
Art Director: Jayne Conte
Cover Design: Bruce Kenselaar
Editorial Assistant: Jesse Power
Copy Editor: Martha Williams
Composition: D&G Limited, LLC

Prentice Hall

©2000 by Prentice Hall, Inc.
Upper Saddle River, New Jersey 07458

All rights reserved. No part of this book may be reproduced, in any form or by any means, without permission in writing from the publisher.

The author and publisher of this book have used their best efforts in preparing this book. These efforts include the development, research, and testing of the theories and programs to determine their effectiveness. The author and publisher make no warranty of any kind, expressed or implied, with regard to these programs or the documentation contained in this book. The author and publisher shall not be liable in any event for incidental or consequential damages in connection with, or arising out of, the furnishing, performance, or use of these programs.

Printed in the United States of America

10 9 8 7 6 5

ISBN 0-13-085037-3

Prentice Hall International (UK) Limited, *London*
Prentice Hall of Australia Pty. Limited, *Sydney*
Prentice Hall Canada Inc., *Toronto*
Prentice Hall Hispanoamericana, S.A., *Mexico*
Prentice Hall of India Private Limited, *New Delhi*
Prentice Hall of Japan, Inc., *Tokyo*
Pearson Education Pte., Ltd. , *Singapore*
Editora Prentice Hall do Brasil, Ltda., *Rio de Janeiro*

Micron Ex. 1022, p. 2
Micron v. YMTC
IPR2025-00294

Chapter 3 Crystal Growth, Wafer Fabrication and Basic Properties of Silicon Wafers 93

3.1 Introduction ... 93
3.2 Historical Development and Basic Concepts ... 94
3.2.1 Crystal Structure ... 97
3.2.2 Defects in Crystals ... 101
3.2.3 Raw Materials and Purification ... 102
3.2.4 Czochralski and Float-Zone Crystal Growth Methods ... 105
3.2.5 Wafer Preparation and Specification ... 109
3.3 Manufacturing Methods and Equipment ... 111
3.4 Measurement Methods ... 111
3.4.1 Electrical Measurements ... 112
3.4.1.1 Hot Point Probe ... 113
3.4.1.2 Sheet Resistance ... 115
3.4.1.3 Hall Effect Measurements ... 117
3.4.2 Physical Measurements ... 117
3.4.2.1 Defect Etches ... 118
3.4.2.2 Fourier Transform Infrared Spectroscopy (FTIR) ... 119
3.4.2.3 Electron Microscopy ... 121
3.5 Models and Simulation ... 122
3.5.1 Czochralski Crystal Growth ... 125
3.5.2 Dopant Incorporation during CZ Crystal Growth ... 128
3.5.3 Zone Refining and FZ Growth ... 131
3.5.4 Point Defects ... 138
3.5.5 Oxygen in Silicon ... 142
3.5.6 Carbon in Silicon ... 143
3.5.7 Simulation ... 144
3.6 Limits and Future Trends in Technologies and Models ... 146
3.7 Summary of Key Ideas ... 147
3.8 References ... 148
3.9 Problems ... 151

Chapter 4 Semiconductor Manufacturing—Clean Rooms, Wafer Cleaning, and Gettering 151

4.1 Introduction ... 154
4.2 Historical Development and Basic Concepts ... 157
4.2.1 Level 1 Contamination Reduction: Clean Factories ... 159
4.2.2 Level 2 Contamination Reduction: Wafer Cleaning ... 161
4.2.3 Level 3 Contamination Reduction: Gettering ... 165
4.3 Manufacturing Methods and Equipment ... 165
4.3.1 Level 1 Contamination Reduction: Clean Factories ... 166
4.3.2 Level 2 Contamination Reduction: Wafer Cleaning ... 167
4.3.3 Level 3 Contamination Reduction: Gettering ... 169
4.4 Measurement Methods ... 169
4.4.1 Level 1 Contamination Reduction: Clean Factories ... 169

Micron Ex. 1022, p. 3
Micron v. YMTC
IPR2025-00294

5.5.7 Advanced Mask Engineering 271
5.6 Limits and Future Trends in Technologies and Models 272
5.6.1 Electron Beam Lithography 273
5.6.2 X-ray Lithography 275
5.6.3 Advanced Mask Engineering 277
5.6.4 New Resists 278
5.7 Summary of Key Ideas 281
5.8 References 281
5.9 Problems 283

Chapter 6 Thermal Oxidation and the Si/SiO_2 Interface **287**

6.1 Introduction 287
6.2 Historical Development and Basic Concepts 290
6.3 Manufacturing Methods and Equipment 296
6.4 Measurement Methods 298
6.4.1 Physical Measurements 299
6.4.2 Optical Measurements 299
6.4.3 Electrical Measurements—The MOS Capacitor 301
6.5 Models and Simulation 312
6.5.1 First-Order Planar Growth Kinetic—The Linear Parabolic Model 313
6.5.2 Other Models for Planar Oxidation Kinetics 322
6.5.3 Thin Oxide SiO_2 Growth Kinetics 326
6.5.4 Dependence of Growth Kinetics on Pressure 328
6.5.5 Dependence of Growth Kinetics on Crystal Orientation 329
6.5.6 Mixed Ambient Growth Kinetics 332
6.5.7 2D SiO_2 Growth Kinetics 333
6.5.8 Advanced Point Defect Based Models for Oxidation 339
6.5.9 Substrate Doping Effects 343
6.5.10 Polysilicon Oxidation 345
6.5.11 Si_3N_4 Growth and Oxidation Kinetics 347
6.5.12 Silicide Oxidation 350
6.5.13 Si/SiO_2 Interface Charges 352
6.5.14 Complete Oxidation Module Simulation 357
6.6 Limits and Future Trends in Technologies and Models 359
6.7 Summary of Key Ideas 361
6.8 References 361
6.9 Problems 364

Chapter 7 Dopant Diffusion **371**

7.1 Introduction 371
7.2 Historical Development and Basic Concepts 374
7.2.1 Dopant Solid Solubility 375
7.2.2 Diffusion from a Macroscopic Viewpoint 377
7.2.3 Analytic Solutions of the Diffusion Equation 379
7.2.4 Gaussian Solution in an Infinite Medium 380

Micron Ex. 1022, p. 4
Micron v. YMTC
IPR2025-00294

8.3.1 High-Energy Implants 466
8.3.2 Ultralow Energy Implants 468
8.3.3 Ion Beam Heating 469
8.4 Measurement Methods 469
8.5 Models and Simulations 470
8.5.1 Nuclear Stopping 471
8.5.2 Nonlocal Electronic Stopping 473
8.5.3 Local Electronic Stopping 474
8.5.4 Total Stopping Powers 475
8.5.5 Damage Production 476
8.5.6 Damage Annealing 479
8.5.7 Solid-Phase Epitaxy 482
8.5.8 Dopant Activation 484
8.5.9 Transient-Enhanced Diffusion 486
8.5.10 Atomic-Level Understanding of TED 488
8.5.11 Effects on Devices 497
8.6 Limits and Future Trends in Technologies and Models 499
8.7 Summary of Key Ideas 500
8.8 References 500
8.9 Problems 502

Chapter 9 Thin Film Deposition 509

9.1 Introduction 509
9.2 Historical Development and Basic Concepts 511
9.2.1 Chemical Vapor Deposition (CVD) 512
9.2.1.1 Atmospheric Pressure Chemical Vapor Deposition (APCVD) 513
9.2.1.2 Low-Pressure Chemical Vapor Deposition (LPCVD) 525
9.2.1.3 Plasma-Enhanced Chemical Vapor Deposition (PECVD) 527
9.2.1.4 High-Density Plasma Chemical Vapor Deposition (HDPCVD) 530
9.2.2 Physical Vapor Deposition (PVD) 530
9.2.2.1 Evaporation 531
9.2.2.2 Sputter Deposition 539
9.3 Manufacturing Methods 554
9.3.1 Epitaxial Silicon Deposition 556
9.3.2 Polycrystalline Silicon Deposition 558
9.3.3 Silicon Nitride Deposition 561
9.3.4 Silicon Dioxide Deposition 563
9.3.5 Al Deposition 565
9.3.6 Ti and Ti-W Deposition 566
9.3.7 W Deposition 567
9.3.8 $TiSi_2$ and WSi_2 Deposition 567
9.3.9 TiN Deposition 568
9.3.10 Cu Deposition 570
9.4 Measurement Methods 572

Micron Ex. 1022, p. 5
Micron v. YMTC
IPR2025-00294

11.2.3 Dielectrics 707
11.3 Manufacturing Methods and Equipment 715
11.3.1 Silicided Gates and Source/Drain Regions 716
11.3.2 First-level Dielectric Processing 718
11.3.3 Contact Formation 719
11.3.4 Global Interconnects 721
11.3.5 IMD Deposition and Planarization 723
11.3.6 Via Formation 724
11.3.7 Final Steps 725
11.4 Measurement Methods 725
11.4.1 Morphological Measurements 726
11.4.2 Electrical Measurements 726
11.4.3 Chemical and Structural Measurements 732
11.4.4 Mechanical Measurements 734
11.5 Models and Simulation 737
11.5.1 Silicide Formation 738
11.5.2 Chemical-Mechanical Polishing 744
11.5.3 Reflow 746
11.5.4 Grain Growth 753
11.5.5 Diffusion in Polycrystalline Materials 762
11.5.6 Electromigration 765
11.6 Limits and Future Trends in Technologies and Models 776
11.7 Summary of Key Ideas 780
11.8 References 781
11.9 Problems 784

Appendices **787**

A.1 Standard Prefixes 787
A.2 Useful Conversions 787
A.3 Physical Constants 788
A.4 Physical Properties of Silicon 788
A.5 Properties of Insulators Used in Silicon Technology 789
A.6 Color Chart for Deposited Si_3N_4 Films Observed Perpendicularly under Daylight Fluorescent Lighting 789
A.7 Color Chart for Thermally Grown SiO_2 Films Observed Perpendicularly under Daylight Fluorescent Lighting 790
A.8 Irwin Curves 791
A.9 Error Function 793
A.10 List of Important Symbols 797
A.11 List of Common Acronyms 798
A.12 Tables in Text 801
A.13 Answers to Selected Problems 802

Index **805**

Micron Ex. 1022, p. 6
Micron v. YMTC
IPR2025-00294

Contents

Preface xi

Chapter 1 Introduction and Historical Perspective **1**

1.1 Introduction 1
1.2 Integrated Circuits and the Planar Process—Key Inventions That Made It All Possible 7
1.3 Semiconductors 13
1.4 Semiconductor Devices 33
1.4.1 PN Diodes 33
1.4.2 MOS Transistors 36
1.4.3 Bipolar Junction Transistors 39
1.5 Semiconductor Technology Families 41
1.6 Modern Scientific Discovery—Experiments, Theory, and Computer Simulation 43
1.7 The Plan For This Book 45
1.8 Summary of Key Ideas 46
1.9 References 46
1.10 Problems 47

Chapter 2 Modern CMOS Technology **49**

2.1 Introduction 49
2.2 CMOS Process Flow 50
2.2.1 The Beginning—Choosing a Substrate 51
2.2.2 Active Region Formation 52
2.2.3 Process Option for Device Isolation—Shallow Trench Isolation 57
2.2.4 N and P Well Formation 60
2.2.5 Process Options for Active Region and Well Formation 63
2.2.6 Gate Formation 71
2.2.7 Tip or Extension (LDD) Formation 76
2.2.8 Source/Drain Formation 80
2.2.9 Contact and Local Interconnect Formation 82
2.2.10 Multilevel Metal Formation 84
2.3 Summary of Key Ideas 90
2.4 Probems 91

Micron Ex. 1022, p. 7
Micron v. YMTC
IPR2025-00294

4.4.2 Level 2 Contamination Reduction: Wafer Cleaning. . . . 173
4.4.3 Level 3 Contamination Reduction: Gettering. . . . 176
4.5 Models and Simulation. . . . 180
4.5.1 Level 1 Contamination Reduction: Clean Factories. . . . 181
4.5.2 Level 2 Contamination Reduction: Wafer Cleaning. . . . 184
4.5.3 Level 3 Contamination Reduction: Gettering. . . . 186
4.5.3.1 Step 1: Making the Metal Atoms Mobile 186
4.5.3.2 Step 2: Metal Diffusion to the Gettering Site. . . . 187
4.5.3.3 Step 3: Trapping the Metal Atoms at the Gettering Site. . . . 190
4.6 Limits and Future Trends in Technologies and Models 193
4.7 Summary of Key Ideas. . . . 196
4.7 References. . . . 196
4.9 Problems 198

Chapter 5 Lithography 201

5.1 Introduction. . . . 201
5.2 Historical Development and Basic Concepts 203
5.2.1 Light Sources. . . . 206
5.2.2 Wafer Exposure Systems. . . . 208
5.2.2.1 Optics Basics—Ray Tracing and Diffraction 209
5.2.2.2 Projection Systems (Fraunhofer Diffraction). . . . 212
5.2.2.3 Contact and Proximity Systems (Fresnel Diffraction) 219
5.2.3 Photoresists. . . . 221
5.2.3.1 g-line and i-line Resists. . . . 223
5.2.3.2 Deep Ultraviolet (DUV) Resists. . . . 225
5.2.3.3 Basic Properties and Characterization of Resists 227
5.2.4 Mask Engineering—Optical Proximity Correction and Phase Shifting. . . 230
5.3 Manufacturing Methods and Equipment. . . . 234
5.3.1 Wafer Exposure Systems. . . . 234
5.3.2 Photoresists. . . . 238
5.4 Measurement Methods. . . . 241
5.4.1 Measurement of Mask Features and Defects 242
5.4.2 Measurement of Resist Patterns. . . . 244
5.4.3 Measurement of Etched Features. . . . 244
5.5 Models and Simulation. . . . 246
5.5.1 Wafer Exposure Systems. . . . 247
5.5.2 Optical Intensity Pattern in the Photoresist 253
5.5.3 Photoresist Exposure. . . . 259
5.5.3.1 g-line and i-line DNQ Resists. . . . 259
5.5.3.2 DUV Resists. . . . 263
5.5.4 Postexposure Bake (PEB). . . . 264
5.5.4.1 g-line and i-line DNQ Resists. . . . 264
5.5.4.2 DUV Resists. . . . 266
5.5.5 Photoresist Developing 267
5.5.6 Photoresist Postbake 270

7.2.5 Gaussian Solution Near a Surface 381
7.2.6 Error-Function Solution in an Infinite Medium 382
7.2.7 Error-Function Solution Near a Surface 384
7.2.8 Intrinsic Diffusion Coefficients of Dopants in Silicon 386
7.2.9 Effect of Successive Diffusion Steps 388
7.2.10 Design and Evaluation of Diffused Layers 389
7.2.11 Summary of Basic Diffusion Concepts 392
7.3 Manufacturing Methods and Equipment 392
7.4 Measurement Methods 395
7.4.1 SIMS 396
7.4.2 Spreading Resistance 397
7.4.3 Sheet Resistance 398
7.4.4 Capacitance Voltage 399
7.4.5 TEM Cross Section 399
7.4.6 2D Electrical Measurements Using Scanning Probe Microscopy 400
7.4.7 Inverse Electrical Measurements 402
7.5 Models and Simulation 403
7.5.1 Numerical Solutions of the Diffusion Equation 403
7.5.2 Modifications to Fick's Laws to Account for Electric Field Effects 406
7.5.3 Modifications to Fick's Laws to Account for Concentration-Dependent Diffusion 409
7.5.4 Segregation 413
7.5.5 Interfacial Dopant Pileup 415
7.5.6 Summary of the Macroscopic Diffusion Approach 417
7.5.7 The Physical Basis for Diffusion at an Atomic Scale 417
7.5.8 Oxidation-Enhanced or -Retarded Diffusion 419
7.5.9 Dopant Diffusion Occurs by Both I and V 422
7.5.10 Activation Energy for Self-Diffusion and Dopant Diffusion 426
7.5.11 Dopant-Defect Interactions 426
7.5.12 Chemical Equilibrium Formulation for Dopant-Defect Interactions 432
7.5.13 Simplified Expression for Modeling 434
7.5.14 Charge State Effects 436
7.6 Limits and Future Trends in Technologies and Models 439
7.6.1 Doping Methods 440
7.6.2 Advanced Dopant Profile Modeling—Fully Kinetic Description of Dopant-Defect Interactions 440
7.7 Summary of Key Ideas 442
7.8 References 443
7.9 Problems 445

Chapter 8 Ion Implantation **451**

8.1 Introduction 451
8.2 Historical Development and Basic Concepts 451
8.2.1 Implants in Real Silicon—The Role of the Crystal Structure 461
8.3 Manufacturing Methods and Equipment 463

Micron Ex. 1022, p. 9
Micron v. YMTC
IPR2025-00294

9.5 Models and Simulation . . . 573
9.5.1 Models for Deposition Simulations . . . 573
9.5.1.1 Models in Physically Based Simulators Such as SPEEDIE . . . 574
9.5.1.2 Models for Different Types of Deposition Systems . . . 582
9.5.1.3 Comparing CVD and PVD and Typical Parameter Values . . . 587
9.5.2 Simulations of Deposition Using a Physically Based Simulator, SPEEDIE . . . 590
9.5.3 Other Deposition Simulations . . . 598
9.6 Limits and Future Trends in Technologies and Models . . . 601
9.7 Summary of Key Ideas . . . 602
9.8 References . . . 603
9.9 Problems . . . 605

Chapter 10 Etching **609**

10.1 Introduction . . . 609
10.2 Historical Development and Basic Concepts . . . 612
10.2.1 Wet Etching . . . 612
10.2.2 Plasma Etching . . . 619
10.2.2.1 Plasma Etching Mechanisms . . . 621
10.2.2.2 Types of Plasma Etch Systems . . . 628
10.2.2.3 Summary of Plasma Systems and Mechanisms . . . 636
10.3 Manufacturing Methods . . . 637
10.3.1 Plasma Etching Conditions and Issues . . . 638
10.3.2 Plasma Etch Methods for Various Films . . . 643
10.3.2.1 Plasma Etching Silicon Dioxide . . . 644
10.3.2.2 Plasma Etching Polysilicon . . . 647
10.3.2.3 Plasma Etching Aluminum . . . 649
10.4 Measurement Methods . . . 650
10.5 Models and Simulation . . . 653
10.5.1 Models for Etching Simulation . . . 653
10.5.2 Etching Models—Linear Etch Model . . . 656
10.5.3 Etching Models—Saturation/Adsorption Model for Ion-Enhanced Etching . . . 663
10.5.4 Etching Models—More Advanced Models . . . 669
10.5.5 Other Etching Simulations . . . 671
10.6 Limits and Future Trends in Technologies and Models . . . 675
10.7 Summary of Key Ideas . . . 676
10.8 References . . . 677
10.9 Problems . . . 679

Chapter 11 Back-End Technology **681**

11.1 Introduction . . . 681
11.2 Historical Development and Basic Concepts . . . 687
11.2.1 Contacts . . . 688
11.2.2 Interconnects and Vias . . . 695

Micron Ex. 1022, p. 10
Micron v. YMTC
IPR2025-00294

Preface

The silicon integrated circuit is surely one of the wonders of our age. The ability to fabricate tens of millions of individual components on a silicon chip with an area of a few cm^2 has enabled the information age.

Basic discoveries and inventions between 1945 and 1970 laid the foundations for these chips. In the past 30 years, chip complexity has increased at an exponential rate, primarily because of the constant shrinking of device geometries, improved manufacturing practice, and clever inventions enabling specific functions to be implemented in new ways. Shrinking geometries permit more devices to be placed in a given area of silicon; improved manufacturing permits larger chips to be economically fabricated; and clever inventions permit functions to be realized in smaller areas. It is widely expected that these historical trends will continue for at least another 10–20 years, resulting in chips that contain billions of components. Such chips will have extraordinary capabilities. We will likely find ourselves in 10–20 years thinking of today's chips as primitive precursors to the chips that will be in manufacturing at that time.

The technology that is used to build silicon integrated circuits today has evolved largely through empirical methods. It often seems that the chip industry moves so rapidly and new products are introduced so often that there is little time to worry about the scientific basis of the technologies used to build these chips. Yet in parallel with the rapid pace of this industry, a strong effort has been proceeding, often behind the scenes, to develop a solid, physically based understanding of the many technologies used in chip manufacturing. Because of the feature sizes of structures in modern chips, this understanding often needs to be on a molecular or atomic level. It is not sufficient any longer to think of silicon oxidation as simply a chemical reaction between silicon and oxygen that grows SiO_2. Today we must understand the detailed bonding between silicon and oxygen atoms and the kinetics that drive this reaction on an atomic basis.

Silicon integrated circuit technology makes use of many diverse fields of science and engineering. The optical steppers which print microscopic patterns on wafers, represent one of the most advanced applications of the principles of Fourier optics. Plasma etching involves some of the most complex chemistries used in manufacturing today. Ion implantation draws upon understanding from research in high energy physics. Thin films on the silicon wafer surface exhibit complex mechanical behavior which stretches our understanding of basic materials properties. And of course, silicon devices themselves are approaching physical sizes at which molecular and atomic scale phenomena involving ideas from quantum mechanics are important. One of the great challenges in integrated circuit manufacturing is the need to draw on scientific principles and engineering developments from such an extraordinarily wide range of disciplines. Integrating the

Micron Ex. 1022, p. 11
Micron v. YMTC
IPR2025-00294

provided substantial inputs and comments. Our own work in this field has been supported over many years by DARPA (the Defense Advanced Research Projects Agency) and by the Semiconductor Research Corporation (SRC) . We owe them a considerable debt of gratitude for making our work possible. We welcome comments or suggestions on this text by email at plummer@ee.stanford.edu, deal@ee.stanford.edu, or griffin@stanford.edu.

Micron Ex. 1022, p. 12
Micron v. YMTC
IPR2025-00294

knowledge from these diverse disciplines has been and will continue to be a great challenge. Scientists and engineers who work in this field need broad understanding and the ability to seek out, integrate and use ideas from many fields.

Over the past 20 years much has been learned about silicon and the other materials that are used in modern chips. Often new knowledge is incorporated in a "model" which may be a mathematical equation describing a process or an atomistic picture of how a particular process works. Models codify knowledge and are an elegant way of expressing what is known. They also provide a way of exchanging ideas between researchers in a particular field, and can be tested experimentally to assess their predictive capability.

Within the last decade, a serious attempt has been made to develop computer simulation tools which can simulate the various technologies used in fabricating chips. These simulation tools are built around models of the physical processes involved. Some simulation tools today use well-established scientific principles to predict experimental results. Optical lithography simulators, which are based on mathematical descriptions of Fourier optics, are a good example. Such tools today can accurately predict the image that will be printed in resist on a silicon wafer, given a particular mask design and a specific exposure system. Other simulation tools rest on less solid ground. Models of dopant diffusion in silicon, for example, use models which are still debated in the scientific community and which are clearly incomplete in terms of describing all the physical phenomena involved. Nevertheless, even these models are very useful today.

This book attempts to describe not only the manufacturing practice associated with the technologies used in silicon chip fabrication, but also the underlying scientific basis for those technologies. Those scientific principles are described in terms of models of the process in many cases. In most chapters, models are discussed in the context of computer simulation programs which have incorporated the models and which use them to simulate technology steps. We make extensive use of simulation examples to illustrate how technologies work and to help in visualizing features of the technologies that are not easily seen any other way. We have found these tools to be powerful teaching aids.

Simulation tools are widely used in the semiconductor industry today to supplement traditional experimental methods. While it is unlikely that simulation will completely eliminate the need for experiments, especially in a fast moving industry like the IC industry, simulators can result in very substantial cost savings in developing new generations of technology and in solving manufacturing problems. It is widely believed that simulation tools will be essential in the future if the rapid progress that has characterized the semiconductor industry is to continue.

This book is organized somewhat differently than other texts on this general topic, in two principal ways. The first is the extensive use of simulation examples throughout the text. These serve several purposes. The first is simply to help explain the scientific principles involved in each chapter. Simulations help to illustrate things like the time evolution of a growing oxide layer, a diffusing dopant profile or a depositing thin film. They are also very useful in illustrating the effects of specific physical phenomena in a process step because it is straightforward in simulators to add or eliminate specific physical models. Simulators provide the only real way in which complex interactions between process steps can be illustrated and understood. Finally, students who spend their

Micron Ex. 1022, p. 13
Micron v. YMTC
IPR2025-00294

careers in this industry will certainly use these tools and understanding their capabilities and limitations will be important in their future work.

The second way in which this book is organized differently is the discussion of a complete process flow early in the book (Chapter 2). While readers new to this field may not appreciate many of the complexities of a CMOS process before studying the later chapters, we have found that an early broad exposure to a complete chip manufacturing process is very helpful in establishing the context for the specific technologies discussed in later chapters. In teaching the material in this book, we usually cover the CMOS process in the first or second lecture somewhat superficially, and then return to the same topic in the last lecture, at which point the details can be more fully discussed.

We have also attempted in each chapter to include some discussion of future trends. Predicting the future is obviously difficult and there is some risk that including this material will simply serve to date this book. Nevertheless, we have found that students are often interested in this topic and at least in general terms, we believe it is possible to predict where silicon technology is heading. The semiconductor industry *National Technology Roadmap for Semiconductors* (the NTRS) provides some guidance in looking to the future.

The material in this book can be covered in a one quarter senior/graduate level course, although not all of the material in each chapter can be covered in one quarter. A semester long course would provide more time to cover the full range of material in the book. If the book is used in connection with a one quarter long course, one option is to minimize the amount of time spent on the Manufacturing Methods and Measurement Techniques sections in each chapter. A set of lecture notes based on figures from the text is available to instructors by contacting the publisher or the authors by email. We have used these notes several times in a one quarter course at Stanford.

Follow-on courses to a basic IC fabrication course can make more extensive use of the simulation tools discussed in this text. We have not used the simulation tools described in this book for homework assignments or for lab assignments in connection with a first course in IC fabrication. We believe that the simulation examples are better used simply as teaching tools in such courses, to illustrate ideas and to clarify physical principles. But in a follow-on course, hands-on experience with these simulation tools is easily possible. Most of the computer tools we use in the book are commercially available and the vendors of these tools are generally anxious to work with university instructors to make the tools available for teaching purposes.

Finally, we acknowledge the many students at Stanford who have helped refine the material in this book by using various draft versions of the text in classes we have taught. Their inputs and suggestions have hopefully made this a better book. For many years we have worked with an energetic group of Ph.D. students and faculty colleagues at Stanford who have helped to develop some of the models and software tools described in this book. We particularly acknowledge Professor Bob Dutton and former Ph.D. students Professor Mark Law (now at the U. Florida) and Dr. Conor Rafferty (now at Lucent Technologies). We are also very grateful to a number of individuals who reviewed draft versions of this book and who provided technical inputs to various chapters. Paul Rissman of Hewlett Packard, Jim McVittie of Stanford, and Mark Law all

Micron Ex. 1022, p. 14
Micron v. YMTC
IPR2025-00294

Etching

10

10.1 Introduction

After thin films are deposited on the wafer surface, they are usually selectively removed by etching to leave the desired pattern of the film on the wafer surface. This process was used many times in the CMOS process flow in Chapter 2 and is summarized in Figure 10–1. In addition to deposited films, parts of the silicon substrate itself may be etched, such as in creating trenches in isolation structures. The masking layer may be photoresist, or it may be another thin film such as silicon dioxide or silicon nitride. Oxide or nitride masks stand up better to etching conditions than photoresist and are often called hard masks. But they themselves must be selectively etched, usually using lithographically defined photoresist as the masking layer. The etching of a thin film is usually done until a different layer is reached underneath. Etching only partway through a layer without reaching an underlying material is sometimes done but can be difficult to control uniformly over the whole wafer. Multilayer structures can be etched sequentially using the same masking layer.

Etching can be done in either a "wet" or "dry" environment. Wet etching involves the use of liquid etchants. The wafers are usually immersed in the etchant solution and the exposed material is etched mostly by chemical processes. While such processes are not common in modern VLSI processing for reasons we shall see, they are sometimes used, as in Figure 2–34 in Chapter 2. Dry etching involves the use of gas-phase etchants in a plasma. Here the etching usually takes place by a combination of chemical and physical processes. Because a plasma is involved, dry etching is often called "plasma etching." This is normally the etching method today and was used many times in Chapter 2 (Figure 2–4 for example).

The ideal etch profile in Figure 10–1 has perfectly straight sidewalls exactly under the edge of the mask. What can happen in reality is shown in Figure 10–2. In Figure 10–2(a) the etching is both vertical and lateral. This leads to undercutting of the photoresist mask and nonvertical sidewalls in the film. In Figure 10–2(b) the photoresist is not perfectly rectangular, with rounded top corners and sloped sides. In addition, the etch rate of the photoresist is nonzero, and the mask itself is etched, or eroded, to some degree. This occurs both on its top and on its sides. This leads to even more lateral etching of the film since the photoresist mask gets narrower as the etching continues. If the substrate is attacked by the etchant as well, then its profile will change. Figure 10–2(b) also illustrates this issue, which is related to the selectivity of the etching process.

Etch selectivity is the ratio of the etch rates of the different materials in an etch process. When the etch rates of the mask and the underlying substrate are near zero,

Micron Ex. 1022, p. 15
Micron v. YMTC
IPR2025-00294

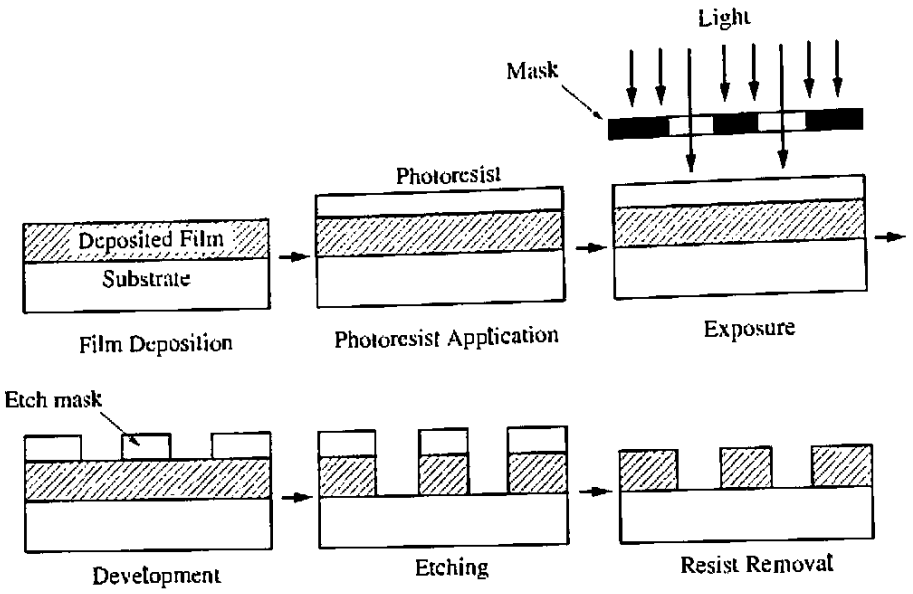


Figure 10–1 General process used in integrated circuit fabrication to define patterned films.

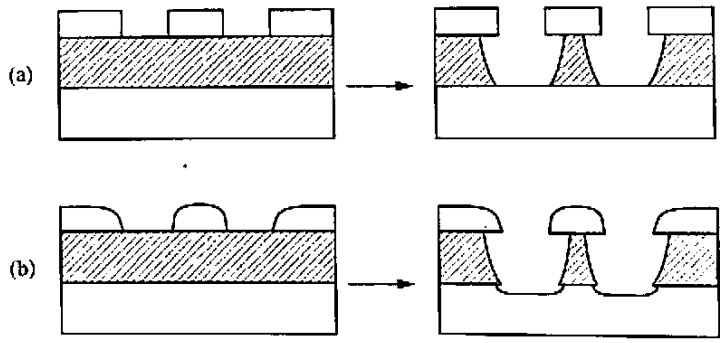


Figure 10–2 Actual etch profiles that can occur. (a) Lateral etching under mask. (b) Rounded photoresist which is further eroded during etching, leading to even more lateral etching. (b) also illustrates etch selectivity.

while the etch rate of the film is appreciable, then the etch selectivity of the film with respect to both the mask and the substrate is high. This is normally a desired situation. If the etch rate of the mask or substrate is significant, then the selectivity is poor. Selectivities, or etch rate ratios, in the range of 25–50 are usually considered reasonable. Different materials have different etch rates usually because of the chemical effects involved with etching, as opposed to the physical effects. Chemical reactions can be very selective whereas physical processes like sputtering tend to be similar for most materials.

Etch directionality is a measure of the relative etch rates in different directions, usually vertical versus lateral, as illustrated in Figure 10–3. Isotropic etching occurs when

Micron Ex. 1022, p. 16
Micron v. YMTC
IPR2025-00294

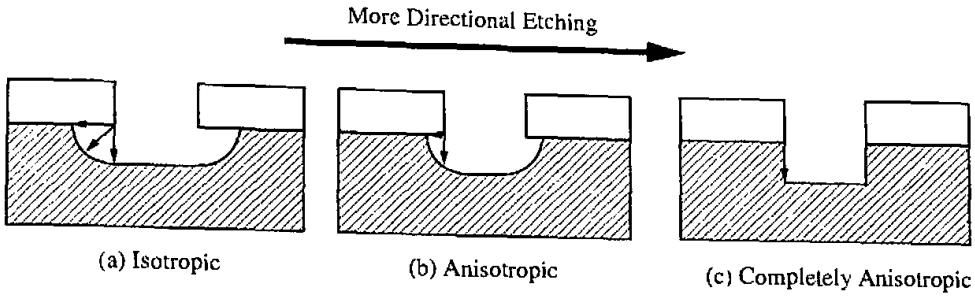


Figure 10–3 Etch profiles for different degrees of anisotropic, or directional, etching: (a) purely isotropic etching; (b) anisotropic etching; (c) completely anisotropic etching.

etch rates are the same in all directions, as in Figure 10–3(a). The etch distance laterally under each side of the mask is the same as vertically under the mask opening. As the opening under the mask approaches zero, the etch profile would approach a perfect semicircle. Figure 10–3(b) shows anisotropic etching, where less etching occurs laterally. Figure 10–3(c) shows completely anisotropic etching, with no etching at all in the lateral direction. Etch directionality is usually related to physical effects in etching such as ion bombardment and sputtering. As we shall see, the more physical an etch process is, the more directional and the less selective it generally is. On the other hand, the more chemical an etch process is, the more selective and the less directional it generally is.

Directionality is often desired in an etch process. Vertical etching maintains lithographically defined feature sizes as they are transferred by etching into underlying films. Vertical etching is also utilized in special applications such as sidewall spacer formation. (Recall Figure 2–30 in the CMOS process flow in Chapter 2.) However, vertical structures that result from vertical etching may also cause problems in subsequent processing. Depositing another layer on top of a structure with vertical steps may cause step coverage problems, as we discussed in Chapter 9. Less steep steps, obtained with less directional etching, would make it easier to obtain good step coverage and would allow easier filling in later deposited layers. Because of shrinking feature sizes, however, modern fabrication methods tend to employ directional etching and vertical steps with little undercutting, and use deposition techniques that achieve good filling and step coverage even for near-vertical structures.

Selectivity is also a requirement. This means that the etch rate of the layer to be etched should be fast compared to the etch rate of the mask and etch rate of the substrate or layer below. Achieving good selectivity and directional etching at the same time is sometimes quite difficult. Other requirements for an etch process are that the gases and liquids used for the etching must be able to be transported to the wafer surface, and the byproducts of the etch process must be transported away easily. The latter means that soluble byproducts are produced in wet etching, and that gaseous or volatile byproducts are produced in dry etching. The etch process should be uniform, safe to use, and should cause minimal damage to structures on the chip. Finally, the etching process should be clean, with low particulate production and little film contamination, and should be cost effective.

Micron Ex. 1022, p. 17
Micron v. YMTC
IPR2025-00294

10.2 Historical Development and Basic Concepts

There are two main methods of etching used in the semiconductor industry: wet etching and dry, or plasma, etching. In the early days of the industry, wet etching was used exclusively. It was a well-established, simple, and inexpensive technology. Wet etching can also be very selective. Eventually, however, the need for smaller linewidths and more vertical structures required new techniques. Plasma etching methods were developed for integrated circuit fabrication and are used for most etching steps today.

In this section we will describe the basic concepts involved in both of these techniques. We will start with wet etching, which we will use to introduce concepts such as selectivity, overetch, etch bias, and anisotropy that are applicable to both wet and dry etching.

10.2.1 Wet Etching

The first etchants used in the integrated circuit industry were simple wet chemical etchants. By immersing the wafers into baths of liquid chemicals, the exposed films could be etched away, leaving unetched those regions of the film that were masked with photoresist or other films. Wet etches were developed for all steps in the fabrication process. A common wet etch for SiO_2 is hydrofluoric acid, HF. The overall reaction is

$$SiO_2 + 6HF \rightarrow H_2SiF_6 + 2H_2O \tag{10.1}$$

Wet etchants work through chemical processes rather than physical processes. In general, wet etchants work by chemically reacting with the film to form water-soluble byproducts or gases, such as the H_2SiF_6 byproduct which is a water-soluble complex in the above example.

In some cases the etching occurs by first oxidizing the surface of the film or material and then dissolving the oxide. For example, a common etchant for silicon is a mixture of nitric acid (HNO_3) and HF. The nitric acid partially decomposes to nitrogen dioxide, NO_2, which then oxidizes the surface of the silicon by the reaction

$$Si + 2NO_2 + 2H_2O \rightarrow SiO_2 + H_2 + 2HNO_2 \tag{10.2}$$

The HF then dissolves the SiO_2 by the reaction given in Eq. (10.1). The overall reaction is

$$Si + HNO_3 + 6HF \rightarrow H_2SiF_6 + HNO_2 + H_2O + H_2 \tag{10.3}$$

Buffering agents are often added to the etch solutions to keep the etchants at maximum strength over use and time. For example, ammonium fluoride (NH_4F) is added to HF to help prevent depletion of the fluoride ions in the oxide etch. This is called "Buffered HF" or BHF, or more commonly BOE for "Buffered Oxide Etch." The addition of ammonium fluoride also decreases the etch rate of photoresist and helps to minimize lifting of the resist during oxide etching. Acetic acid, CH_3COOH, is often added to the nitric acid/hydrofluoric acid silicon etch to limit the dissociation of the nitric acid.

Wet etches can be very selective because they depend on chemistry. The limiting steps in most etch processes are usually the chemical reactions in which the etch species react

Micron Ex. 1022, p. 18
Micron v. YMTC
IPR2025-00294

with the film, forming the soluble byproducts. The selectivity, S, of an etch process between two materials, 1 and 2, is simply the ratio of their etch rates, r, in that etchant, or

$$S = \frac{r_1}{r_2} \tag{10.4}$$

Material 1 is usually the film being etched, and material 2 is either the masking material (photoresist or perhaps silicon dioxide) or the material below the film. We often speak of an etch process for material 1 having a certain selectivity over (or "with respect to," or just "to") material 2. For a large selectivity ($S>>1$) we say that the etch process for material 1 has good selectivity over material 2.

Selectivity is important for a number of reasons. First, the selectivity for the material to be etched with respect to the mask determines how thick the mask material must be so that the mask is not completely removed during the etching process. Second, all etch processes generally employ some amount of overetching in order to ensure that the desired etching process has gone to completion. Thus underlying films are normally subjected to the etchant for some period of time toward the end of the etch period. The selectivity for the material being etched with respect to the underlying material determines how much etching of the underlying materials occurs.

Example 1 μm of SiO_2 is being etched on top of a Si substrate. The etch rate of the oxide is 0.40 μm min^{-1}, and the etch selectivity of the oxide with respect to the silicon is 25-to-1. If the etch is done for three minutes, how much of the underlying Si is etched?

Answer From Eq. (10.4), the etch rate of the Si can be calculated:

$$S = \frac{r_1}{r_2} \Rightarrow 25 = \frac{0.40\ \mu\text{m min}^{-1}}{r_{Si}} \Rightarrow r_{Si} = 0.016\ \mu\text{m min}^{-1}$$

The Si is only exposed to the etch after the overlying oxide is completely etched off. The time required to etch away the oxide equals 1 μm/0.40 μm min^{-1}, which equals 2.5 minutes. Therefore, the Si is etched for 0.5 minutes. Hence, the amount of Si etched is 0.016 μm min^{-1} * 0.5 min, which equals 0.008 μm, or 8 nm.

Most wet chemical etchants etch isotropically. The exceptions to this are those which are sensitive to crystallographic orientation. For example, some etchants etch much slower in the <111> direction in crystalline silicon as compared to the other directions. But most commonly used wet etches etch equally in all directions. In Figure 10–3(a) we saw how isotropic etching results in etching underneath the edge of the mask. The amount of undercutting is called the "etch bias." This is shown in Figure 10–4(a). Here we assume that the selectivity of the etch with respect to both the mask and the substrate is infinity (i.e., no etching at all of those materials). The etch thickness or depth is

Micron Ex. 1022, p. 19
Micron v. YMTC
IPR2025-00294

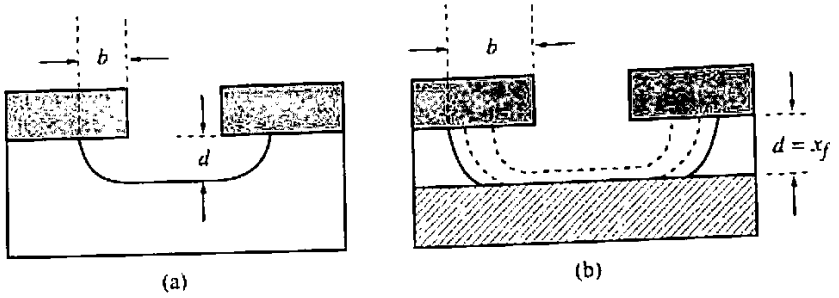


Figure 10–4 Illustration of etch bias and overetch. In (a) the etch bias, b, is shown for a given etch depth, d. In (b), overetching is illustrated where etching is continued even after the etch depth, d, equals the film thickness, x_f, with the result that the etch bias increases.

d and the bias is b. For perfectly isotropic etching b would equal d, but only if etching is stopped before the bottom of the film is reached.

As mentioned earlier, some overetching is normally part of every etch process. If each layer were of uniform thickness, and the etch were perfectly uniform through time and space, then overetching would theoretically not be needed. The etch time required would be based on the previously determined etch rate or on other endpoint detection methods, to be discussed later. It would not even matter what the etch selectivity over the layer beneath is in that case. However, the thickness of films is not perfectly uniform, and they do not always etch exactly uniformly. So some overetch is always done in manufacturing to ensure that the etch goes to completion everywhere. This is illustrated in Figure 10–4(b). In this figure we again assume that the selectivity with respect to the mask and substrate are infinite and that the etching is purely isotropic. The bias b now increases with time as the overetch continues. The amount of overetching needed, usually measured in terms of time or % time, can be determined by estimating the uncertainties in etch rates and in the nonuniformities of the thicknesses and then calculating the worst case etch time needed. Ten to twenty percent overetches are common. This ensures that while some of the structures may be overetched, none are underetched. We will see later that when the etching is anisotropic, overetching is also required to remove residual film from steps in the topography.

Example A 0.5-μm layer of silicon dioxide on a Si substrate needs to be etched down to the Si. Assume that the nominal oxide etch rate is r_{ox} (in μm min^{-1}). There is a ± 5% variation in the oxide thickness and a ± 5% variation in the oxide etch rate. (a) How much overetch is required (in % time) in order to ensure that all the oxide is etched? (b) What selectivity of the oxide etch rate to the Si etch rate is required so that a maximum of 5.0 nm of Si is etched? (Assume the overetch calculated in part (a) is done.)

Answer (a) The nominal etch time = x/r_{ox} = $0.5/r_{ox}$ (x = thickness in μm.) The overetch is done to make sure all the oxide is etched for the worst case condition; that means for the thickest oxide and the slowest etch rate. The thickest oxide =

Micron Ex. 1022, p. 20
Micron v. YMTC
IPR2025-00294

0.5 * 1.05 = 0.525 μm. The slowest etch rate = r_{ox} * 0.95 μm min^{-1}. The time to etch the worst case = x/r = 0.525/(r_{ox} * 0.95) = 0.553/r_{ox} min. The amount of overetch, in % time, is just the worst case etch time divided by the nominal etch time = (0.553/r_{ox})/(0.5/r_{ox}) = 1.106 or 10.6% overetch.

(b) The maximum amount of Si that will be etched will occur under the thinnest oxide being etched at the fastest etch rate. The thinnest oxide is 0.95 * 0.5 μm = 0.475 μm. The fastest etch rate is r_{ox} * 1.05 μm min^{-1}. The time to etch through that oxide is x/r = 0.475/(r_{ox} * 1.05) = 0.4523/r_{ox} min. The time that the Si is exposed to the etch is equal to the total etch time (0.553/r_{ox}, as calculated in part (a)) minus the time it took to etch the thinnest oxide, etching at the fastest rate, or

$$(0.553/r_{ox}) - (0.4523/r_{ox}) = 0.1003/r_{ox} \text{ min}$$

We want to etch 0.005 μm or less of the Si, so

$$r_{Si} = x/\text{time} = 0.005/(0.1003/r_{ox}) \text{ μm min}^{-1}$$
$$= 0.050 * r_{ox} \text{ μm min}^{-1}$$

The selectivity of oxide etch rate to Si etch rate is therefore:

$$r_{ox}/r_{Si} = r_{ox}/(0.050 * r_{ox})$$
$$r_{ox}/r_{Si} = 20{:}1$$

Since overetching is usually done, it is important that the selectivity with respect to the layer below be as high as possible or else some etching of that layer will occur during the overetch. On the other hand, if the selectivity is very large, one cannot indiscriminately overetch. This would cause unwanted undercutting or bias.

The above examples assume infinite etch selectivity of the film with respect to the mask; that is, the etch rate of the mask is zero. But there will be some finite etch rate of the mask, which is usually photoresist. What will happen? Obviously the mask will etch at some rate during the etching of the film. This is shown in Figure 10–5(a) for the case of isotropic etching and a rectangular-shaped mask. Here Δm is the amount of mask etched, the same in all directions in this case. This is called mask erosion. Obviously the extent of lateral etching will increase beyond what would be expected without any mask erosion. For completely anisotropic (vertical) etching, etch erosion should not be a problem as long as the mask is perfectly rectangular in shape. The etch will only occur from the top. Only if the mask is etched all the way through would any difficulties arise.

In fact, the mask shape is usually not perfectly rectangular but often has rounded corners or sloped sides. Mask erosion leading to extra undercutting can occur even for completely anisotropic etching, as illustrated in Figure 10–5(b). With a finite etch rate for the mask, there will be equal vertical etching at all points of the mask. At the sloped edge, a finite amount of the mask will be etched away. This will allow lateral erosion of

Micron Ex. 1022, p. 21
Micron v. YMTC
IPR2025-00294

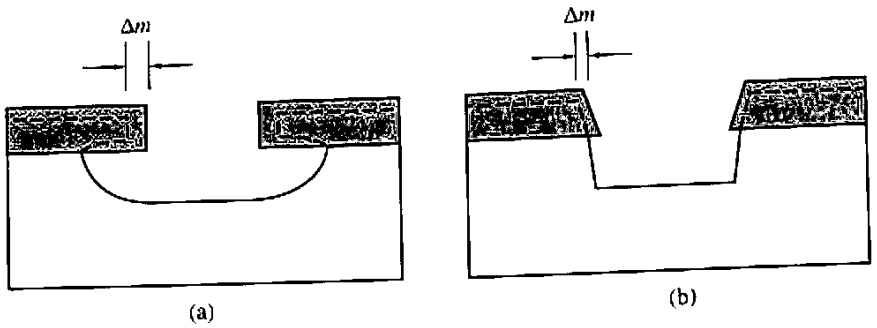


Figure 10–5 Illustration of mask erosion. In (a), there is an idealized rectangular mask and isotropic etching of the mask and the substrate. In (b), there is a sloped mask and anisotropic etching. In both cases more lateral etching of the substrate occurs as a result of the mask etching, or erosion.

the mask, shown by Δm in the figure, and etching of the film in this thin region will occur. This will result in undercutting with respect to the original mask edge, even for perfectly anisotropic, or vertical, etching.

Etching is often neither perfectly anisotropic nor perfectly isotropic, as was shown in Figure 10–3(b). We can define the degree of anisotropy of a film, A_f, as

$$A_f = 1 - \frac{r_{\text{lat}}}{r_{\text{ver}}} \tag{10.5}$$

where r_{lat} and r_{ver} are the etch rates in the lateral and vertical directions, respectively. In Figure 10–4, this would correspond to

$$A_f = 1 - \frac{b}{d} \tag{10.6}$$

Isotropic etching [Figure 10–3(a)] would have an anisotropy of 0, completely anisotropic etching [Figure 10–3(c)] would have an anisotropy of 1, and general anisotropic etching [Figure 10–3(b)] would have an anisotropy between 0 and 1. For a structure etched exactly to the bottom of the film, with no overetch, the anisotropy would be

$$A_f = 1 - \frac{b}{x_f} \tag{10.7}$$

where b is the bias and x_f is the film thickness.

Example Consider the structures shown in Figure 10–6. A 0.5-μm-thick oxide layer is etched to achieve equal structure widths and spacings (S_f). The etch process produces

Micron Ex. 1022, p. 22
Micron v. YMTC
IPR2025-00294

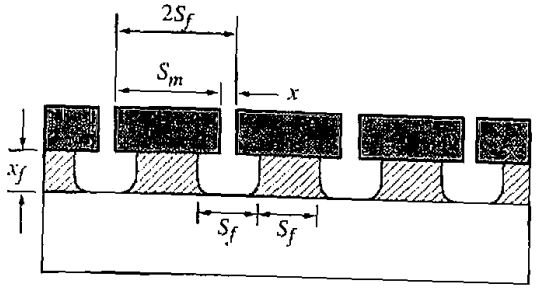


Figure 10–6 Structure and dimensions needed to fabricate features with equal widths and spaces (S_f) for a mask size of S_m, film thickness of x_f, and degree of anisotropy of A_f. x is the spacing between the masks and is usually the minimum lithographic feature. (After [10.1].)

a degree of anisotropy of 0.8. If the distance between the mask edges, x, is 0.35 μm, what structure spacings and widths are obtained? Neglect any overetch.

Answer To obtain equal widths and spacings, S_f, the mask width, S_m, must be made larger to take into account the anisotropic etching. Since

$$S_m = S_f + 2b$$

where b is the bias on each side, and using Eq. (10.7) we can now rewrite S_m as

$$S_m = S_f + 2x_f(1 - A_f)$$

which is the dimension of the mask needed. [This makes sense. For isotropic etching ($A_f = 0$), S_m is a maximum, and for completely anisotropic etching ($A_f = 1$), S_m is a minimum and equal to S_f.] The distance between the mask edges, x, is usually the minimum feature size that can be lithographically resolved. Since

$$x = 2S_f - S_m$$

x can be rewritten, using the expression above for S_m, as

$$x = S_f - 2x_f(1 - A_f)$$

Rewriting this in terms of S_f gives

$$S_f = x + 2x_f(1 - A_f) \tag{10.8}$$

Plugging the above numbers into Eq. (10.8) gives

$$S_f = 0.35\mu m + 2(0.5\mu m)(1 - 0.8)$$
$$= 0.55\ \mu m$$

Eq. (10.8) shows that the structure size approaches the minimum lithographic dimension only when the film thickness gets very small (not always practical) or as the anisotropy gets close to 1. This means completely vertical etching. Unfortunately, wet etching does not result in vertical etching, but rather isotropic etching where A_f is a minimum. These considerations give some insight into the reasons wet chemical etching is not very commonly used in chip fabrication today.

Micron Ex. 1022, p. 23
Micron v. YMTC
IPR2025-00294

Table 10–1 Common wet chemical etchants for various thin films used in IC fabrication

Material	Etchant	Comments
SiO_2	HF (49% in water) "straight HF"	Selective over Si (i.e., will etch Si very slowly in comparison). Etch rate depends on film density, doping.
	NH_4F:HF (6:1) "Buffered HF" or "BOE"	About 1/20 th the etch rate of straight HF. Etch rate depends on film density, doping. Will not lift up photoresist like straight HF.
Si_3N_4	HF (49%)	Etch rate depends strongly on film density, O, H in film.
	H_3PO_4:H_2O (boiling @ 130–150°C)	Selective over SiO_2. Requires oxide mask.
Al	H_3PO_4:H_2O:HNO_3:CH_3COOH (16:2:1:1)	Selective over Si, SiO_2, and photoresist.
Polysilicon	HNO_3:H_2O:HF (+ CH_3COOH) (50:20:1)	Etch rate depends on etchant composition.
Single crystal Si	HNO_3:H_2O:HF (+ CH_3COOH) (50:20:1)	Etch rate depends on etchant composition.
	KOH:H_2O:IPA (23 wt. % KOH, 13 wt. % IPA)	Crystallographically selective; relative etch rates: (100): 100 (111): 1
Ti	NH_4OH:H_2O_2:H_2O (1:1:5)	Selective over $TiSi_2$
TiN	NH_4OH:H_2O_2:H_2O (1:1:5)	Selective over $TiSi_2$
$TiSi_2$	NH_4F:HF (6:1)	
Photoresist	H_2SO_4:H_2O_2 (125°C)	For wafers without metal.
	Organic strippers	For wafers with metal.

Before we describe techniques which do result in more anisotropic etching, we will look at some of the wet etch solutions that have been used, and are still used to some extent, in the Si integrated circuit industry. Table 10–1 gives a brief sampling of some of the common solutions and compositions.

The etch rate of a material in a particular etchant depends on the specific composition of the etch solution, and the etch rate can vary by orders of magnitude for different compositions of the same constituents. The rates of chemical reactions are strong functions of temperature, so the etch rates using wet, or chemical, etchants should be functions of temperature as well. For example, the etch rate of silicon dioxide in a 6:1 Buffered Oxide Etch (BOE) can change by a factor of two for a 10°C change in temperature [10.2].

Etch rates also depend on the composition and density of the films. For example, the etch rate of undoped, undensified CVD silicon dioxide in BOE is about 5 nm sec^{-1}, while the etch rate of phosphorus doped (8 atomic %) CVD silicon dioxide is about 9 nm sec^{-1}. On the other hand, the etch rate of densified (annealed at 800–1000°C), undoped CVD silicon dioxide is only about 1.5 nm sec^{-1}, the same as for thermal oxide. Clearly, the composition of the etchant and film, the density of the film, and the etch solution all affect the wet etch rates significantly.

The etch rate can also depend on the crystallographic orientation in some cases. In Table 10–1, the etch rates for two crystallographic directions in Si using KOH are given.

Micron Ex. 1022, p. 24
Micron v. YMTC
IPR2025-00294

One sees that the etch rate for this etchant in the [100] direction is much faster than in the [111] direction, because the (111) planes are the most closely packed and etch more slowly. This can be used to form v-grooves on the surface of a (100) Si wafer because the {111} planes intersect the surface at a 54.7° angle.

10.2.2 Plasma Etching

While wet chemical etching was successfully used in the early days of integrated circuit manufacturing, it has been largely replaced by plasma, or dry, etching. There are two main reasons for this.

The first reason is that very reactive chemical species are produced in a plasma which can often etch more vigorously than species in a nonplasma environment. One of the first widespread uses of plasma etching was in the early 1970s to etch PECVD silicon nitride, used as the final passivation layer in integrated circuits. This film is difficult to etch with wet chemical etchants. Wet HF can etch it, but the etch rate is quite low, and the process is not selective with respect to SiO_2 which is often underneath. Boiling phosphoric acid was commonly used instead. But this etchant often lifts off photoresist masks so that a mask of SiO_2 has to be used, requiring its own masking and etching steps. A better etch process was sought. It was soon discovered that by using a CF_4/O_2 gas mixture in a plasma atmosphere, atomic fluorine is produced which can etch the nitride film much more easily. In addition, a photoresist mask is not lifted off in this process, making the process much simpler.

The second, and more important, reason why plasma etching has supplanted wet etching is the fact that directional or anisotropic etching is possible with plasma etch systems. Directional etching is needed to minimize undercutting and etch bias, which then allows smaller and more tightly packed structures. This directional etching is due to the presence of ionic species in the plasma and the electric fields that direct them normal to the wafer surface.

Plasma etch systems can be designed so that either the reactive chemical components or the ionic components dominate. In many cases, a combination of ionic and reactive chemical species, usually acting in a synergistic manner, are utilized. The net etch rate can be much faster than the sum of the individual etch rates when they are acting alone. In addition, by utilizing both components this way, directionality can be achieved while maintaining an acceptable degree of selectivity.

A basic plasma etch system is shown schematically in Figure 10–7. This is similar to the PECVD and RF sputtering systems shown earlier in Figures 9–14 and 9–28. In these etch systems a low-pressure (1 mtorr – 1 torr) gas is used in the chamber. By applying a high electric field across two electrodes, some of the gas atoms are ionized, producing positive ions and free electrons and creating a plasma, as discussed in Chapter 9. In plasma etching systems, the energy is supplied by an RF generator, usually operating at 13.56 MHz. As we saw in Chapter 9, a voltage bias develops between the plasma and the electrodes. This is due to the difference in mobility of the electrons and the ions. Initially, the more mobile electrons are lost to the electrodes at a faster rate than the slower ions. This results in the plasma being biased positively with respect to the electrodes. For a symmetric RF plasma system, with the two electrodes of equal area, the

Micron Ex. 1022, p. 25
Micron v. YMTC
IPR2025-00294

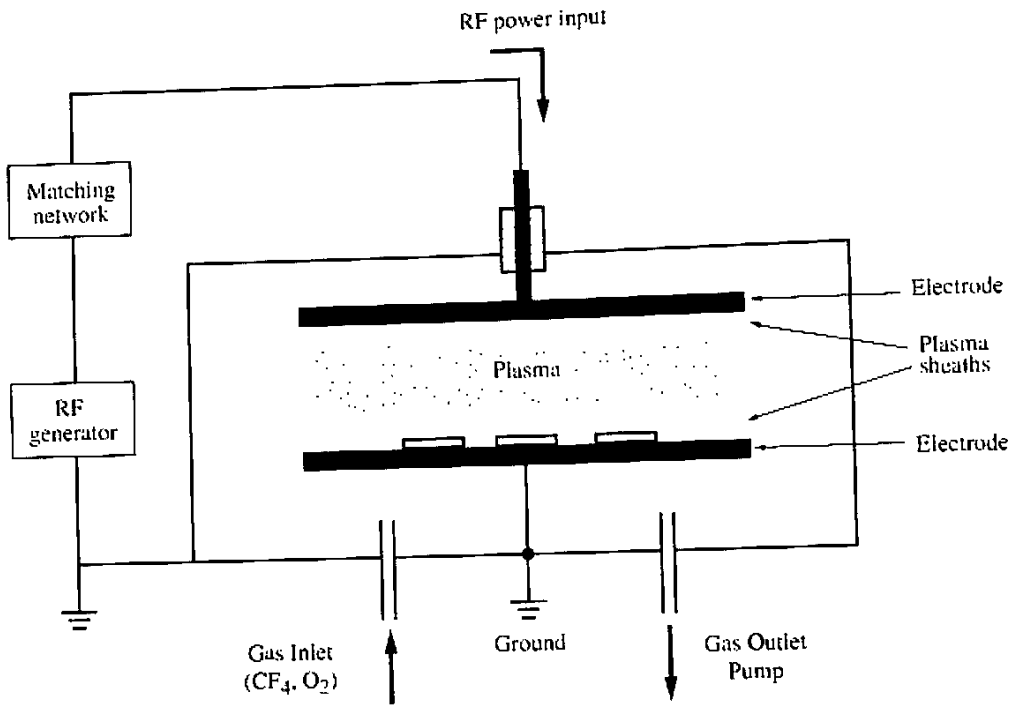


Figure 10–7 Schematic diagram of an RF-powered plasma etch system.

voltage distribution that develops is shown by the solid curve in Figure 10–8 (repeated from Figure 9–29). The sheaths are the regions next to each electrode where the voltage drops occur and correspond to the dark regions of the plasma.

The sheaths form to slow down the electron loss so that it is equal to the ion loss per RF cycle and so the average current to the electrodes is zero. Whereas the heavy ions respond to the average sheath voltage, the light electrons respond to the instantaneous voltage. However, due to the self-biasing, they only cross the sheath during a short period per cycle when the sheath voltage and thickness are near their minimum. During most of the RF cycle the electrons are turned back at the sheath edge, resulting in the sheaths, on the average, being deficient or depleted of electrons. This depletion of electrons in the sheath results in the sheath being dark because of the lack of electron/atom collisions and subsequent relaxation by light emission. In the bulk of the plasma, both ionization and excitation events occur, the latter producing the characteristic glow of the plasma. The lack of electrons in the sheath also increases the impedance of the sheath compared to the plasma bulk resulting in the main voltage drop being across the sheaths. If one of the electrodes is made much smaller in area, then the voltage distribution becomes asymmetric with a much larger voltage drop occurring from the plasma to the smaller electrode, as shown by the dashed curve in Figure 10–8. As described in Chapter 9, this happens because the RF current density must be much higher at the smaller electrode in order to maintain current continuity throughout the system. Therefore the fields must be higher at the smaller electrode.

Micron Ex. 1022, p. 26
Micron v. YMTC
IPR2025-00294

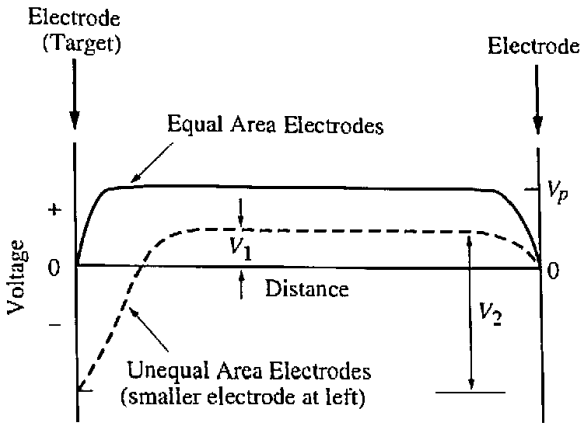


Figure 10–8 Steady-state voltage distribution in RF-powered plasma etch systems. (See Figure 9–27 and the associated text for a more complete discussion of this figure.)

For etching materials other than photoresist (for which O_2 is used) the reactant gases in the plasma are usually halide containing species, such as CF_4, Cl_2, and HBr. Sometimes small amounts of other gases, such as H_2, O_2, and Ar are also added. The high-energy electrons in the plasma can cause a variety of reactions to occur with the reactant gases, including electron-induced ionization, dissociation, recombination, and excitation reactions, as illustrated in Figure 10–9. The plasma will thus contain free electrons, ionized molecules, neutral molecules, ionized fragments of broken-up molecules, and free radicals. For example, in a CF_4 plasma, there will be electrons, CF_4, CF_3 (and other CF_X fragments), CF_3^+ and F. CF_3 and F are free radicals—very reactive species. Typically there will be about 10^{15} cm^{-3} neutral species (1 to 10% of which may be free radicals) and 10^8–10^{12} cm^{-3} ions and electrons. The actual numbers of the different species will depend on the balance between generation and loss or recombination reactions for each.

In standard plasma etch systems, the plasma density (the concentration of ions or electrons in the main plasma, which are virtually equal) and the ion energy as it travels across the sheath to strike the wafer are closely coupled. As the RF power increases, more ions are created, increasing the density, and the sheath voltage increases as well, increasing the ion energy. This coupling comes about because of the capacitive nature of the coupling between the RF current and the plasma [10.3].

10.2.2.1 Plasma Etching Mechanisms

The two main types of species involved in plasma etching are the reactive neutral chemical species and the ions. It is the reactive neutral species—free radicals in many cases, but sometimes other reactive species such as Cl_2—which are primarily responsible for the chemical component in plasma etch processes. It is the ions that are responsible for the physical component. They can work independently, or as we will see, they can work

Micron Ex. 1022, p. 27
Micron v. YMTC
IPR2025-00294

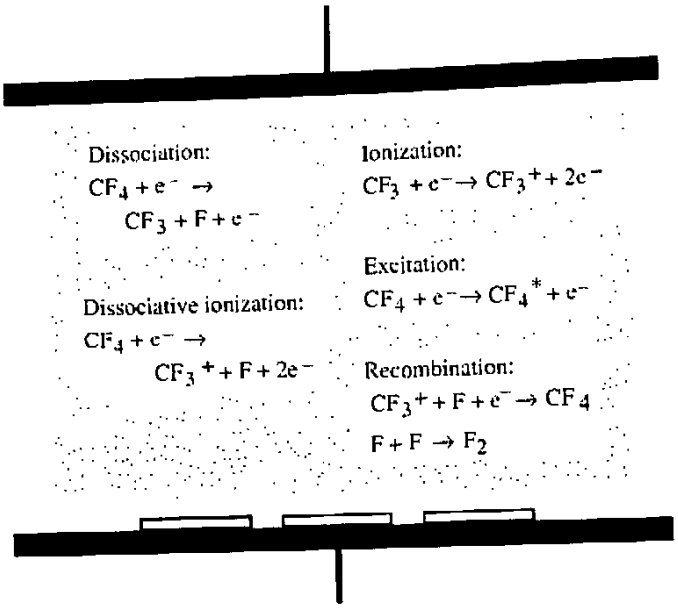


Figure 10–9 Typical reactions and species present in a plasma used for plasma etching.

together in a synergistic manner. When the reactive neutral species act by themselves, the process or mechanism is called chemical etching. Ions acting by themselves can result in physical etching, or sputtering. When the reactive neutral species and ions act in a synergistic fashion, this is called ion-enhanced etching. We will now describe each of these mechanisms.

Chemical Etching Chemical etching of materials in plasma systems is commonly done by free radicals. Free radicals are electrically neutral species that have incomplete bonding; that is, they have unpaired electrons. Examples are the fluorine free radical, F, and the neutral CF_3 free radical. Both of these can be produced by the reaction between free electrons in the plasma and CF_4, for example,

$$e^- + CF_4 \rightarrow CF_3 + F + e^- \tag{10.9}$$

Because of their incomplete bonding structure, free radicals are highly reactive chemical species. Free fluorine, with seven electrons in its outer shell instead of the energetically favorable set of eight, would much rather be bonded to other atoms so that all electrons are paired. It will therefore react quickly with other species to achieve that bonded state. The idea in plasma etching is for the reactive neutral species to react with the material to be etched, Si for example. The byproduct should be a volatile species

Micron Ex. 1022, p. 28
Micron v. YMTC
IPR2025-00294

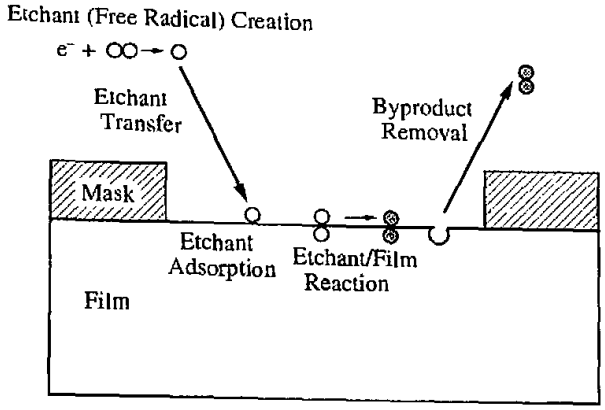


Figure 10–10 Processes involved in chemical etching during plasma etch process.

(that is, easily vaporized or evaporated into the gas phase) that leaves the surface, exposing more Si to be etched. This is illustrated in Figure 10–10. In fact, the fluorine free radical will react with Si via the reaction

$$4F + Si \rightarrow SiF_4 \tag{10.14}$$

to produce the gas SiF_4 (although there may be intermediate steps and species in that reaction). Thus a CF_4 plasma can be used to etch Si. It is important in etch processes that the byproducts of the etch, as well as any unreacted etchants, be removed from the surface for the etching to continue. Figure 10–10 shows a simple etch process, but more complex reactions may occur, involving multiple species and steps.

Gas additives can be used to increase the production of the reactive etch species and thereby increase the chemical etching rate. For example, oxygen is often added to a CF_4 plasma. The oxygen reacts with dissociated CF_4 species (CF_3 or CF_2, for example), which reduces the recombination of those species with F, thereby increasing the amount of free F. This enhances the chemical etching. However if too much O_2 is added, the etchant becomes too diluted or the surface is oxidized by the O_2, and the etching decreases.

We saw earlier that wet chemical etching occurs isotropically. The chemical component of plasma etching, when acting by itself, also occurs isotropically. Two factors lead to this behavior: an isotropic arrival angle distribution and a low sticking coefficient, with the latter usually more important. When we model and simulate plasma etching later in this chapter, we will closely follow the approach we used for deposition processes. That is, we will consider the incoming fluxes of species from the plasma to the wafer surface including the angular distribution of the various fluxes. This will be quantified by the $\cos^n\theta$ distribution, where a value of 1 for n describes an isotropic distribution (that is, coming in at all angles equally so that the normal component to the surface follows a $\cos\theta$ distribution) and a value of n larger than 1 describes a more directed distribution toward the surface. As in the deposition models we assume that all un-ionized

Micron Ex. 1022, p. 29
Micron v. YMTC
IPR2025-00294

chemical species arrive at the wafer surface at all angles. Since the free radicals are neutral species, the flux of the chemical component of plasma etching has an isotropic arrival angular distribution, or n equals 1.

We also consider the sticking coefficient of the species, as defined by Eq. (9.25), and repeated here.

$$S_c = \frac{F_{\text{reacted}}}{F_{\text{incident}}} \tag{10.11}$$

A high sticking coefficient (equal to 1) means that the reaction, and etching, occur the first time the species strikes the surface. A lower sticking coefficient means that before the species reacts, it can leave the surface—usually assumed to occur at a random angle—and strike the surface somewhere else. One might guess that free radicals would have very high sticking coefficients, since they are so reactive. However, as in deposition processes, the chemical reactions that occur in chemical etching often require multiple steps, and multiple atoms or species, all in the right proportions. In addition, the availability of suitable sites on the surface, competing reactions, and surface recombination of species can be issues. These issues result in most free radicals having effective sticking coefficients that are low, on the order of 0.01 to 0.05 for F etching of Si, for example. Thus the chemical etch species bounce around a lot and tend to maintain random angles of flight even under masks and other surface features. The fluxes for chemical species are illustrated in Figure 10–11(a).

These two properties of the reactive neutral species in plasma systems—isotropic arrival angles and low sticking coefficients—result in the fact that purely chemical etching acts in an isotropic or near-isotropic manner. Only if the sticking coefficient is relatively large would shadowing by the topography and etch mask become important. (Sticking coefficients on the order of 0.1 may actually occur for some purely chemical

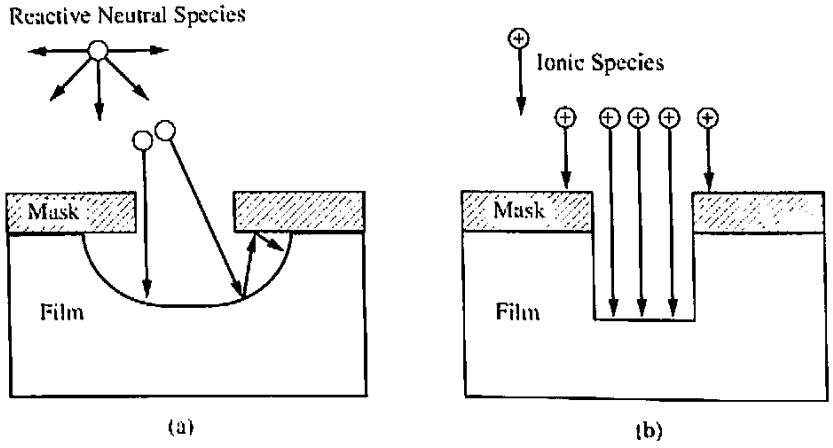


Figure 10–11 Fluxes of species in plasma etching: (a) fluxes of reactive neutral chemical species (such as free radicals), with a wide arrival angle distribution and low sticking coefficient; (b) fluxes of ionic species, with a narrow, vertical arrival angle distribution and high sticking coefficient (assumed equal to 1).

Micron Ex. 1022, p. 30
Micron v. YMTC
IPR2025-00294

plasma etching cases [10.4].) In that event somewhat more anisotropic etch profiles can result. In general, though, pure chemical plasma etching results in isotropic or near-isotropic etching. We must reiterate that this is only for the chemical component acting independently, or for a purely chemical etch process. As we shall see shortly, the reactive chemical species and the ions can work in a synergistic manner so that the etching is not isotropic at all.

Since free radicals etch by chemically reacting with the material to be etched, the process can be very selective, as discussed earlier for wet chemical etching. Thus any chemical component to plasma etching will be relatively selective, as compared to the physical component.

In some cases, reactive neutral species other than free radicals may be involved in chemical etching. An example is in the plasma etching of Al by the Cl_2 molecule. For the same reasons given above, these reactive neutral species would have the same etching properties as the free radicals, namely isotropic profiles and selective chemical etching.

Physical Etching The other main species that participate in plasma etching are the ions that are present. Because of the voltage drop between the plasma and each electrode and the resulting electric field across each sheath, positive ions will be accelerated toward each electrode. Since the wafers are placed on one of the electrodes, then the ionic species such as Cl^+ (or Ar^+ in a purely physical sputter etch system) will be accelerated to the wafer surface. This striking of the wafer surface results in the more physical component of etching. The flux of ions toward the wafer surface is much more directional than the flux of neutral free radicals because of the directionality of the electric field from the plasma to the surface of the wafer. Thus the etching will be much more directional and more anisotropic. In fact it is usually assumed that all the ions arrive normal to the wafer surface, as shown in Figure 10–11(b), meaning that n is very large in the $\cos^n\theta$ distribution. Because the ions etch by more physical processes, rather than chemical, the etching will be much less selective. It is also assumed that once each ion strikes the surface, it does not strike the surface again somewhere else (or if it does, it does not have enough energy to do anything). This means that the sticking coefficient is effectively one. This also leads to more anisotropic behavior.

Ions can etch material in plasma systems by physical sputtering. Sputtering was discussed in Chapter 9, where we saw how sputtering of elemental, compound, or alloy targets was utilized to deposit material on the surfaces of wafers. We also saw how sputtering of the wafer itself could be done during a simultaneous deposition of material in order to planarize or fill features. Sputtering occurs by ions, accelerated by an electric field, striking the atoms on the surface of a material and physically dislodging them. The sputtering process is often described by a sputtering yield defined in Chapter 9 as the number of atoms or molecules ejected from the target per incident ion and is a measure of the sputter efficiency. As discussed in Chapter 9, the sputter yield is a function of incident angle, and it is this property that allows for planarization and filling in bias-sputtering deposition techniques. Because of the physical nature of sputtering by ion species arriving normal to the wafer surface, very anisotropic etching occurs, with profiles similar to that shown earlier in Figure 10–3(c).

Micron Ex. 1022, p. 31
Micron v. YMTC
IPR2025-00294

When ionized reactive species such as Cl^+ and CF_3^+ are involved in sputtering, chemistry can also be important in determining the effective sputtering yield since these ions do have the potential of reacting chemically with surface atoms. Such effects can enhance the sputtering yield compared to Ar^+ sputtering, although the magnitude of these effects is usually small compared to ion-enhanced etching, which involves both neutral and ionized species and which we describe next.

Ion-Enhanced Etching Another way that ions participate in plasma etch processes is through ion-enhanced etching. It was recognized many years ago that the ions and reactive neutral species do not always act independently in an etch process. This was easily deduced when it was observed that the etch rate measured is not always just the sum of the two components acting independently; in many cases it is much higher. As a classic example of ion-enhanced etching, Figure 10–12 shows the etch rate of silicon as XeF_2 gas and Ar^+ ions are introduced to the surface. First XeF_2 gas (not a plasma, so there is no physical component at all) is introduced into the chamber and very little etching occurs. Then an Ar^+ ion beam is directed toward the surface and the etch rate increases ten times. Finally the XeF_2 gas is turned off so that only ion sputtering occurs, and the etch rate becomes almost zero. The chemical and physical species are obviously working in a synergistic manner.

This synergistic process is also demonstrated in the shape of the etch profiles that result. In ion-enhanced etching, both chemical and physical components are acting, but the profiles are not just a linear combination of isotropic chemical etching and anisotropic physical etching as illustrated in Figure 10–3(b). Instead, the profile for ion-enhanced etching is much more like the case for physical etching acting alone, as in Figure 10–3(c). If the chemical component in the etch system is increased, the vertical etching is increased but not the lateral etching, which is not what would be expected from chemical etching. In addition, the etch rate in many cases is much higher (>10 times) than that calculated from the measured ion flux assuming normal sputtering yields in the absence of neutral species; hence it is not likely that the observed plasma

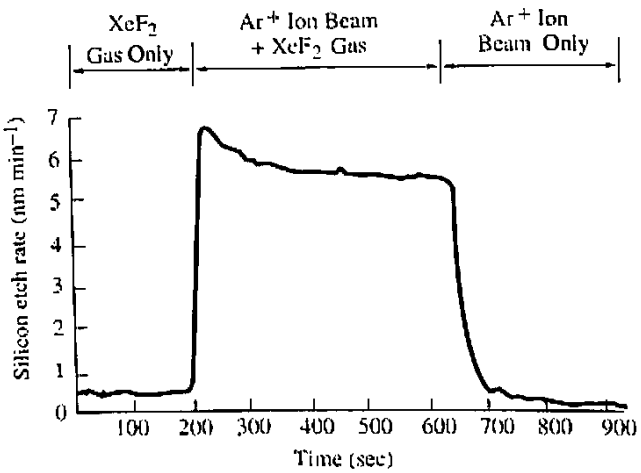


Figure 10–12 Etch rate of silicon as XeF_2 gas (not plasma) and Ar^+ ions are introduced to the silicon surface. Only when both are present does appreciable etching occur, illustrating synergistic etching behavior between chemical and ionic species. (After [10.5, 10.6].)

Micron Ex. 1022, p. 32
Micron v. YMTC
IPR2025-00294

etch behavior in these cases is due simply to an ionized chemical species, such as CF_3^+. Observed saturation effects, which we will describe later, also support this dual component model involving both neutral and ion species.

In this type of etch process, the chemical components (the free radicals or other reactive neutral species) and the physical components (the ions) in the plasma somehow work together to etch the material, with both components required at each point for the process to work. In addition, because of the required chemical component and the chemical processes that occur, good selectivity can be obtained. So not only can one achieve very anisotropic etch profiles, but also a high degree of selectivity as well. This is something that is very difficult to achieve when the two components work independently. In addition, high etch rates can be achieved. Thus gas chemistries and etch conditions are usually chosen to promote ion-enhanced etching and to suppress independent chemical and physical etching.

There have been many explanations and mechanisms proposed for this type of cooperative etch process. In most of the models the ion bombardment enhances one of the steps of the chemical etch process, such as surface adsorption, etching reaction and formation of byproduct, or removal of byproduct or unreacted etchant. For example, the ion bombardment causes damage (breaking bonds, etc.) which makes the surface more apt to chemically react with the radical. Or the ion bombardment accelerates the formation of volatile byproducts. Or the ion bombardment may dislodge or sputter away etch byproducts which would otherwise tend to stay on the surface and impede the etch process. The removal of byproducts can also include secondary, or indirect, byproducts. It has been found that a chemically inert residue is often formed from etching or sputtering photoresist. In addition, species from the plasma may deposit on the surface. These layers that are formed or deposited, whatever their source, inhibit chemical etching either by physically blocking the chemical etch species or by reacting with them and depleting them. But the inhibitors can be removed, or prevented from forming, by ion bombardment, leading to anisotropic etching. In fact, these inhibitors are often intentionally produced on the surface by providing sources in the gas which enhance their formation so that more directional etching is achieved. In a particular ion-enhanced etch process, one or more of the above mentioned mechanisms (damage induced, inhibitor removal, etc.) may be occurring.

Whatever the exact mechanism for ion-enhanced etching, and it is often difficult to distinguish between them, directional etching occurs because of the directionality of the ions. The enhancement of the process, whether of enhancement of etch reaction or of inhibitor removal, occurs only where the ions strike the surface. Since the ions are striking normal to the wafer surface, the enhancement will occur normal to the wafer surface. This directional enhancement will result in directional, anisotropic etching. This is illustrated in Figure 10–13(a) for the case when the chemical etch reaction is enhanced by ion bombardment. It is assumed in this figure that etching by the neutral (radical) species alone without ion bombardment, the so-called "spontaneous chemical etching," is negligible, leading to no lateral etching at all. In Figure 10–13(b) the process of inhibitor formation and removal is illustrated, which also results in anisotropic etching. Ion bombardment on the horizontal surfaces removes the inhibitor there but leaves the sidewall inhibitor to protect against lateral chemical etching.

Micron Ex. 1022, p. 33
Micron v. YMTC
IPR2025-00294

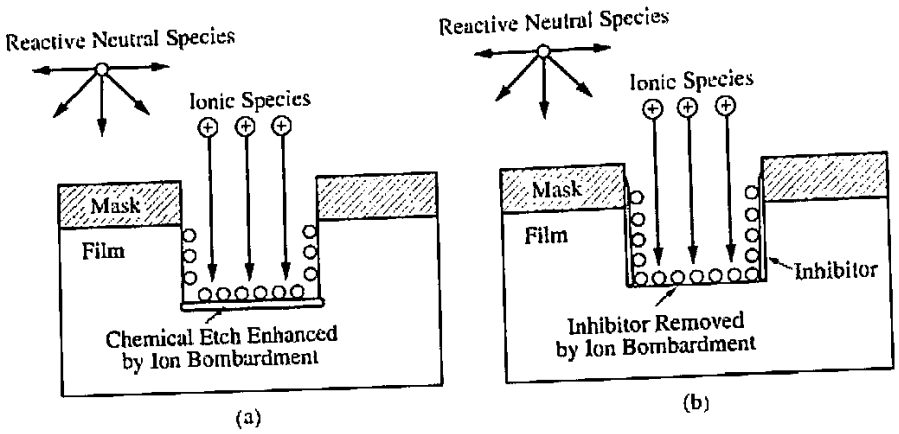


Figure 10–13 Illustration of ion-enhanced etching. In (a) the chemical etch reaction is enhanced by ion bombardment. In (b) an inhibitor is formed which is removed by ion bombardment, allowing chemical etching to proceed. In both cases, anisotropic etching results.

Even with ion-enhanced etching and no spontaneous chemical etching, the slope of the resulting sidewall may not always be exactly vertical. For example, the ion flux may not always be perfectly normal to the wafer surface and can result in slightly bowed sidewalls. Also, when inhibitors form or are deposited during etching, sloped sidewalls can result if the inhibitor formation or deposition rate is very high relative to the etch rate of the inhibitor and substrate, as demonstrated in Figure 10–14. Changing the relative deposition/etch rates by changing the etch chemistry or plasma conditions can be used, in fact, to tailor the desired slope if less than vertical sidewalls, without any undercutting, are desired in specific applications. But the important point still is that very anisotropic etching can be achieved when ion-enhanced etching is occurring.

Selectivity occurs in ion-enhanced etching because chemical reactions are involved in this type of etch process, and chemical reactions are by nature selective. To achieve the needed selectivity, one must choose the proper etchant gas (either F, Cl, or Br based, with or without oxygen or other species added, for example) and other etching conditions which favor the etching of the film over the mask material and the underlying films. With ion-enhanced etching, one can achieve good etch selectivity while still obtaining very directional etch profiles.

10.2.2.2 Types of Plasma Etch Systems

Different types of plasma etch systems and modes of operation have been developed to etch films in semiconductor structures which take advantage of the different species present in a plasma and the different etch mechanisms that can operate. We will now describe these different etch systems or modes, focusing on the advantages and disadvantages of each.

Plasma Etching in Barrel Etchers One of the earliest plasma systems developed was the barrel etcher, named because of its shape, and is shown in Figure 10–15. In this

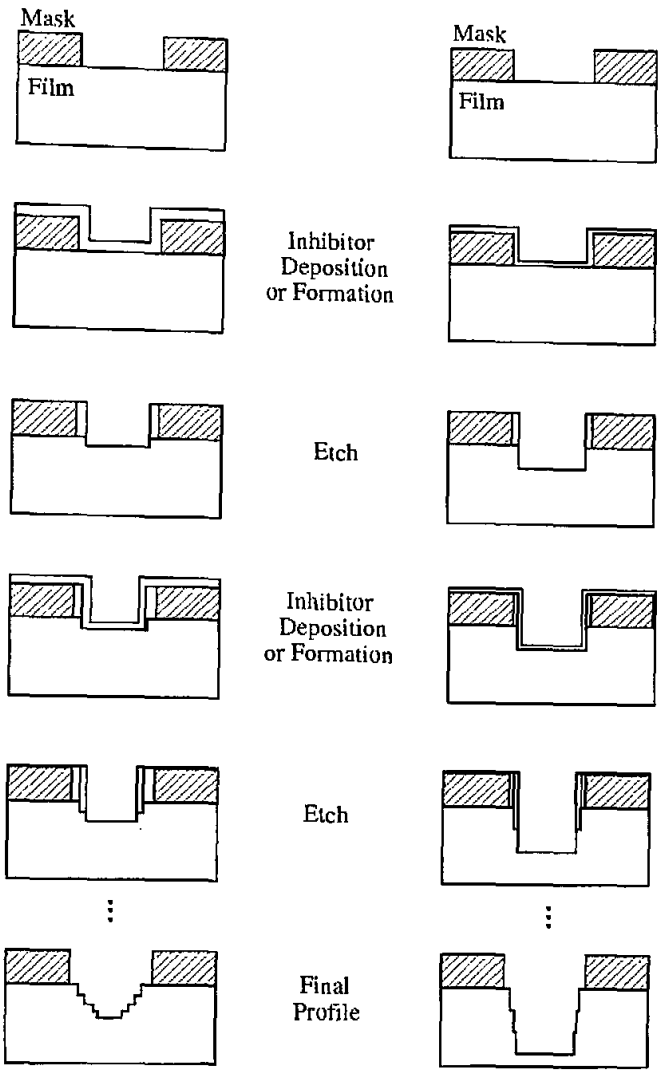


Figure 10–14 Illustration of the effect of the inhibitor deposition rate-to-etch rate ratio on the resulting sidewall slope. The different relative rates of inhibitor deposition and etch rate lead to different slopes of sidewall [10.4].

configuration, the electrodes are curved, wrapping around the quartz tube and the wafers are placed vertically in a substrate holder which sits in the middle of the tube. After evacuating the tube, reactant gases are introduced and RF power is applied to the electrodes. A plasma is generated but is kept away from the wafers themselves by the use of an etch tunnel, a perforated metal shield between the wafers and the electrodes. Reactant chemical species, such as F, diffuse from the plasma where they are generated, through the shield and to the wafers. There they can etch the wafers. Because the plasma and ions are kept away from the wafers by the shield, and the wafers do not sit

Micron Ex. 1022, p. 35
Micron v. YMTC
IPR2025-00294

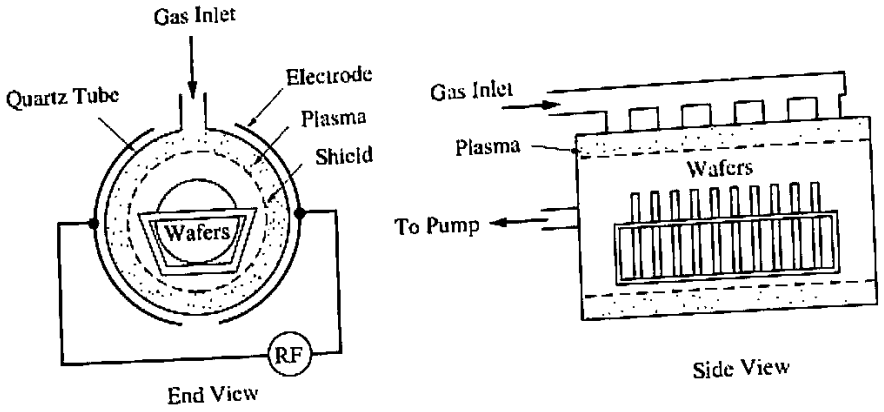


Figure 10–15 Schematic illustration of barrel etch system, in which purely chemical plasma etching occurs.

on either of the electrodes, no ionic bombardment of the wafers occurs. Thus the etching is purely chemical.

Because the etching is purely chemical, it can be very selective. It also causes very little damage to the surface because of the lack of ion bombardment. Also, it is a rather simple process and the throughput can be high with the closely stacked wafers. But because the etching is purely chemical, it is isotropic. This results in significant undercutting or mask bias. In addition, the etch uniformity across each wafer is not very good, especially from the outside of each wafer to the inside, because of the long diffusion path for the reactive species between the wafers.

As a result of the isotropic etching and nonuniformities, barrel etchers are used only for noncritical etch steps. In fact they are mostly limited to photoresist removal, using an O_2 plasma, where masking is not even done. This is called photoresist ashing, or just ashing, since the reaction between the oxygen and the hydrocarbon-based photoresist is the same as burning, producing CO_2 and H_2O. A long overetch is usually done in barrel etchers to compensate for the nonuniformities. This is allowable because of the high selectivity of the chemical etching processes used in these systems.

Similar to barrel etchers in principle but a little different in configuration are "downstream plasma etchers." Microwave or RF power can generate a plasma upstream in one chamber, while the wafers are placed in a separate but connected chamber "downstream" from the plasma. The neutral reactive chemical species can diffuse from the plasma in one chamber to the wafers in another, while the ions do not. Hence purely chemical etching occurs, resulting in good selectivity and little ion bombardment damage, but in isotropic etching. These are also called "afterglow etchers." These are also used for nonmasked etching steps, such as removing silicon nitride masks used for LOCOS processes.

Plasma Etching in Parallel Plate Systems—Plasma Mode Parallel plate etch systems, as shown earlier in Figure 10–7, are commonly used for plasma etching of films. This is very similar to the PECVD system described in Chapter 9, except that etch gases

Micron Ex. 1022, p. 36
Micron v. YMTC
IPR2025-00294

are used instead of deposition gases. Having this configuration with the wafers sitting on one of the electrodes and directly facing the other electrode gives much better etch uniformity than the barrel etcher design. In addition, it allows for the bombardment of ions on the wafer surface. The voltage distribution that develops from the RF source was shown in Figure 10–8. The voltage distribution is symmetric for equal area electrodes, with voltage drops across each sheath to the electrodes in the range of 10–100 V. As discussed earlier, this voltage drop accelerates the ions to the surface of the wafer, which is sitting on one of the electrodes. This results in a physical component to etching due to ion bombardment, as well as a chemical component due to the neutral reactive species. The physical component means that anisotropic etching is possible.

In symmetric parallel plate systems, with a gas pressure from 100 mtorr to 1 torr, the physical etch component is usually not very significant compared to other parallel plate configurations. In fact, the ion bombardment is even less since the bottom electrode is the grounded electrode in this setup. Since the chamber walls are also usually grounded and thus electrically connected to the bottom electrode, this effectively increases the size of that electrode. This means that the voltage drop from the plasma to that electrode is even smaller, as was shown in Figure 10–8 (the wafers would sit on the right side electrode for the dashed curve in that figure), and weaker ion bombardment would occur. One problem with etching in this mode is that with the large voltage drop to the top electrode, significant sputtering of that electrode can occur, causing contamination problems.

When the electrodes themselves are of equal area and the bottom electrode on which the wafers sit is grounded, making the effective size of the bottom electrode larger, then the etching is said to be operating in the plasma mode. Both chemical and physical components of etching are present in this mode, but as stated earlier the physical component is often rather weak, and highly directional etching is hard to achieve. However, the etching is still rather selective, and better uniformity and etch directionality are achieved compared to barrel etchers.

Plasma Etching in Parallel Plate Systems—Reactive Ion Etching Mode The parallel plate etch system can be modified to enhance the physical component of the etching by increasing the energy of the ions bombarding the wafers. This is achieved by having the electrode on which the wafers sit be smaller than the other electrode. Not only can the lower electrode be made physically smaller than the upper electrode, but the upper electrode can be the one that is grounded and electrically connected to the chamber walls. This makes the upper electrode effectively much larger. The bottom electrode is now much smaller than the upper electrode, and the voltage distribution is as shown in Figure 10–8, with the wafers on the left-hand side in this case. A much larger voltage drop occurs from the plasma to the wafers, in the 100–700 V range, resulting in more energetic ion bombardment of the wafer. With stronger ion bombardment, more directional etching can be achieved.

When the wafers sit on a smaller electrode, the etching is said to be operating in the Reactive Ion Etching or RIE mode. A better name for this might be "reactive and ion etching," since two types of species, the neutral reactive species and the ion species, are involved. In the RIE mode, both the physical ion component and the chemical reactive neutral component are important. They can act separately, but as we described earlier,

Micron Ex. 1022, p. 37
Micron v. YMTC
IPR2025-00294

gas chemistries and etch conditions are usually chosen so that they act together in a synergistic manner.

Even more directional etching can be attained by lowering the gas pressure. A lower pressure means fewer ion collisions during transit across the sheath in the gas phase, resulting in a more directed ion flux toward the wafer. Decreasing the pressure also increases the sheath voltage (that is, the voltage drop from the plasma to the wafer), which increases the ion energy. But decreasing the pressure can also decrease the plasma density (fewer gas atoms available to be ionized or converted into radicals), so that the pressure cannot be lowered too much. Reactive ion etch systems generally operate in the 10–100 mtorr range.

RIE systems can look very much like parallel plate plasma mode etchers (Figure 10-7) except that the RF power is supplied to the other electrode (to the bottom wafer holding electrode so that the top electrode is grounded with the chamber). and the size of the bottom electrode in the RIE case may be somewhat smaller. Single-wafer systems are often used for better control over each wafer. To increase the batch size other configurations have been used historically, such as with several electrode pairs stacked vertically above one another in a single chamber. Magnetic fields are often added to enhance plasma density and lower operating pressures.

Vertical RIE systems have also been developed. Here the wafers sit vertically against the inside electrode, which is often hexagonally shaped—hence the name, hexode batch etcher. The outside barrel chamber acts as the outer electrode. With its large size compared to the inner electrode, etching in the RIE mode can occur. Triode systems have also been developed. These are similar to the bias-sputtering systems discussed in Chapter 9, and add a second separate RF power supply to control the bias of the wafers. This separates plasma generation from ion energy, the latter being determined by the wafer bias. However, this independent control is only partially achieved using this technique with two capacitively coupled sources, and the plasma can suffer from nonuniformity. Also, the additional internal electrodes can cause contamination problems.

Operating in the RIE mode results in stronger ion bombardment than in the plasma mode, and a more physical component in the etching. While this leads to more directional etching, the higher enegy ions striking the surface can cause radiation or lattice damage, charging, and trenching. These will be discussed in more detail later. In addition, the higher physical component can lead to less selectivity. However, by choosing proper etch chemistries and utilizing ion-enhanced etching, an acceptable degree of selectivity can be achieved in these systems while still being able to etch material with excellent dimensional control. As a result, RIE etching is used extensively in the integrated circuit industry.

Etching in High-Density Plasma Systems A new type of plasma etch system that is becoming more popular is the High-Density Plasma (HDP) etch system. Like triode RIE etchers, these systems separate the plasma density and ion energy by using a second excitation source to control the bias voltage of the wafer electrode. But instead of using two capacitively coupled RF sources as in the triode systems, a different type of source for the plasma is used. The plasma generation source is non-capacitively coupled and produces a very high density plasma ($10^{11} - 10^{12}$ ions cm^{-3}) without itself generating a large sheath bias, utilizing a variety of methods. These include Electron Cyclotron

Micron Ex. 1022, p. 38
Micron v. YMTC
IPR2025-00294

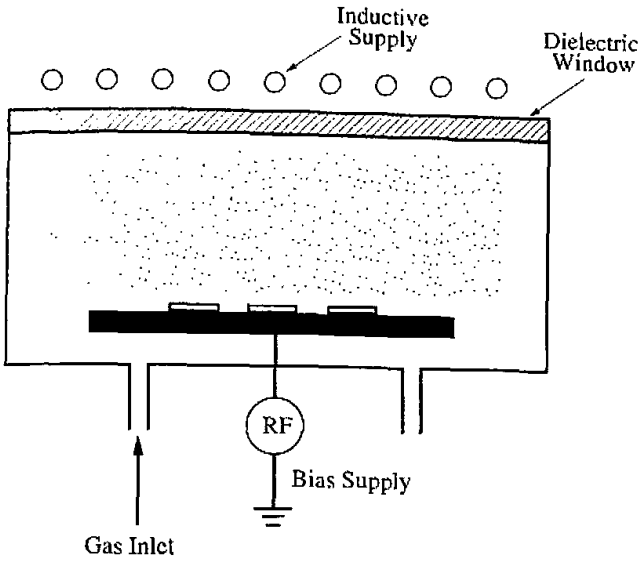


Figure 10–16 Schematic diagram of High-Density Plasma (HDP) etch system. This configuration is powered by an Inductively Coupled Plasma (ICP) source which produces and controls the high-density plasma. The RF wafer bias independently controls the ion energy.

Resonance (ECR) and Inductively Coupled Plasma (ICP) sources. The ICP method is becoming popular due to its much simpler design and equipment. A schematic diagram of an ICP high-density etch system is shown in Figure 10–16.

HDP etch systems are similar to the HDPCVD deposition systems described in Chapter 9. In those systems, the high-density plasma is produced using the same type of power sources, producing the reactive species for deposition as well as ionic species. A separate power source is used to bias the wafer in order to control the ion bombardment on the surface that is used for simultaneous biased sputtering. In Figure 9–45 in Chapter 9 we illustrated an ECR-powered HDPCVD system, which would be similar to an ECR HDP etch system. Similarly, an ICP high-density plasma CVD system would be very similar to the etch system shown in Figure 10–16.

In HDP etch systems, very high plasma densities are produced compared to standard RIE etch systems. Therefore lower pressures can be utilized, in the 1–10 mtorr range, while still achieving high ion fluxes and etch rates. A lower gas pressure means that even more directed etching can be achieved because of fewer gas-phase collisions in the sheath. In standard RIE systems, increasing the power increases the plasma density (and ion flux), allowing for higher etch rates, but also increases the sheath bias and ion energy, leading to more substrate damage. One could raise the pressure in standard RIE systems to produce a higher ion density while keeping the ion energies low, but the etching would become more isotropic due to more gas phase collisions in the sheath. In HDP systems, with the decoupling of the plasma density and ion energy, many ions can be produced at low pressures with low ion energies. As a result, ion bombardment damage can be kept low while maintaining high etch rates and good anisotropic etching. In addition, a lower ion energy usually gives better selectivity than higher ion energy.

Etching in HDP systems is similar to etching in the RIE mode, with a large physical component due to the ions combined with a chemical component involving the reactive neutrals (although the ionized species may themselves also contribute an appreciable chemical component to etching in these systems [10.6]). Therefore both directional etching and reasonable selectivity are possible. But in the HDP systems, the ion flux is

Micron Ex. 1022, p. 39
Micron v. YMTC
IPR2025-00294

even higher than in standard RIE systems, resulting in higher etch rates at lower pressures. And the higher ion flux, along with the lower pressures, leads to even more directional etching. The separate power sources allow independent control of ion density and ion energy, providing more flexibility in the etch process.

Sputter Etching and Ion Milling The sputter etching and ion milling techniques are at the other end of the spectrum from purely chemical systems; these are purely physical etching methods. We discussed sputtering in detail in Chapter 9, in which sputtering of a target was done to produce species for deposition. We also described how simultaneous sputtering of a film being deposited can be done to help with planarization of the film as well as filling in high aspect ratio spaces or holes. In sputter etching, physical bombardment of films with chemically inert ions, such as argon ions, produced in a plasma is used to etch the film. Figure 10–17 shows an RF sputtering system. The size of the cathode is minimized relative to the anode, which includes the chamber walls, to maximize the ion bombardment. The ion energies in these systems are large, greater than 500 eV, in order to get appreciable etching of films. While these systems are not normally used to etch thin films today, they do illustrate some important points about physical etching, and they have been used in the past.

The main advantages of sputter etching are that all materials can be etched this way and the etching is very directional, or anisotropic. The principle disadvantage is that selectivity is poor because little or no chemistry is involved. The sputtering rate, which is the same as the etch rate, depends on the sputtering yield. This is the efficiency of dislodging or removing an atom from the sputtered material by each impinging ion. The sputter yields of most materials by argon ions are fairly similar. This means that most materials can be sputter etched with about the same efficiency and that this method can often be used when other etch methods do not work. But this also means that the selectivity will not be good. The best selectivity ratios achievable are only about two-to-one. The sputtering yield is usually a function of incident angle. This can lead to faceting, which can be good or bad depending on the desired topography. The fact that

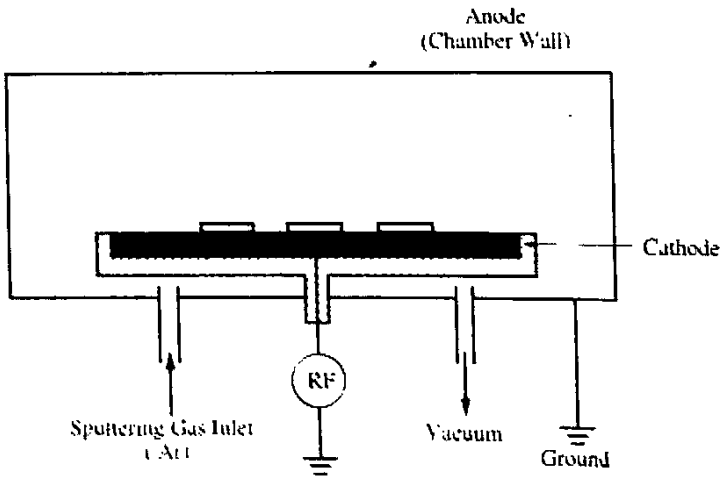


Figure 10–17 Illustration of sputter etch system.

all the etching is done by the highly directional ions means that highly directional etching can occur.

There are a few other problems associated with sputter etching. These would also be problems with any other method that utilizes energetic ion bombardment, such as reactive ion etching, but they are worse for sputter etching which is purely physical. One of these problems is called trenching, or "microtrenching." Along the sides of masking layers, some of the ions will glance off the sides and strike the films at the bottom corner. Hence these corner regions will receive a higher ion flux than if the sidewall were not there. This causes enhanced etching at the edges, resulting in trenches, as illustrated in Figure 10–18(a). Another problem is in redeposition. In a nonselective physical process other layers will be sputtered as well. These sputtered materials can be redeposited elsewhere, including in the region that is being etched. This is illustrated in Figure 10–18(b).

A third problem is lattice or radiation damage. During sputtering, the surface is subjected to bombardment of energetic ions, electrons, and photons. Ion bombardment can lead to displaced atoms and implanted atoms below the surface. Radiation damage can lead to electron traps being produced in gate oxides. Another problem is surface charging. This is associated with the bombardment of the wafer surface with charged ions and electrons. Because of nonuniformities that can exist in the plasma, dielectric materials can be charged by the local differences between ion and electron fluxes. This can lead to tunneling current damage to thin dielectrics. It can also lead to etch profile distortion. This is because the paths of the incoming charged ions will be affected by the presence of the charged regions, either positive or negative, as shown in Figure 10–18(c), and lead to uneven etching.

In ion milling, some of the problems associated with charged species are eliminated. In this technique, a confined plasma is used to generate a broad beam of Ar^+ ions. This is done by using a set of grids to extract and accelerate ions from the plasma chamber toward the target wafer to be etched. A separate electron source is used to supply electrons to neutralize the ion beam. This setup allows for more independent control over

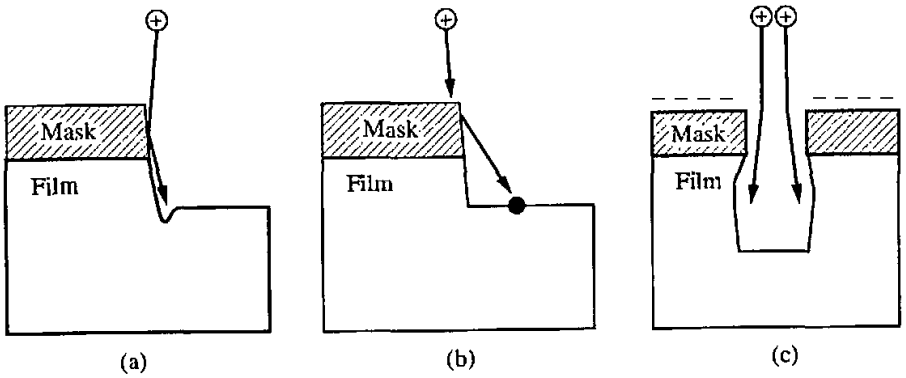


Figure 10–18 Problems associated with sputter etching (or any etching that has a high degree of physical/ionic etching): (a) trenching at bottom of sidewalls; (b) redeposition of photoresist and other material; (c) charging and ion path distortion.

Micron Ex. 1022, p. 41
Micron v. YMTC
IPR2025-00294

the ion energy and ion density, which are usually closely coupled in a normal plasma system. An amount of reactive species may also be added to, or replace, the Ar in ion milling systems. These species may include CF_4, CCl_4, or O_2. This will add some amount of selectivity to the process. This method is called "Reactive Ion Beam Etching," or RIBE.

Ion beams can also be focused and then used to sputter, or etch, very small areas. This is called the Focused Ion Beam (FIB) technique. It can be used in advanced lithography applications to expose/etch resist instead of electron beams. It is commonly used to repair masks. It can also be used to cut or etch regions of films and substrates to expose cross sections for observation. The ions in this are often He^+, N^+, Ar^+, Xe^+, and most commonly Ga^+.

10.2.2.3 Summary of Plasma Systems and Mechanisms

Figure 10–19 summarizes the different types of plasma etch systems in terms of some of the operating and etch properties. Of course there are wide variations in the properties for different types of systems, and overlaps occur between the different types of etching. For example, the ion energy in HDP etch systems can be the same or lower than in RIE systems, and the selectivity can be better as well. And the selectivity in both HDP and RIE systems can be very good while still achieving anisotropy by choosing the right etch chemistries and utilizing ion-enhanced etching. But the basic trends shown are useful in understanding the differences in the various types of plasma etching systems.

Figure 10–20 summarizes some of the different etch processes that occur in plasma etching which affect the two-dimensional etch profile. Not all the processes would occur simultaneously of course—inhibitor formation and trenching would not just occur on one side with undercutting on the other, for example, but the figure does illustrate the many complex phenomena that can occur during plasma etching.

We have described the similarities between etching and deposition systems several times. PECVD systems are similar to parallel plate etch systems operating in the plasma

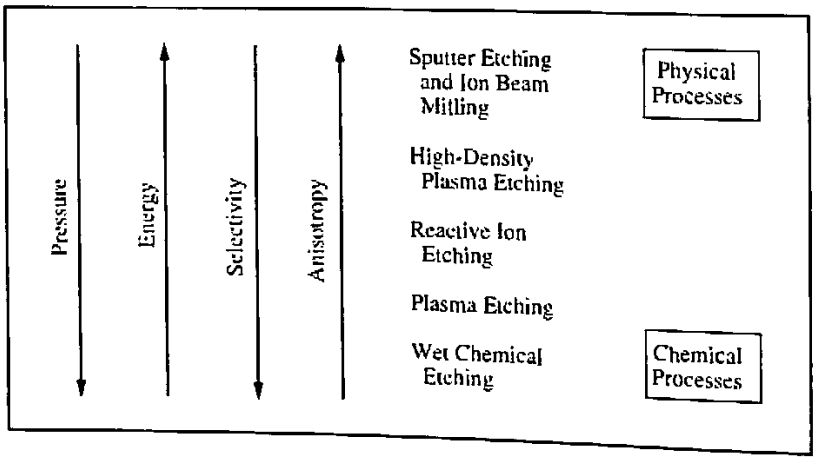


Figure 10–19 Summary of trends of different etch systems.

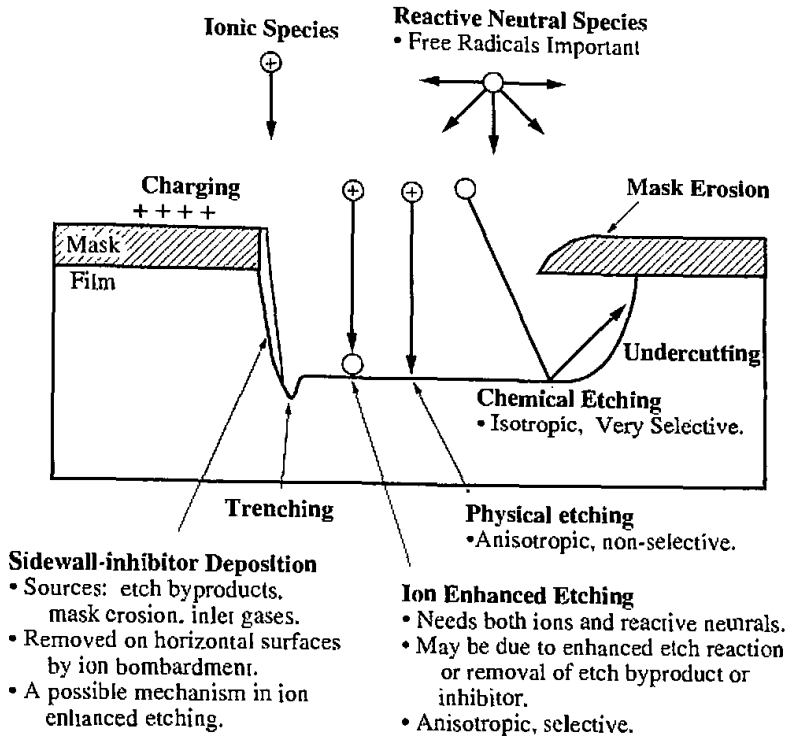


Figure 10–20 Summary of different processes occurring in plasma etching. (After [10.4].)

mode. There are reactive neutral species for either deposition or etching, with a minimum of ionic bombardment in either case. There are also similarities between deposition systems that utilize wafer sputtering, such as bias-sputtering and HDPCVD systems, and reactive ion and HDP etch systems. Bias-sputtering and HDPCVD deposition systems combine deposition of materials and sputter etching of the surface. Both of these processes also occur in reactive ion etching and HDP etching systems. Etching of the wafer surface is done using ion bombardment as well as chemical processes. But "deposition" is also commonly done in these etch systems in which inhibitor layers are "deposited" on the surface to promote anisotropy. These inhibitors form from byproducts of the etch process and the chemistry of the etch gases is often chosen to enhance their formation. This is called inhibitor deposition. So both deposition and etching occur in these deposition systems and etch systems. It is only the degree and type of deposition or etch that is different in specific systems. Many of the same concepts and models apply to both.

10.3 Manufacturing Methods

In this section we will describe some of the specific manufacturing methods used in plasma etching and some of the important issues related to manufacturing. We will limit ourselves to plasma etching here because of its dominance in current integrated circuit

Micron Ex. 1022, p. 43
Micron v. YMTC
IPR2025-00294

manufacturing. Limited information on wet chemical etching was given in Table 10–1. Most films in current semiconductor manufacturing are etched using parallel plate plasma systems in the RIE mode or using HDP systems.

10.3.1 Plasma Etching Conditions and Issues

The main parameters that can be directly controlled during plasma etching in standard parallel plate etch systems are RF power, pressure, gas compositions, and flow rates. (Some systems allow control of the self-bias, or sheath voltage, and the RF power is adjusted so that a particular bias is achieved.) Power densities of 0.1 to 5 W cm^{-2} are commonly used in parallel plate, capacitively coupled RF plasma systems, usually at 13.56 MHz with excitation voltages of 100–1500 volts RMS. Increasing the RF power increases the plasma density. In standard parallel plate systems, increasing the RF power also increases the self-bias or sheath voltage, which is the voltage drop between the plasma and the electrodes. This increases the ion energy. Ion energies produced are in the 10- to 700-eV range. Higher ion energy results in a higher sputtering yield which results in a higher physical component of etching but can also result in more surface damage.

In HDP systems, with separate power sources for the plasma and wafer bias, one can achieve high plasma densities and high fluxes, without necessarily getting high ion energies. In those systems, the power density on the wafer is in the 0.1–3 W cm^{-2} range. The resulting ion energies can range from 10 to 500 eV. A higher source power is used to generate the plasmas, in the 3- to 10-W cm^{-2} range.

The pressure in plasma etching systems ranges from 1 mtorr to 1 torr, with standard RIE systems operating in the 10- to 100-mtorr range and HDP systems in the 1- to 10-mtorr range. Increasing the pressure causes more gas-phase collisions to occur, decreasing the directionality of the etching. Increasing the pressure also increases the plasma density (since there are more atoms or molecules to begin with), but only up to a point. Above a certain pressure, depending on the etch system and operating parameters, the collisions between the gas molecules and electrons limit the energy of the electrons and thereby limit the ionization rate. Thus the plasma density decreases at higher pressures. In addition, increasing the pressure lowers the sheath voltage [10.7], thereby lowering the ion energy.

The etch rate, to first order, is proportional to the flux of active species, which would be the neutral chemical species and the ionic species. The flux of ionic species equals its concentration times its velocity. In plasma systems, increasing the power increases the plasma density and therefore increases the ion concentration in the plasma. The ion velocity in the plasma (by the electron temperature in the plasma) does not change to first order with a change in power at the sheath edge and determined. (The velocity across the sheath does increase as the power is increased in a parallel plate system, or as the wafer bias power is increased in a high-density plasma system. But the concentration of ions decreases proportionally across the sheath, so as to keep the flux constant across the sheath [10.11].) Thus the ion flux, being equal to the product of the ion concentration and velocity in the plasma at the sheath edge, would increase with power. The effect of increasing the pressure on the ion flux is less clearcut, and different systems show different relationships.

Micron Ex. 1022, p. 44
Micron v. YMTC
IPR2025-00294

The etch rate due to the ion component would be proportional to the ion flux, as well as to the sputtering yield, or the effective sputtering yield in ion-enhanced processes as we will discuss later. The effective sputtering yield itself can be dependent on ion energy (approximately proportional to the square root of the energy), which for parallel plate systems would be dependent on the RF power. In parallel plate systems, increasing the RF power increases the ion energy which increases the sputtering yield. Likewise, increasing the pressure can decrease the ion energy and sputter yield, decreasing the etch rate with pressure. In HDP systems, one can change the ion energy and thus the sputtering yield, independent of the plasma density and flux, by changing the separate bias voltage control. One can thus increase the physical etch rate by directly increasing the bias voltage.

One might assume that the chemical flux would be increased by increasing the power, which would increase the plasma density, and the generation of reactive neutral radicals. However, perhaps due to the complex chemistry occurring, this is not often observed. Generally the chemical flux increases with pressure. Thus the etch rate which depends on this flux generally increases with pressure. The behavior of the overall etch rate as a function of pressure can get quite complicated when the etching depends on both the chemical and ion components. A more detailed examination of chemical and ion fluxes and how they relate to the etch process will be given in the models and simulation section. In general, decreasing the pressure too far—below about 10 mtorr for standard RIE systems and about 1 mtorr for HDP systems—will result in too low a plasma density and too low an etch rate for practical purposes.

The gas composition—which gases are used and in what proportions—and flow rates can also be controlled and are used to help achieve the desired etch properties. We will discuss different gas compositions used to etch various films below. The flow rate often has a minor effect on etch rate. Increasing the flow rate will initially increase the etch rate by producing more reactive species. But the actual supply of reactant species depends on the balance between generation and loss of species in the plasma, and a steady state is reached where the etch rate will become independent of gas flow. If too high a flow rate occurs, the etch rate may actually decrease since the residence time of the gas may become less than the lifetime of the active species produced in the plasma.

Usually the temperature of the etch system, including the wafer, is not intentionally raised during etching. The plasma supplies the energy for the etch process and heating the gas or wafer would not significantly increase the etch rate or improve the process. An exception to this is in aluminum etching in which the system, including the chamber walls, is heated to 35–65°C to help keep the species volatile and assist in the removal of the byproducts. Without intentional heating, the wafers may still heat up due to the plasma processes and ionic bombardment—temperatures of 90–100°C can be encountered on wafer surfaces. It is important to control and minimize the temperature rise on the wafers. Sidewall inhibitor deposition actually decreases as the temperature goes up in most cases, resulting in less directional etching. The trend in recent years is for better control of temperature and removal of heat from the wafers by developing better wafer chuck systems, including electrostatic chucks, which uniformly extract heat from the wafers.

At the beginning of this chapter we mentioned several desired properties or qualities of etch processes. These included selectivity, etch profile control, uniformity,

Micron Ex. 1022, p. 45
Micron v. YMTC
IPR2025-00294

minimal substrate damage, and low contamination. We now consider how these issues relate to manufacturing concerns.

Selectivity involves the chemical component of etching. It is achieved primarily by choosing the particular chemical reactants, in the proper proportions, that favor the etching of one material over another. Changing the plasma conditions, such as the wafer bias and sheath voltage, can also affect selectivity in some cases. Achieving selectivity will be discussed later in the context of some common etch chemistries used for films in integrated circuit fabrication.

Etch profile control means obtaining the desired shape of the etch profile. For most applications in today's technology this means obtaining vertical, or near-vertical, sidewalls. Directional etching, either with ion-enhanced mechanisms or physical sputtering, is basically due to the ion or physical component and can be enhanced by increasing the ion directionality (by decreasing the pressure, for example), increasing the ion flux (by increasing the RF power, for example), or by increasing the effective sputtering yield (by increasing the RF power or bias voltage, for example). Less vertical or more sloped sidewalls may sometimes be desired—adequate filling or conformal deposition of subsequent layers may require a slightly sloped underlying topography. Producing less vertical sidewalls could be accomplished by reversing the above mentioned parameter trends. Sloped sidewalls can also be produced by allowing a certain amount of mask erosion to occur and using a tapered mask. While this allows the slope to become less vertical, it does so by increasing the width of the etched region, as we will show later in a simulation.

The etch profile can also be altered by changing the etchant gases. More vertical sidewalls can be obtained by using etchant gas species that have a lower spontaneous chemical component and which have appreciable etching only where there is ion bombardment, such as by ion-induced damage or byproduct removal mechanisms. One can also choose a chemistry that favors inhibitor formation. The inhibitor layer obstructs the spontaneous chemical etching and allows for ion-enhanced etching, resulting in very vertical etching. If the inhibitor forms too quickly relative to the etch rate, nonvertical sidewalls can result, as discussed earlier and illustrated in Figure 10–14. Figure 10–21 shows how the sidewall angle can be changed by changing the relative composition of C_2H_6 in the Cl_2/C_2H_6 etchant chemistry to etch polysilicon. Adding C_2H_6 increases the sidewall polymer formation (or "deposition") relative to the etch rate, causing the sidewall to be less vertical. In this manner, the etch profile can be tailored to the desired shape.

It is interesting that while plasma etching is rather insensitive to temperature, the deposition of an inhibitor layer often shows a negative activation energy with respect to temperature. In a plasma, the bond breaking and forming, which often limit film deposition, is rather temperature insensitive since most of the energy for this is supplied by the plasma energy and not thermal energy. However, the desorption of the deposited inhibitor layers increases with temperature, so that the net temperature dependence of inhibitor deposition is actually negative.

Etch uniformity means uniform etch rates across a wafer and from wafer to wafer. In batch systems, wafer-to-wafer uniformity involves the proper design of equipment so that the plasma and gas flows are uniform across the wafers in the system. Single-wafer systems have been developed to achieve better control over each wafer and to elimi-

Micron Ex. 1022, p. 46
Micron v. YMTC
IPR2025-00294

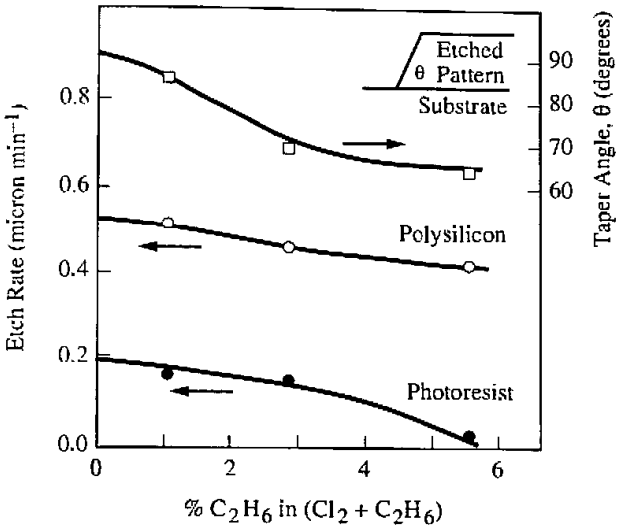


Figure 10–21 Etch rate of polysilicon and photoresist, and resulting taper angle as a function of C_2H_6 in Cl_2/C_2H_6 etch chemistry. More C_2H_6 results in more sidewall inhibitor formation and deposition relative to etching. (After [10.8].)

nate the wafer-to-wafer problems. Uniformity across a single wafer can still be a problem. Sometimes wafers develop "bulls-eye" patterns where the outside etches faster than the inside. This is usually due to depletion effects as the gas flows from the outside of the wafer to the inside.

Another kind of problem related to etch uniformity is called the "loading effect." There are two types of loading effects: macroscopic loading and microscopic loading. Macroscopic loading refers to the phenomenon in which more wafers in a chamber or more area exposed on a wafer to be etched results in a slower etch rate. This occurs because of the depletion of etchant species that occurs as the material is being etched. It is hard to predict to what extent this will occur due to the complex balance between species in the plasma and on the wafer surface. For the same reasons it is often difficult to control—increasing the flow rates does not always help.

Microloading occurs when etch rates vary over small distances on the surface of the wafer. This can occur when differences in the density of the unmasked area occur over small distances, resulting in differences in etch rates, just as in macroscopic loading. Microloading can also occur due to differences in aspect ratios. This effect is known as "Aspect Ratio Dependent Etching" or ARDE. It is also known as RIE "lag." As shown in Figure 10–22, the etch rate is different for different aspect ratios, with a lower etch rate for higher aspect ratio (smaller width) trenches. Different mechanisms have been suggested to explain this, each of which may be important under certain conditions. These include (1) depletion or trapping of the reactant species, or other conductance limitations, as the species travel to the bottom of the trench; (2) distortion of ion paths due to charging; and (3) shadowing effects involving either neutrals or ions. In the last case, collisions in the sheath may cause ions to be off-axis so that the number which reach the bottom is reduced due to simple geometrical shadowing. In each case, a narrower width decreases the chance that the reactant species, either ionic or reactive neutral, makes it to the bottom, thereby reducing the etch rate at the bottom. Etching at a lower pressure would reduce this effect if the shadowing mechanism were important, since reducing

Micron Ex. 1022, p. 47
Micron v. YMTC
IPR2025-00294

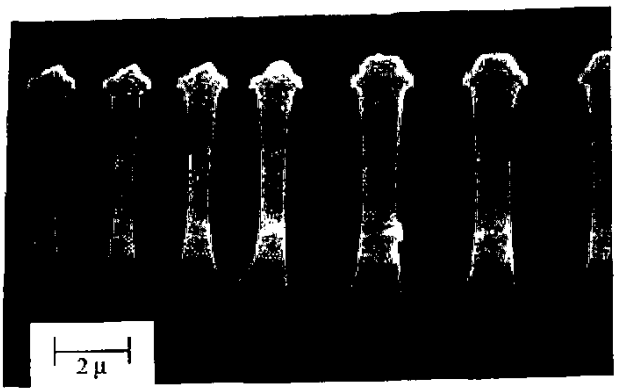


Figure 10–22 Example of Aspect Ratio Dependent Etching (ARDE) in silicon trench etching. The depth of etching decreases as the lateral feature size decreases [10.10].

the pressure would decrease the collisions in the gas phase and hence reduce shadowing effects. This is seen to be true experimentally [10.9] for some conditions, and we will simulate this later in the chapter.

Other uniformity issues involve differences in etching due to local variations in the film itself. The etch rate is a function of the density of the film, as one would expect, but also of the doping of the film [10.11]. Since these can vary locally across the film, the etch rate will vary as well.

Because of nonuniformities in the etch rate, and because the film itself may be of nonuniform thickness across the wafer or wafer to wafer, a certain amount of overetching is done to ensure that complete etching is achieved everywhere on the wafer. This is often 10–20%, in terms of time, past the endpoint detection. (*In situ* measurement and monitoring techniques, including endpoint detection, will be discussed in the measurement techniques sections.) Even more overetching may be required when anisotropic etching is done over nonplanar topography. Figure 10–23 illustrates this for purely vertical anisotropic etching of a conformally deposited film, where an additional time would be required to etch away the corner region. "Stringers" can results if strings of the material are left unetched at the bottom of the corner. Of course, this phenomenon can be taken advantage of in order to produce self-aligned spacers, as we discussed in Chapter 2 (Figure 2–30). In that case, no extra overetch would be done and the remaining oxide at the corner would be left as a spacer. The structure shown in the right side of Figure 10–23 would result, with the very narrow self-aligned spacer having a width approximately equal to the deposited film thickness.

Contamination and particulates can be reduced by reducing the pressure. Fewer contaminants are in the system and there is reduced polymerization of some etch species at lower pressures. Unwanted residues are often due to polymeric byproducts of the etch process. These can often cause problems with incomplete etching. If residues are left in contacts (or vias) after etching the contacts in a dielectric, high contact resistance can result. Reducing residue formation can be done by the proper choice of reactant gases. However, often polymeric formation is desired in order to achieve etch anisotropy, as discussed earlier, and gases are selected to promote such polymeric formation. In that case it is important to eliminate any unwanted residues from the etched surface following the etch process. Overetching can help remove residues in some situations. But in the

Micron Ex. 1022, p. 48
Micron v. YMTC
IPR2025-00294

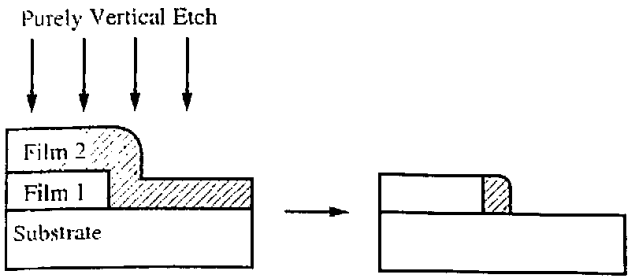


Figure 10–23 Overetching of a film over a step would be required to remove material at corner. In this example, completely anisotropic etching is assumed to emphasize this concept. This phenomenon can be used in producing self-aligned oxide spacers, in which no extra overetching is done so as to intentionally produce the structure at the right.

case of via etching, it may make it worse since sputtering of the underlying metal onto the sidewalls makes the sidewall residue harder to remove. One safe way to remove etch residues is by using a selective chemical etch after the plasma etch.

10.3.2 Plasma Etch Methods for Various Films

Most reactant gases for plasma etching contain halogens, generally Cl and F, and sometimes Br. Free radicals of these species can easily be produced in a plasma which can efficiently etch many films, and volatile etch products commonly result with these species. The exact choice of reactant gases to etch a specific film depends on a variety of factors, the most important being (1) etch selectivity to underlying films; (2) anisotropic etching; and (3) volatility of main etch byproducts.

Since in an etch process it is necessary to remove the byproducts from the surface, keep them off the wafer and pump them out of the system, the volatility of the main byproducts is an important consideration in choosing the gas chemistry. The volatility, or tendency to evaporate, depends on how tightly bound the species is to the surface. Table 10–2 lists the boiling points of typical etch products. The boiling point is an indicator of the volatility of a species—the lower the boiling point, the lower the surface binding energy and the higher the volatility. One can see that if Al is etched with a fluorine chemistry, AlF_3 would be the main byproduct. But the boiling point of AlF_3 (actually the sublimation temperature since it transforms directly from solid to gas without going through a liquid phase) is quite high at 1291°C. This means that the etch byproduct will be tightly bound to the surface with a very low vapor pressure, and even with ion bombardment it would be difficult to remove and keep off the surface. On the other hand, the byproduct of a chlorine-based etchant would be $AlCl_3$ with a boiling point (sublimation temperature again) of 177.8°C. This indicates looser bonding to the surface and a much more volatile species, so that a chlorine-based etchant would be a much better choice to etch Al. Having a volatile, weakly bound main etch byproduct is important when choosing an etch chemistry for a particular film. It is important to note that other, sometimes intermediate, byproducts may form during the etch process, and their removal or conversion to a more volatile species can be a rate limiting step in the etch process.

Table 10–3 lists some common chemistries used in plasma etching films in integrated circuit fabrication. These etchants are chosen mostly based on issues associated with byproduct volatility, etch selectivity, and etch profiles. The exact etch profiles and

Micron Ex. 1022, p. 49
Micron v. YMTC
IPR2025-00294

Table 10–2. Boiling points of typical etch products (After [10.12]).

Element	Chlorides	Boiling Point (°C)	Fluorides	Boiling Point (°C)
Al	$AlCl_3$	177.8 (subl.)	AlF_3	1291 (subl.)
Cu	CuCl	1490	CuF	1100 (subl.)
Si	$SiCl_4$	57.6	SiF_4	− 86
Ti	$TiCl_3$	136.4	TiF_4	284 (subl.)
W	WCl_6	347	WF_6	17.5
	WCl_5	276	WOF_4	187.5
	$WOCl_4$	227.5		

selectivities will depend on the specific system and plasma conditions. We will next discuss the plasma etching of three films, silicon dioxide, polysilicon, and aluminum, in a little more detail. In doing so we hope to illustrate some of the major issues involved in plasma etching and in choosing the etch chemistries.

10.3.2.1 Plasma Etching Silicon Dioxide

Fluorine-based chemistries are usually used to etch silicon dioxide. The volatility of the main etch product, SiF_4, is very high as indicated by its low boiling point in Table 10–2 and thus the SiF_4 can easily leave the surface via thermal desorption. Fluorine can etch the SiO_2 by reaction of the fluorine free radical, with the overall reaction given by

$$4F + SiO_2 \rightarrow SiF_4 + O_2 \tag{10.12}$$

CF_2 and CF_3 free radicals may also be directly involved in the case of fluorocarbon etchants, in which case CO-containing byproducts would also be produced.

Etching with a significant isotropic component can result using source gases such as NF_3, SF_6, CF_4, or CF_4/O_2 mixtures. CF_4 dissociates to form free F in a plasma via the reaction given in Eq. (10.9). As mentioned earlier, adding O_2 to the CF_4 gas significantly increases the F free radical production and hence increases the etch rate as well as makes the etch profile more isotropic. Too much oxygen, though, can decrease the etch rate due to dilution [or by reversing the reaction in Eq. (10.12) and redepositing oxide on the surface]. These gas sources with relatively high free F concentrations will etch the oxide; however, depending on the conditions, the etching can result in undercutting. In addition, the etch selectivity over silicon or polysilicon, which is often underneath the oxide, is poor. The anisotropy can be enhanced by increasing the ion bombardment and lowering the pressure [10.14], but the selectivity over silicon is still generally poor with these chemistries.

The key to making the etching of silicon dioxide very anisotropic as well as much more selective over Si is to reduce the amount of F free radical production and increase the carbon content. Doing so will decrease any spontaneous isotropic etching by free

Micron Ex. 1022, p. 50
Micron v. YMTC
IPR2025-00294

Table 10–3. Typical or representative plasma etch gases for films used in IC fabrication (After [10.1, 10.4, 10.13, 10.14].)

Material	Etchant	Comments
Polysilicon	CF_4	Isotropic or near isotropic (significant undercutting); fair to no selectivity over SiO_2.
	CF_4/H_2,	Very anisotropic; nonselective over SiO_2.
	CF_4/O_2, SF_6,	Isotropic or near isotropic; good selectivity over SiO_2.
	HBr, Cl_2, Cl_2/HBr/O_2	Very anisotropic; most selective over SiO_2.
Single-crystal Si	same etchants as polysilicon	
SiO_2	SF_6, NF_3, CF_4/O_2, CF_4	Can be near isotropic (significant undercutting); anisotropy can be improved with higher ion energy and lower pressure; poor or no selectivity over Si.
	CF_4/H_2, CHF_3/O_2, C_2F_6, C_3F_8	Very anisotropic; selective over Si.
	CHF_3/C_4F_8/CO	Anisotropic; selective over Si_3N_4.
Si_3N_4	CF_4/O_2	Isotropic; selective over SiO_2 but not over Si.
	CF_4/H_2	Very anisotropic; selective over Si but not over SiO_2.
	CHF_3/O_2, CH_2F_2	Very anisotropic; selective over Si and SiO_2.
Al	Cl_2	Near isotropic (significant undercutting).
	$Cl_2/CHCl_3$, Cl_2/N_2	Very anisotropic; BCl_3 often added to scavenge oxygen.
W	CF_4, SF_6	High etch rate; nonselective over SiO_2.
	Cl_2	Selective over SiO_2.
Ti	Cl_2, $Cl_2/CHCl_3$, CF_4	
TiN	Cl_2, $Cl_2/CHCl_3$, CF_4	
$TiSi_2$	Cl_2, $Cl_2/CHCl_3$, CF_4/O_2	
Photoresist	O_2	Very selective over other films

fluorine. The etching that then occurs involves other fluorine species and is strongly ion enhanced. In addition, polymer inhibitor formation will be increased, also suppressing lateral etching. Furthermore, selectivity over Si will be greatly enhanced.

One way to reduce the relative amount of F free radicals is by adding H_2 to the CF_4 gas. The hydrogen reacts with the fluorine to produce HF which reduces the amount of atomic F. Another possibility is to use more fluorine-poor and more carbon-rich gas species, such as CHF_3, C_3F_8, or C_2F_6. With fewer F free radicals, any spontaneous (non-ion-enhanced) chemical etching by these species is reduced. Appreciable etching happens only where ion bombardment occurs, perhaps involving an ion-induced damage or bond-breaking process, leading to anisotropic etching. CF_2 or CF_3 free radicals, rather than free F, are believed to be involved in the etch mechanism in these fluorine-deficient gas mixtures [10.14]. Increasing the carbon-to-fluorine ratio with these etchants also increases the amount of polymer inhibitor formed, or deposited, during the etching [10.6]. With a CF_4 or CF_4/O_2 gas, little or no polymer forms on the surface. However with a higher carbon concentration relative to fluorine in the gas mixture,

Micron Ex. 1022, p. 51
Micron v. YMTC
IPR2025-00294

more polymer formation will occur relative to etching. With a thick polymer inhibitor layer present, etching can not occur on vertical surfaces where there is little ion bombardment to remove the polymer inhibitor layer. Any lateral etching is suppressed, and near vertical sidewalls can result.

Of course, as even more carbon is added to the system and the deposition of the polymer becomes faster relative to the etching of the polymer and film, then sloped sidewalls (without mask undercutting) can result, as discussed earlier and illustrated in Figures 10–14 and 10–21. CHF_3 has a higher ratio of C to F than CF_4 does so that more polymer forms, in fact enough so that sloped sidewalls often result. If pure CHF_3 produces excess inhibitor deposition for particular plasma conditions, then O_2 could be added to react with the carbon and reduce the polymer deposition and change the etch profile. Other species such as CO_2 or CF_4 may also be added to CHF_3 for this purpose. Figure 10–24 conceptually illustrates the different etch profiles in SiO_2 that could result when different amounts of inhibitor formation occur.

Reducing the fluorine-to-carbon ratio also greatly improves the etch selectivity of SiO_2 over Si. This is because polymer formation preferentially occurs on Si surfaces compared to SiO_2 surfaces during the etch process. This may be due to the fact that carbon in the polymer reacts with the oxygen from the oxide, forming carbon monoxide, which results in much less accumulation of polymer on the oxide surface. With more polymer on the Si, its etching is slower, resulting in a higher SiO_2 to Si etch selectivity. Figure 10–25 shows how the etch rates of Si and SiO_2, and hence the selectivity, vary as H_2 is added to a CF_4 gas mixture [10.15]. The etch selectivities of oxide over $TiSi_2$ and TiN, which are important when etching contact or via holes in multilayer structures, are enhanced in this same manner by adding H_2 to the fluorocarbon etchant.

Changing the etchant chemistry may also change the etch rate of the mask. As seen in Figure 10–25, the etch rate of photoresist changes significantly as the H_2 content in the H_2/CH_4 gas mixture changes, with a lower H_2 content (and less F production) resulting in a higher etch rate. Adding O_2 to a CHF_3 mixture similarly increases the etch rate of the photoresist. The resulting mask erosion can cause the etch profile of the SiO_2 to change, as we will illustrate in the models and simulation section (Figure 10–33), and may alter the profiles shown above in Figure 10–24.

A relatively large bias voltage is often used for SiO_2 etching (in the 400- to 500-V range). This is needed to help remove the polymers. After the SiO_2 etching is complete, including a suitable overetch, any remaining polymer residue must be removed, espe-

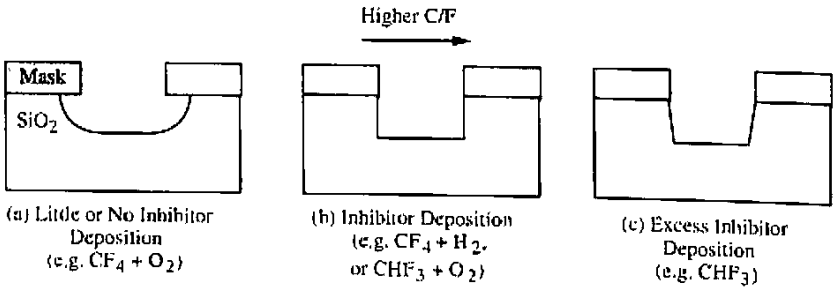


Figure 10–24 Effect of inhibitor deposition on resulting etch profile. The profiles shown assume no mask erosion, which may occur for different etch chemistries. The actual profiles obtained will also depend on the specific etch system and plasma conditions.

Micron Ex. 1022, p. 52
Micron v. YMTC
IPR2025-00294

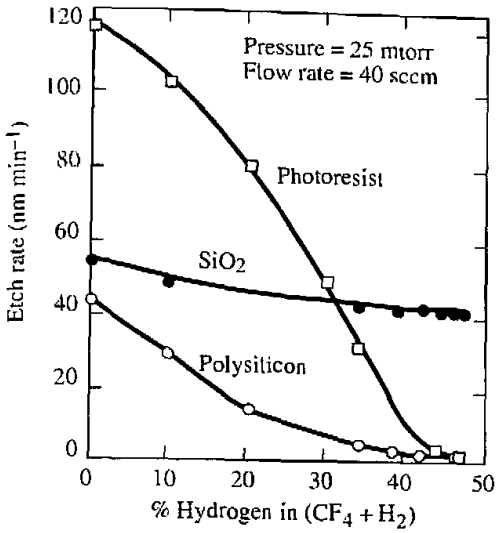


Figure 10–25 The etch rates of Si and SiO_2 (and photoresist) as H_2 is added to a CH_4 gas mixture. (After [10.15].)

cially in contact holes. The polymer can be removed by an O_2 or CF_4 plasma treatment. CF_4 is better at removing all the polymer and even some damaged substrate, but it cannot be over done since it has poor selectivity over Si and there can be lateral etching. A lower energy is used for the cleanup step so as not to damage the exposed material below. Also helpful is an anneal treatment; the polymer appears to break down at temperatures higher than $\approx 280°C$.

It should be clear from the discussion in this section that there are many details and subtleties associated with developing a particular manufacturing recipe for plasma etching. We will return to some of these issues in the models and simulation section.

10.3.2.2 Plasma Etching Polysilicon

The choice of etch chemistry for polysilicon depends on the same factors as etching silicon dioxide: byproduct volatility, selectivity, and anisotropy. Another issue is the presence of the ubiquitous native oxide layer on the film's surface, requiring an initial "breakthrough" etch step to remove it.

F-based etchants could be used for polysilicon etching because of the volatility of SiF_4. However, etching polysilicon with SF_6, CF_4, or CF_4/O_2 has a relatively large isotropic component due to the high concentration of F free radical species produced in such plasmas combined with little polymer formation. We saw that with etching SiO_2, anisotropy can be enhanced by reducing the relative F component and increasing the carbon component, thus decreasing the spontaneous etching, increasing polymer formation, and enhancing ion-induced etching. Adding H_2 to CF_4 can accomplish this. But doing so also increases the etch rate of SiO_2 relative to Si by preferentially forming a polymer on the Si. This is good when etching SiO_2 but bad when etching polysilicon when a high selectivity over the underlying SiO_2 is required. (Recall the structure in Figure 2–26 in the CMOS process flow in Chapter 2 for an example of why good selectivity over SiO_2 might be important.) Thus with a fluorine chemistry it is difficult

Micron Ex. 1022, p. 53
Micron v. YMTC
IPR2025-00294

to achieve both anisotropic etching and good selectivity of polysilicon over silicon dioxide at the same time.

If anisotropy is not important, then adding O_2 to CF_4 allows etching polysilicon with good selectively over silicon dioxide since the etch rate of the Si is increased by O_2 much more than that of SiO_2. But the etch will be fairly isotropic. One approach with fluorine chemistry when both anisotropy and selectivity with respect to an underlying oxide are desired is to switch the gas chemistry during the etching. One would start with an anisotropic etch, with a CF_4/H_2 mixture for example, and then when the etch is almost done, switch to an etch chemistry that is selective over SiO_2, using CF_4/O_2 for example. This will, however, result in some undercutting of the polysilicon.

Anisotropic and selective etching of polysilicon can be achieved simultaneously using Cl-based etchants. The byproduct volatility is a little lower with Cl than with F, but is still acceptable. Cl_2, HCl, or $SiCl_4$ can be used. These have a lower purely chemical component to etching than the F-containing etchants, and less lateral etching of Si occurs than with F. The etch rate in the vertical direction is significantly increased by ion bombardment, perhaps by surface bond breaking or by enhancing byproduct removal. Thus the etching of Si with Cl can be fairly anisotropic even without a polymer inhibitor layer present. Along with being anisotropic, the etch selectivity of Si to SiO_2 is high. For one thing, there is no polymer inhibitor layer that may form preferentially on the Si, as in the fluorine case, and degrade selectivity. Also, chlorine etches SiO_2 rather slowly. Furthermore, removing or minimizing the carbon in these systems is seen to significantly lower the etch rate of SiO_2 by chlorine—carbon evidently plays a role in the SiO_2-Cl etch reaction and enhances the etching at low carbon concentrations. Therefore the etch selectivity of Si to SiO_2 can be quite high, typically over 100, for these anisotropic, chlorine-based etchants. The anisotropy can be enhanced even more by adding a small amount of O_2. The O_2 reacts with the Si film, or with etch reaction byproducts that have adsorbed on the sidewall to form a nonpolymer, SiO_2-based inhibitor layer. The O_2 also helps with selectivity over oxide by removing any carbon that comes from photoresist erosion. Keeping the wafer temperature low, by providing helium backside heat conduction for example, also improves the anisotropy by enhancing inhibitor deposition.

Cl-based etchants exhibit a large doping sensitivity. High n^+ levels can increase the polysilicon etch rate by up to 25 times, and can increase the spontaneous etching and undercutting. An SiO_2-based inhibitor can block this. Cl-based chemistries etch the polysilicon slower than F-based chemistries, and mixtures of the two types have been used. The addition of SF_6 also reduces trenching. Trenching at gate edges can be a problem with chlorine etching, with the underlying gate oxide being damaged. Chlorinated flourocarbons, such as C_2ClF_5, have also been used for etching polysilicon but are out of favor since they are believed to cause environmental damage by depleting the ozone layer.

The most popular etchants used currently for polysilicon are chemistries based on bromine, the next halogen after F and Cl in the periodic table. HBr and Br_2 are commonly used. These act in a similar fashion to the Cl-based etchants, etching with a low purely-chemical component and without a polymer inhibitor, and are even more anisotropic and selective over oxide. Trenching of the underlying oxide is less of a problem as well. But the etch rates of Br-based chemistries are even slower than Cl-based

Micron Ex. 1022, p. 54
Micron v. YMTC
IPR2025-00294

chemistries, and they are often used in a mixture with Cl_2 in current polysilicon etch processes. As with etching with Cl, adding O_2 in these noncarbon containing gases promotes inhibitor formation, perhaps by forming SiO_2 from the Si film, and thereby increases the anisotropy. The O_2 also helps with selectivity over oxide by removing any carbon that might result from photoresist erosion. One drawback to the use of HBr and Cl_2 is their high toxicity which puts more stringent requirements on equipment and gas handling systems.

Polysilicon, like single-crystal silicon, usually has a small native oxide layer present on the surface, even after cleaning. This must be removed prior to etching. Since the etchants used for the main polysilicon etch have low-oxide etch rates, the etch must be initially modified to increase the oxide etch rate. This is called a breakthrough step. During the first 5 to 10 seconds of the poly etch, one can lower the selectivity with respect to oxide by adding an etchant such as CF_4 or by increasing the RF power to enhance the physical component of etching and etch the thin oxide layer from the surface.

An overetch step after the main etch is also important for polysilicon etching. This not only allows for deposition and etch nonuniformities, but also for the presence of stringers at steps, as discussed earlier and illustrated in Figure 10–23. This overetch step is often done at a lower RF power to increase the selectivity over oxide. A final postetch "cleanup" step is done to remove any sidewall layer material. While polymeric (carbon containing) layers would need an O_2 plasma strip, followed by an HF dip, inorganic layers usually need only an HF dip.

To produce shallow trench isolation structures, etching of the silicon is a critical process step as described in Chapter 2 (Figures 2–6 to 2–9). Achieving the desired etch profile and selectivity to mask layers is important, and many of the same ideas regarding polysilicon etching would apply. Using a Cl- or Br-based etchant can give good selectivity over silicon dioxide or silicon nitride mask layers and provide good anisotropy, as described above. Using Cl etchants alone can result in harmful ion-induced trenching at the bottom corners, so Br etchants are often used—either by themselves or in combination with Cl etchants. The slope of the etch profile can be tailored by including gas additives, such as O_2, to promote inhibitor deposition, and multistep etch processes may be utilized to achieve the desired profile.

10.3.2.3 Plasma Etching Aluminum

Plasma etching of aluminum interconnect lines has been a challenge for process engineers, but successful strategies have been developed to overcome the many problems associated with this film. Again, byproduct volatility, selectivity, and anisotropy are issues, as well as native oxide on the surface. In addition, a potential corrosion problem as well as Cu doping in the film lead to more difficulties.

Because of the presence of a native oxide, Al_2O_3, on the Al film surface, an initiation or breakthrough etch step must be done before the main Al etch step. Ion bombardment, or sputtering, is usually done to remove this film in conjunction with chemical scavenging. Argon sputtering can be used, but gases such as BCl_3, $SiCl_4$, CCl_4, or BBr_3 are often used to scavenge the O_2 and H_2O and remove Al_2O_3 on the Al surface by both physical and chemical means. A load lock system is required to control the H_2O level.

Micron Ex. 1022, p. 55
Micron v. YMTC
IPR2025-00294

The byproduct of etching Al with F-based chemistries, AlF_3, is not very volatile as discussed earlier, so that a Cl-based chemistry is most often used for the main Al etch step. Cl_2 is commonly used, and Cl_2 (not a free radical, but still a reactive neutral species) can directly etch the Al. However Cl_2 etches Al isotropically, producing an undercut, and ion bombardment has little effect on the etch rate (unlike the etching of Si by Cl_2). To suppress lateral etching of the Al and obtain vertical profiles, sidewall inhibitor formation is needed. Therefore inhibitor sources or promoters are often added to the gas mixture. These include $CHCl_3$, $CFCl_3$, CCl_4, and N_2. Resist erosion plays a significant role in supplying inhibitor material in Al etching, and N_2 enhances the inhibitor formation from photoresist, perhaps forming a CN polymer. BCl_3 also seems to promote inhibitor formation. The etch rate and selectivity over silicon dioxide are acceptable for Cl-based chemistries.

Al interconnect lines usually contain Si and Cu, which can complicate the etching. While Si is readily etched by Cl, Cu is not (the volatility of the Cu byproducts by halogen etching is quite low). Ion bombardment and often higher temperatures are needed. We will describe in Chapter 11 how Ti and/or TiN layers are often used above and below Al layers in the interconnects. These are usually etched at the same time as the Al, and Cl-based chemistries can readily etch them as well.

An overetch step is especially important for Al etching to remove the residues, both from the inhibitor layers and the Cu precipitates that can remain. The difficulty in Cu precipitate and residue removal depends on the Al deposition conditions, with a higher deposition temperature giving larger precipitates and more residues.

Corrosion of the etched Al line can be a problem when it is exposed to the ambient. Residual chorine on the sidewall and in the resist can react with water to form HCl. The HCl can then etch the Al. Cu in the films enhances this electrochemical reaction. It is important to passivate the Al film after the etching and before it is exposed to air. The wafer can be heated to 100°C or 150°C to drive off the Cl. Or the Cl can be buried under a CHF_3 polymer, which is then wet etched. But the common method has been to expose the wafer to an F-containing plasma, such as a CF_4 plasma. The chlorine is replaced by fluorine on the Al surface, passivating it. An O_2 plasma then removes the photoresist, and a deionized H_2O bath removes any remaining chlorine. A wafer rinse may also be done before the ashing to help remove the water-soluble chlorides before they are converted by the ashing to insoluble metal oxides [10.16]. A newer process uses an H_2O plasma to both pacify the surface and to remove the resist.

We end this section with a short comment regarding the use of freons, or fluorocarbons. Chlorinated flourocarbons without any hydrogen, such as C_2ClF_5 or $CClF_3$, are believed to deplete the ozone layer in the upper atmosphere. There has been a trend to replace these with safer source gases in the semiconductor industry.

10.4 Measurement Methods

Measurement techniques for etching can be separated into two types: post-etch measurements and *in situ* measurements. Post-etch measurements are generally performed outside the etch chamber. *In situ* measurements are done inside the chamber as the

Micron Ex. 1022, p. 56
Micron v. YMTC
IPR2025-00294

etching is occurring for diagnostic and monitoring purposes. The most important type of monitoring is that done for endpoint detection.

Post-etch measurements for etching are performed to characterize the etch process. The resulting line width can be measured using an optical microscope. Observing the wafer under a microscope can also indicate whether some of the film still remains in the patterned areas due to underetching. However optical observations and measurements are difficult for submicron lines. A much more accurate method for line width measurement is the Scanning Electron Microscope (SEM), discussed in earlier chapters. More automated versions of SEMs have been especially designed for linewidth observation and measurement for both lithography and etching. Measurements from above the wafer looking down assume that the sides of the etched film are vertical. Obviously this may not be so. To observe and measure the actual profile of the etched film, cross-sectional SEM images are used. An example was shown in Figure 10–22. This method requires cleaving the sample and is done on test wafers, usually when developing the process. Linewidth measurements of etched films using electrical testing methods were discussed in Chapter 5.

Other post-etch measurement techniques include composition and contamination measurements. Small amounts of polymeric residues may remain which can have detrimental affects on later processing and circuit behavior. Surface analysis techniques such as Auger Electron Spectroscopy (AES) and X-ray Photoelectron Spectroscopy (XPS) can be used to detect and measure chemical species left on the film or in the near-surface region. XPS is often used to give bonding information and can distinguish whether carbon detected on the surface is bonded to fluorine in C-F_2 structures or to the silicon in the substrate with C-Si bonding, for example. This helps to determine the actual source of the contaminant or residue and the mechanism for its production.

Measuring damage induced by plasma processing is important. Physical damage, in terms of dislocations, trenching, and surface roughening, can be measured by TEM or SEM. Electrical damage, including charging and electron traps, is measured using device or electrical measurements, often using MOS capacitors as discussed in Chapter 6.

In situ measurements are performed inside the etch chamber while the etch process is taking place. The most important type of *in situ* measurement is that done for endpoint detection. Due to the physical component in most plasma etching, selectivity is not 100 percent. Therefore it is important to end the etching soon after the film has been etched to the bottom (allowing for a certain amount of overetch, of course). Some sort of *in situ* measurement is required to do this.

One way to detect the endpoint is to measure the thickness of the film as it is being etched. If one does not want to etch all the way through the film, the endpoint thickness may be some finite value. This method would also give etch rate information as well. An *in situ* thickness measurement technique for optically transparent films, such as silicon dioxide, is interferometry. This method determines the thickness of the film by measuring the interference of optical beams—using either light from a laser or from the plasma itself—reflected from the top and bottom of the etched layer. As the material is etched, oscillations in the reflected signal occur as constructive and destructive interference occurs. The period of oscillation is related to the change in film thickness, x_f, via the relationship

Micron Ex. 1022, p. 57
Micron v. YMTC
IPR2025-00294

$$\Delta x_f = \frac{\lambda}{2n} \tag{10.13}$$

where λ is the wavelength of the laser light and n is the refractive index of the film. Therefore, for each complete cycle in the reflected signal, the film has been etched Δx_f. When the film has been etched completely, the oscillations cease. For nontransparent films, such as metals, techniques using reflectivity differences between the film and the layer underneath can be used. A major disadvantage in film thickness techniques is that the information is obtained from only a small area of the wafer which may not be fully representative of other regions. Recent single-wafer systems use an array of sensors to measure the thickness change at many points on each wafer. One advantage to these systems is that they can accurately measure the ongoing etch rate during an etch process, which can be valuable information concerning the process.

The most common methods for endpoint detection are those which monitor the reacting species or reaction products of an etch process. Optical spectroscopy or mass spectroscopy can be used, but the former is more common. In optical emission spectroscopy a photosensor detects and measures the emitted radiation, through a window into the chamber, from the various species in the plasma as a function of wavelength. In a plasma, light is emitted by exited atoms and molecules as electrons relax from one energy state to another (which is why the plasma glows). Each species emits light in a characteristic spectrum which can be used to identify the particular atom or molecule. (See Figure 4–18.) For example, the fluorine free radical emits light at 703.7 nm (among other wavelengths) as it relaxes from a plasma-induced excited state. Monitoring this wavelength can be used to determine the relative concentration of the fluorine free radical in the plasma. Endpoint detection is done by either monitoring the reacting species or the reaction products.

As an example, consider the etching of SiO_2 on Al by CF_4 chemistry. The main etch reaction occurring here involves the fluorine free radical which is produced in the plasma. As the etching begins, F is consumed by the etch process, forming SiF_4. Therefore the signal from F emission is decreased. When the etching finishes, the concentration of F increases, and its signal goes back up. The endpoint is thus indicated by the increase of the reactant species. Alternately, the endpoint can be indicated by the increase or decrease in the emission signal of an etch product. For example, in etching SiO_2 by CHF_3, one reaction that can occur is between the carbon on the SiO_2 surface and oxygen, producing CO. Monitoring CO at its characteristic 483.0-nm wavelength can be used to detect the presence of CO. When the CO signal decreases below a certain point, the etch is determined to be over. This method, in contrast to thickness measurements, takes its information from the gas phase and thus averages over a much larger region. Therefore, a more average endpoint is determined. Loading effects can occur, since the signal from either the reactants or products will depend on how much material is being etched. In addition, the exact quantification of the signal to concentrations is difficult and some calibration is necessary to determine at what point the etch is completed. However, this method is relatively simple and usually a good indicator of when the etching is complete, and is the most common method in current technology.

Micron Ex. 1022, p. 58
Micron v. YMTC
IPR2025-00294

The technique of optical emission spectroscopy, in addition to being used as an endpoint determination method, is also used in diagnostics of plasma etch processes. By following the emission signals, the relative concentrations of the various species present during the etching process can be measured throughout the etch process. This can give valuable information concerning the various mechanisms occurring and the roles of the different species.

In situ measurements can also be utilized for process control applications. For example, loading effects could be monitored and changes in equipment parameters could be made automatically and instantaneously, based on the feedback from such measurements. Such measurements could also be used to determine when chambers must be cleaned due to buildup of etch residues on the chamber walls.

10.5 Models and Simulation

We have described the different types of underlying mechanisms important for plasma etch processes: chemical etching by reactive chemical species; physical etching by bombardment or sputtering of ionic species; and ion-enhanced etching involving both types of species acting in a synergistic manner. As in Chapter 9, we will describe physically based models that predict the shape, or topography, that results from specific etching technologies. These models are implemented in a variety of simulation tools including SPEEDIE [10.17], TAURUS-TOPOGRAPHY [10.18], and ATHENA [10.19], as well as other topography simulation tools mentioned in the previous chapter. We will show examples from all three of these simulators. In this section we will first describe how physically based simulators model plasma etching. Since there are a number of similarities to the models described in Chapter 9 for simulating deposition of thin films, we will refer the reader to that chapter for some of the specific details.

10.5.1 Models for Etching Simulation

As in the simulation of deposition, plasma etching can be simulated by considering the fluxes of species that come from the plasma and strike the surface of the wafer. In Figure 10–20 we schematically illustrated the fluxes of species coming from the plasma and the various processes that occur on the wafer surface during etching of the films. In physically based topography simulators, the flux of each type of species is calculated, in particular the component of the incoming flux normal to the surface at each point. Because of the relatively low pressures used in etch systems and large mean free paths compared to the feature size on the wafer surface, it is usually assumed that free molecular flow is the dominant gas-phase transport mechanism near the surface, that is, there is no boundary layer diffusion process. The net etch rate at each point is then calculated using an expression that relates the etch rate to the different fluxes. The exact form of that expression depends on the model that is used. We will describe some of these models and expressions in the next section. With the etch rate determined at each location,

Micron Ex. 1022, p. 59
Micron v. YMTC
IPR2025-00294

the appropriate amount of material is removed, the boundary is moved, and the profile can evolve as the etching continues. The etch rate at each location can change with time as the etching progresses because the fluxes that reach each location on the surface can change due to changing geometrical effects, such as flux shadowing.

As in deposition modeling, the flux of species arriving from the plasma and striking the wafer surface can be calculated using Monte Carlo techniques. For example, the distribution of ions in terms of arrival angle at the surface and of energy can be calculated as a function of system parameters, such as gas pressure, composition, and RF settings. This explicitly takes into account the collisions that occur in the plasma and in the sheath, and the acceleration across the sheath to the wafer. There have been several simulation tools developed, including a version of SPEEDIE, that take this approach. However, we again will utilize a simpler approach and define the incoming fluxes analytically on a plane just above the surface. We specify the maximum, unobstructed flux of each species—ions or chemical, for example—and the angular distribution of each.

The angular distribution is assumed to be of the form

$$F_{\text{direct}}(\theta) = F^{\circ} \cos^{n}\theta \tag{10.14}$$

where F_{direct} is the normal component of the flux coming in at angle θ, F° is the flux at θ = 0 degrees, and θ is the angle from the vertical direction. By adjusting n from 1 to large numbers, one can obtain isotropic to anisotropic distributions of arrival angles, respectively. This was illustrated in Figure 9–25 in Chapter 9. With $n = 1$, the distribution is isotropic, with fluxes coming from all directions equally. Higher pressure, more collisions in the gas phase, and shorter mean free path would all lead to a more isotropic arrival distribution. In etching, neutral chemical species are usually assumed to arrive at the top surface isotropically, and $n = 1$ is usually used. For $n > 1$, a tighter distribution of arrival angles would occur. This means that the fluxes arriving at each point on the surface are more directed, or more anisotropic. In etch models, the ionic species—accelerated across the sheath to the wafer surface due to the electric field—are assumed to arrive at the surface approximately perpendicular to the wafer and very anisotropically, and $n = 10$ to 80 is usually used.

Figure 10–26 illustrates the species and fluxes that occur in plasma etching that are included in physically based etch simulators. This is analogous to the fluxes used in deposition modeling (see Figure 9–35). The ionic species are involved in the physical component of etching, and the reactive neutral species would include those species involved in the chemical component of etching, and would primarily be the free radicals. Another type of species is the deposited, or deposition, species. These would include material that is deposited in the form of inhibitor layers, often carbon polymeric material. These would be analogous to the neutral species that deposit in the deposition models. As we mentioned earlier in this chapter, the same processes (deposition, chemical etch, ion bombardment, etc.) often occur in both deposition and etch processes.

As in deposition modeling, the total flux of each type of species arriving at each position will be the sum of that coming directly from the plasma (a direct flux) plus that coming from somewhere else on the surface of the wafer (an indirect flux). The indirect fluxes may be a result of reemission or resputtering from another location. In Chapter 9 many of those processes and the equations used to describe them were presented.

Micron Ex. 1022, p. 60
Micron v. YMTC
IPR2025-00294

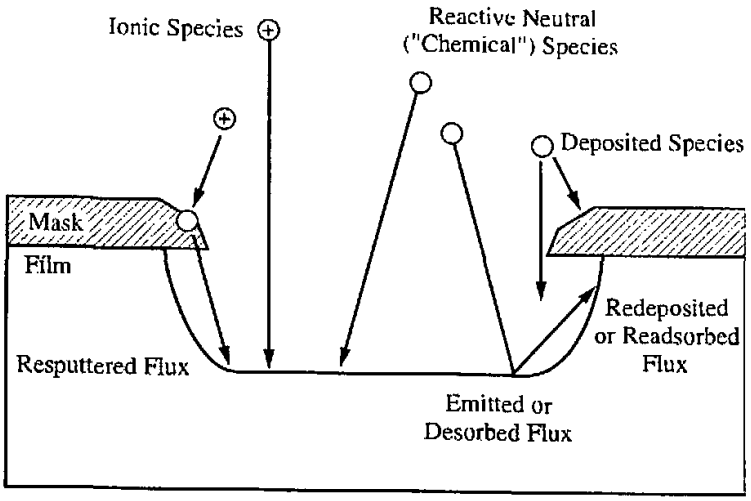


Figure 10–26 Illustration of fluxes, both direct and indirect, that are used in physically based etch simulations.

One of the important sources of indirect flux is that due to reemission of the etch reactant before it can react and etch. This is described by the sticking coefficient. The sticking coefficient is defined, as in Chapter 9 and earlier in this chapter, as the ratio of the flux of species that actually deposit or react at each location on the surface, to the flux of incident species:

$$S_c = \frac{F_{\text{reacted}}}{F_{\text{incident}}} \tag{10.11}$$

Therefore S_c times the chemical flux hitting the surface at each point is the net flux that actually etches, and $(1 - S_c)$ is the fraction of the flux that is reemitted. These reemitted atoms or molecules can then travel to other locations on the surface and etch material there. If S_c is set to a low number ($S_c << 1$) for the chemical species, as is usually the case, then isotropic etching can occur for purely chemical etch processes. Most of the chemical species move in all directions from place to place, as was illustrated in Figure 10–11(a), with a net result that etching is isotropic.

It is usually assumed that the angular distribution of the desorbed or emitted flux follows an ideal cosine distribution ($n = 1$ in $\cos^n\theta_i$ emitted distribution, where θ_i is the angle relative to the surface normal); that is, the emitted species are emitted in an ideal fashion from a small area on the surface. In SPEEDIE it is currently assumed that only the neutral species can be emitted from the surface; for ionic species the sticking coefficient is assumed to be one. This does not mean that all ionic species are successful in etching, or sputtering, an atom or atoms from the surface. It just means that the ions that do not etch any material are not reemitted to etch elsewhere.

In Chapter 9, we described how it has been experimentally determined that surface diffusion for SiO_2 deposited by both LPCVD and PECVD methods was not important —the results could be modeled better with the reemission and redeposition process. A similar experiment has been done to distinguish between the two processes in plasma

Micron Ex. 1022, p. 61
Micron v. YMTC
IPR2025-00294

etching of silicon [10.20, 10.21]. By modeling the undercut profiles, it was determined that using the reemission/readsorption model, with a low sticking coefficient, works better than using the surface diffusion process in the simulation. Thus surface diffusion of the species is often not included as a model in etch simulators.

Physical etching occurs by sputtering when ions strike the surface. Sputtering occurs when the incoming ion transfers enough energy to the wafer surface to break the bonds holding a surface atom in place. The sputtering yield, Y, is defined as the number of atoms or molecules ejected from the target per incident ion and is a measure of the sputtering efficiency. Therefore Y times the ion flux striking the surface at each point determines how much physical etching occurs for a given ion flux .

The sputter yield, Y, is a function of ion energy, the mass of the incoming ion and the target material (the wafer surface material, in this case), and the incident angle, θ, at point i, with a normal incidence being 0°. As we discussed in Chapter 9, ions coming in at low angles are reflected from the surface and do not transfer significant energy to the surface atoms, while ions coming perpendicular to the surface knock surface atoms further into the film and not off. The maximum sputtering yield occurs usually at somewhere from 40–70°. This is usually modeled as was described in Figure 9–39.

In some of our models we will use K_i, the ion-induced etch yield, or the effective sputtering yield. Like Y, it is a measure of how many atoms or molecules of substrate are etched per incident ion but can include the synergistic effects with the chemical component, resulting in higher values for it than normal physical sputtering yields. K_i generally has similar properties as Y, angle and energy dependencies for example. For cases of purely physical sputtering, K_i would just equal Y.

All of the geometrical issues involved in the etching process are taken into account in physically based etch simulators. That is, the net flux of each type of species at each point on the surface is calculated based on the relative orientation of that point to all sources of fluxes. This includes fluxes from the plasma source (the direct flux) and from all other points on the surface (the indirect fluxes). The view angles to all other sources of fluxes, as well as the angular distribution emitted from each source, are taken into account in the calculation of the arriving flux at each point.

Once the net flux of each type of species is calculated at each point on the surface, the etch rate can then be calculated at each point. This is determined by the specific etch model used in the simulation. We will next consider some of the models and corresponding etch rate expressions that etch simulators use to model plasma etching.

10.5.2 Etching Models — Linear Etch Model

Different types of etch models have been developed and are available in simulators. Some of these models are for specific types of etching equipment—for high-density plasma etch systems or for sputter etch systems, for example. However, there are also some more general-purpose models. These were developed to model the different types of mechanisms that occur during plasma etching: physical, chemical, and ion-assisted etching, and which can occur in any of the plasma etch systems. We will concentrate on those models, and two in particular: the linear etch model and the saturation/adsorption etch model, both of which are used in the SPEEDIE simulator.

Micron Ex. 1022, p. 62
Micron v. YMTC
IPR2025-00294

The simplest model for etching assumes that the chemical and ionic components act independently of each other and combine in a linear fashion. This is the basis of the linear etch model in SPEEDIE. Other simulators include similar models. It is assumed in this model that the etch rate due to each component is linearly proportional to the flux of that component. Studies of chemical etching do show a linear dependence of etch rate on the chemical flow rate or flux for certain conditions [10.5, 10.22]. Likewise, the etch rate in the presence of ionic bombardment is seen to be linearly dependent on the ion current or flux over a range of conditions [10.23]. The two terms are then added together, so that

$$\text{Etch rate} = \frac{(S_c K_f F_c + K_i F_i)}{N} \tag{10.15}$$

The density, N (in cm^{-3}), is that of the film being etched. F_c is the chemical (reactive neutral, free radical) flux and F_i is the ion flux at each point on the surface. S_c is the sticking coefficient, which is between 0 and 1. K_f and K_i are the relative rate constants for the two processes and can include any stoichiometric factors. In practice, K_f is often used as a fitting parameter for the purely (non-ion-enhanced or "spontaneous") chemical etching. As described above, K_i is the ion-induced etch yield and is related to the number of ions needed to remove one atom or molecule for the material being etched. It is essentially equivalent to the physical sputtering yield, Y, but can be greater than Y in some cases as we will discuss. K_i can be a function of incident angle and ion energy. Like K_f, it is often used as a fitting parameter.

One can see that the net etch rate at each point is just the linear combination of purely chemical etching and ion-driven etching, with each term linearly dependent on the appropriate flux. The etch profile would likewise be a linear combination of the two components, with chemical etching occurring equally in all directions plus the physical, ion-driven etching occurring primarily in the vertical direction.

While being simple, with no coupling between the components, the model may be appropriate for certain conditions. It would be valid when the etch process is purely chemical, in which case the ion flux would be zero, and the etch rate is simply proportional to the chemical flux. Purely chemical etching would occur in a barrel etcher or in an after-glow system, for example, where the ions are prevented from striking the wafer surface. It could even occur in a parallel plate system if little or no inhibitor layer is formed and there is a very high concentration of free radicals in the plasma and only spontaneous chemical etching occurs. For purely chemical etching, the etch profile would be completely isotropic and look like Figure 10–3(a). This model would also be valid when the etch process is only dependent on the ion flux, as in solely physical etching, in which case the first term would be zero. This would occur, for example, in a sputter etch system where only high-energy, chemically inert Ar^+ ions are used. When the etch rate is simply proportional to the ion flux with no chemical term, the profile would look like Figure 10–3(c), with vertical or near-vertical etching and no undercutting.

The model would also be applicable when the etch process does have both chemical and physical etching components, but the two act independently of each other. Or at least they each appear as if they are independent in that they do not limit the action of the other for a given range of conditions. For example, the physical, ionic component in

Micron Ex. 1022, p. 63
Micron v. YMTC
IPR2025-00294

this model (the second term in the rate expression) does not, in fact, have to be due to purely physical sputtering. It could actually be ion-enhanced etching, but operating in a regime where the chemical component in that mechanism is high enough, due to a relatively high flux of neutrals, for example, and is not limiting the ion-driven etching, as we will describe later. In that regime the ion-enhanced etching would act as if it were purely physical and not dependent on the chemical flux, that is, simply proportional to the ion flux. In that case, K_i is often much greater than the normal physical sputtering yield. [And if there is no spontaneous chemical etching, the profile would look like that for purely physical etching, Figure 10–3(c).] In addition, any adverse effect the ion bombardment might have on the spontaneous chemical etch term, by depleting the surface chemical species for example, may not be significant at lower ion fluxes or higher neutral fluxes [10.21]. When two (seemingly) independent etch components are present, isotropic chemical and directional ionic, the etch profile would look like Figure 10–3(b), a linear combination of the profiles for spontaneous chemical etching and ion-driven etching. So in general, the simple linear etch model would be appropriate when one or two independent, or seemingly independent, etch components are present, resulting in a range of etch profiles.

Example Silicon is plasma etched for 5 minutes and the process follows the linear etch model. The flux of chemical species, F_c, on an unobstructed flat surface is equal to 2.5×10^{18} atoms $cm^{-2}\,sec^{-1}$, the sticking coefficient is 0.01, and K_f is 0.2. The flux of ionic species, F_i, on a flat surface is equal to 1×10^{16} atoms $cm^{-2}\,sec^{-1}$ and K_i is 1. The density of Si is 5.0×10^{22} atoms cm^{-3} A photoresist mask is used so that a wide trench is etched in the Si. (There is no etching of the photoresist.) How far is the Si etched in the vertical direction (away from the mask edge), and how far is the Si etched in the lateral direction right under the mask for these conditions?

Answer For the linear etch model, Eq. (10.15):

$$\text{Etch rate} = \frac{(S_c K_f F_c + K_i F_i)}{N}$$

In the vertical direction, there would be both chemical and ion fluxes, and the total etch rate in this model would simply be the sum of those components. Away from the mask edge we assume no shadowing effects, so F_c and F_i are the unobstructed chemical and ion fluxes, respectively, given above. Therefore

$$\text{Etch rate(vert)} = \frac{(0.01 * 0.2 * 2.5 \times 10^{18}\text{cm}^{-2}\text{sec}^{-1} + 1 * 1 \times 10^{16}\text{cm}^{-2}\text{sec}^{-1})}{N}$$

$$= \frac{1.5 \times 10^{16}\text{cm}^{-2}\,\text{sec}^{-1}}{N}$$

Micron Ex. 1022, p. 64
Micron v. YMTC
IPR2025-00294

The density of Si, N, is 5.0×10^{22} atoms cm^{-3}, so the Si etched in the vertical direction is

$$\text{Etch depth(vert)} = \frac{1.5 \times 10^{16} cm^{-2} sec^{-1}}{5.0 \times 10^{22} cm^{-3}} * 300 \text{ sec} = 9.0 \times 10^{-5} cm = 0.9 \mu m$$

In the lateral direction, right under the mask edge, there is virtually no ion flux ($F_i \approx 0$). Therefore only the chemical flux term is used in the etch rate expression and it is assumed that the chemical flux is the same in all directions (due to the isotropic arrival distribution and, especially, the low S_c), so that

$$\text{Etch depth(lat)} = \frac{(0.01 * 0.2 * 2.5 \times 10^{18} cm^{-2} sec^{-1} + 0)}{5.0 \times 10^{22} cm^{-3}} * 300 \text{ sec}$$

$$= 3 \times 10^{-5} cm = 0.3 \ \mu m$$

There is more etching in the vertical direction than in the lateral direction, and a profile such as that in Figure 10–3(b) occurs in this case.

This model has been used to accurately simulate the etching of Si under certain conditions. For example, Singh and colleagues [10.20] etched Si using a CF_4/O_2 plasma. As we noted earlier, this can result in isotropic etching, with a very strong chemical component. They used the etch system in the plasma mode, with symmetric electrode areas, which minimizes any ion bombardment. In addition, an oxide etch mask was used rather than photoresist so that the formation of a carbon-containing inhibitor layer was minimized. The etch profiles obtained were virtually isotropic and they were able to model them with the linear etch model in SPEEDIE and assuming no ion component. A value of 0.04 was used for S_c.

This same group [10.21] etched Si using an SF_6 plasma, but now observed a mixture of chemical and physical etching. Etch profiles similar to that in Figure 10–3(b) were obtained, with notable undercutting but not completely isotropic. They were able to accurately model the profiles again with the linear etch model, with a chemical-to-physical component ratio of 2:1. They actually identified the physical component as an "ion-assisted mechanism" as opposed to purely physical sputtering but modeled it with a simple linear dependence on ion flux, independent from the isotropic chemical flux. Ulacia and colleagues [10.24] did similar experiments etching Si using a SF_6/C_2ClF_5 plasma and modeled it with the linear etch model. (Again the physical component was identified as ion-enhanced, but following a linear relationship with ion flux.) They were able to vary the chemical-to-physical ratio from 4:1 (near-isotropic) to approximately 1:1 and then to 1:20 (almost perfectly anisotropic) by changing the SF_6:C_2ClF_5 ratio and the amount of carbon in the system, and model the resulting etch profiles quite well with the linear etch model for a specific set of conditions.

Micron Ex. 1022, p. 65
Micron v. YMTC
IPR2025-00294

We now describe a series of plasma etch simulations using the SPEEDIE simulator and the linear etch model just described. As with the SPEEDIE deposition simulations in Chapter 9, we will use analytical $\cos^n\theta$ distributions for arrival angles (as opposed to Monte Carlo calculations of gas-phase processes). A value of n equal to 1 results in an isotropic arrival angle distribution, relative to the vertical direction. A value of n higher than 1 results in a more anisotropic arrival distribution, with a more directed downward distribution such as occurs with ionic species. In all the simulations presented in this section, we etch a silicon substrate using a photoresist mask. The top layer is 1-μm thick photoresist, with a slightly sloped window defined in it.

The first simulation uses the linear etch model, and Eq. (10.15) to govern the etch rate at each point. Pure chemical etching is illustrated first in Figure 10–27(a). The simulation time is 240 seconds, and each of the contours corresponds to a 30-second time step in the etching. The arrival angle distribution parameter, n, for chemical is set to one, indicating an isotropic arrival angle distribution. The maximum unobstructed direct flux of neutral species is set to 5×10^{18} cm^{-2}sec^{-1}. This corresponds to the total integrated direct flux of chemical species arriving from all directions and hitting a flat, unobstructed surface. Knowing the angular distribution of arriving atoms and the geometry of the surface, SPEEDIE can convert this to the direct chemical flux normal to the surface, $F_{c(direct)}$, at each point. The value of the maximum direct chemical flux used in the simulations is usually determined by knowing the chemical rate on a flat surface, in which case it is directly equal to F_c, or is determined by fitting experimental profiles to the simulations. The ion flux is set to zero in this simulation, so that the etch is purely chemical. A low value for the sticking coefficient, S_c, is used for the chemical species, equal to 0.01, ensuring that F_c is equal everywhere and the chemical component to etching occurs isotropically. A value of 0.2 is used for K_f. Negligible etching of the photoresist occurs in these simulations.

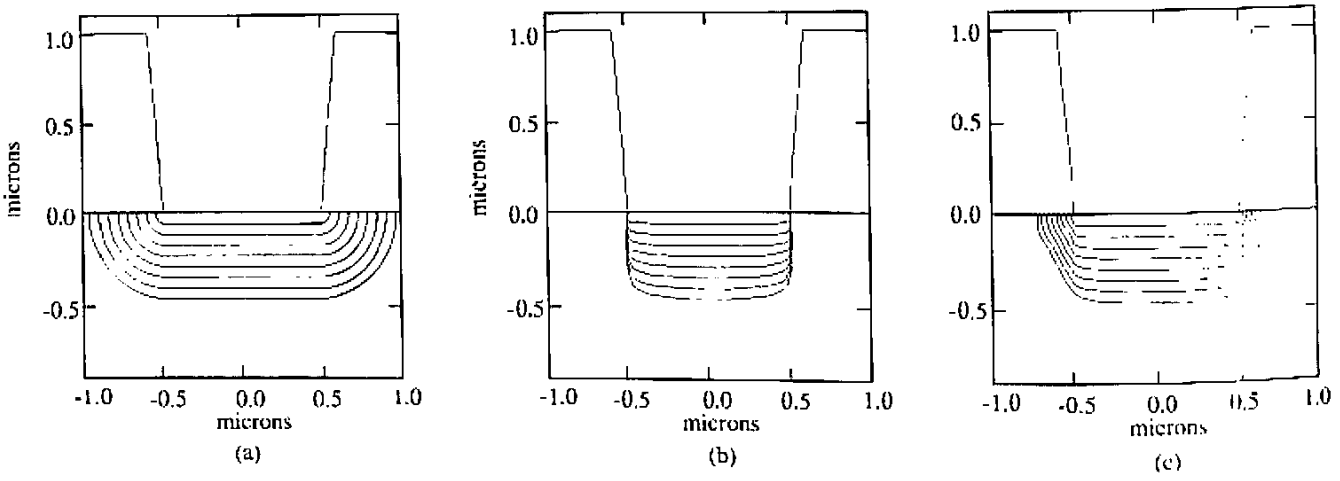


Figure 10–27 SPEEDIE simulations for etching of Si with linear etch model: (a) all chemical etching, showing isotropic etching; (b) all physical or ionic etching, showing very anisotropic etching; (c) half-chemical, half-ionic etching, showing a combination of isotropic and anisotropic etching. The different curves correspond to different times in the etch simulation.

Micron Ex. 1022, p. 66
Micron v. YMTC
IPR2025-00294

Next only physical, ionic etching is illustrated using the same linear etch model. The chemical flux is set to zero while the maximum ionic flux is set to $1 \times 10^{16}\ cm^{-2}\,sec^{-1}$. Setting $n = 80$ means that nearly all the ionic flux will arrive from the vertical direction. K_i is set to 1. Figure 10–27(b) shows the results. Very anisotropic etching results as expected. Purely physical etching would occur in a sputter etch system (although one would expect etching of the resist as well in that case). This etch behavior could also occur, and be modeled in the same manner, for an ion-enhanced mechanism for conditions where the chemical component is not limiting the ion-driven etching anywhere in the structure, and where there is no spontaneous chemical etching.

Now we combine both chemical etching and physical/ionic etching in the linear etch model. As we discussed this model assumes that the two components are acting independently, or else in a regime where neither is limiting the action of the other. Here we use $2.5 \times 10^{18}\ cm^{-2}sec^{-1}$ for the chemical maximum flux and $0.5 \times 10^{16}\ cm^{-2}sec^{-1}$ for the ionic maximum flux, and the same values for S_c, K_f, and K_i we used above. This results in relatively equal contributions of the ionic and chemical components since the $S_cK_fF_c$ and K_iF_i products [see Eq. (10.15)] are equal. The resulting etch profile is shown in Figure 10–27(c). Different degrees of anisotropy can be achieved by varying the relative amounts of the two components. This behavior could occur in a plasma system in which there is both chemical etching and ionic sputtering acting separately. It could also occur where there is some spontaneous chemical etching, not affected by ion bombardment, as well as ion-enhanced etching for conditions in which the chemical component is not limiting the etching.

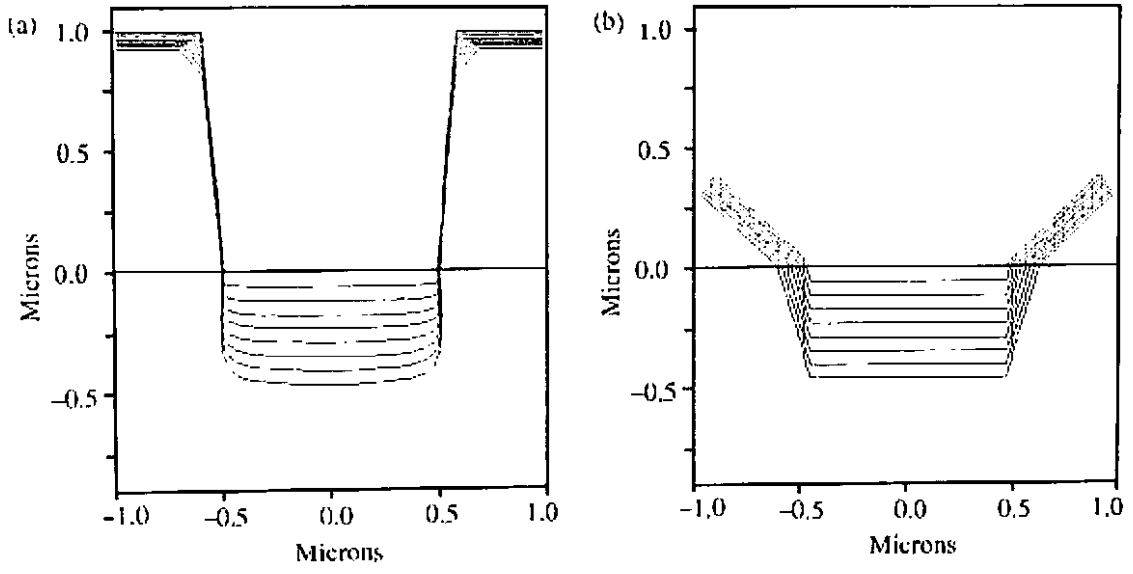


Figure 10–28 SPEEDIE simulations for etching of Si with linear etch model for physical-only etching with etching of photoresist included: (a) angle-dependent sputtering of photoresist included, showing faceting; (b) initial taper of photoresist changed, allowing for mask erosion due to vertical physical etching. A wider area of silicon is etched, and sloped sidewalls in the Si result.

Micron Ex. 1022, p. 67
Micron v. YMTC
IPR2025-00294

Next we allow for some physical etching of the photoresist. We first allow for some angle-dependent physical sputtering of the photoresist during physical-only etching. We do this by increasing the value of K_i for the photoresist from 0 to 0.3. In Figure 10–28(a) we see the faceting that occurs at the top corners. Next we change the initial shape and thickness of the photoresist mask. We start with a thin mask, only 0.4 μm thick at the sides, which slopes diagonally to the opening. When physical etching occurs, the edge of the mask will be etched away, illustrating the phenomenon of mask erosion. Figure 10–28(b) shows the result. The etching away of the mask results in a wider etched area in the silicon, and nonvertical sidewalls. Changing the etch chemistry to change the amount of mask erosion can be utilized to obtain a desired etch profile.

We next illustrate the concept of Aspect Ratio Dependent Etching (ARDE). As discussed earlier this is the phenomenon in which the depth of etching decreases as the aspect ratio increases. One possible mechanism for this is that ion-neutral collisions in the sheath cause ions to be off-axis, making their arrival angle distribution wider. The less directed flux means that fewer ions reach the bottom of the etched trench due to view angle or shadowing considerations. With fewer ions getting to the bottom for the narrower openings, less vertical etching occurs, whether it is purely physical etching or ion-enhanced etching. This is simulated in the following two figures using the linear etch model. First we repeat the physical-only etching of Figure 10–27(b), except that we change the arrival angle distribution factor, n, for ions from 80 to 10, as might occur if the gas pressure were higher and more gas phase collisions take place, for example. This widens the arrival angle distribution a little, but the ions are still fairly directed downward. Figure 10–29(a) shows the result. More bowing of the sides results as compared to the $n = 80$ example in Figure 10–27(b), and this type of profile is seen in some etch

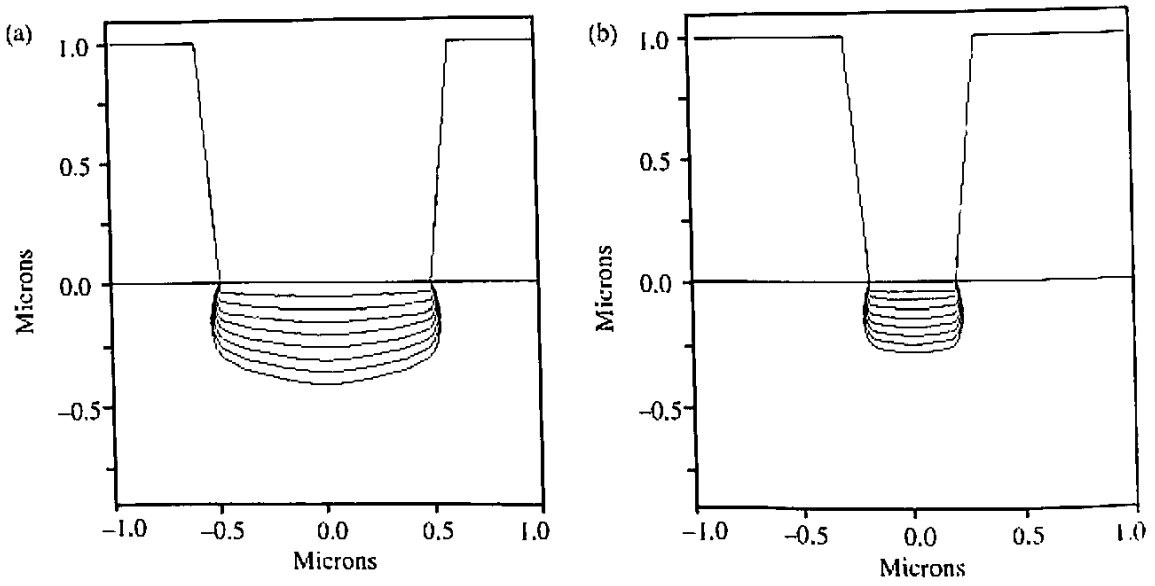


Figure 10–29 SPEEDIE simulations for etching of Si with the linear etch model illustrating Aspect Ratio Dependent Etching (ARDE). Physical-only etching (with arrival angle distribution factor $n = 10$) is done for two different mask opening widths: (a) mask opening = 1 μm; (b) mask opening = 0.4 μm. Deeper etching occurs for the wider mask opening.

Micron Ex. 1022, p. 68
Micron v. YMTC
IPR2025-00294

systems. Now we decrease the window in the photoresist down to 0.4 μm. The resulting etch profile is shown in Figure 10–29(b). The depth of etching is clearly reduced. (The same effect is not seen if n were left at 80 for the two widths.) With the slightly wider angular distribution of arrival angles for the ions, the etch depth is less for the narrower mask opening than the wider opening even though all the other etch conditions are the same. Therefore, the etching could be different for different feature sizes on the same wafer, even if the features are right next to each other.

Interestingly enough, in some etch systems and under certain conditions, a reverse ARDE effect is sometimes observed where wider etch features etch less than narrower ones. Both forward and reverse ARDE has been simulated in SPEEDIE using the "Simuletchdepo" model, to be described later, which includes a modified saturation/adsorption etch term combined with a polymer deposition term [10.25]. In that modeling, the transport of the neutral species down the trench is important for the aspect ratio dependence.

In summary, the linear etch model is relatively simple, combining the chemical and physical components in a linear fashion. It can be used in a physically based simulator such as SPEEDIE to simulate etch profiles with different degrees of anisotropy, for a variety of etch systems. It can also model effects such as ARDE and mask erosion. While simple, the model may in fact be adequate for particular plasma etch situations, even for ion-enhanced etching under limited conditions. But it does not model the coupling between the chemical and physical components that can occur, particularly the synergistic interactions in ion-enhanced etching.

10.5.3 Etching Models — Saturation/Adsorption Model for Ion-Enhanced Etching

To account for the physical and chemical components acting together, and not independently, another model is needed. As was described earlier, the etching is often not just simply the sum of the two individual components, as in the linear etch model. In ion-enhanced etching the two components act in a synergistic manner, and the etch rate can be much higher than the sum of the two separate rates. Likewise, the etching can be limited by the deficiency or lack of either of the two components. Ion-enhanced etching can be due to a variety of mechanisms. Any one of the steps of the chemical etch process may be enhanced by ion bombardment, such as the reaction of the etchant and the surface material, or the removal of etch byproducts. Inhibitor layers, formed as a result of the etch process, may require ion bombardment to remove them.

What is needed in the model is an expression that allows for the etch rate to be larger than the sum of the two components acting independently. In fact, it may be the case that the presence of both components is needed for the etching to occur. Without any ion bombardment, for example, a byproduct layer may not be removed and no chemical etching can proceed. Without any chemical processes, the ion sputtering alone may be negligible. This means that the two components are acting in series, as opposed to in parallel. It also means that the deficiency of one component can limit the total etch rate, even as the other component is increased. This leads to saturation effects—increasing the flux of one of the components will increase the etch rate to a point, but then the rate will saturate due to the lack of enough of the other

Micron Ex. 1022, p. 69
Micron v. YMTC
IPR2025-00294

component. These results have all been observed experimentally [10.6, 10.23, 10.26, 10.27, and 10.28].

A model for ion-enhanced etching that captures the above behavior is the saturation etch model. This model is also commonly called the Langmuir adsorption or the saturation/adsorption etch model and includes surface coverage issues involving species adsorbing on and leaving the surface in its formulation. While we will derive a simple expression below based on one type of ion-enhanced etching mechanism (ion-enhanced byproduct removal), its results are generally applicable to many different mechanisms in which ion bombardment enhances one or more of the steps in the etch process. It is really a phenomenological model which can incorporate many simultaneous reactions and kinetics into its simple form. Many versions of this basic model have been developed to include a variety of processes and chemistries, but they are all similar in idea and approach [10.26, 10.28, 10.29, 10.30, 10.31, and 10.32].

For this simple analysis we consider both reactive neutral species and ions striking a surface during an etch process. The neutral species are adsorbed on the surface and chemically react with the surface material, forming etch products which contain both reactant species and film atoms. The ions striking the surface can enhance the removal of the etch byproducts from the surface, perhaps by sputtering or dislodging the loosely held byproducts or by inducing their conversion to more volatile species which then spontaneously desorb [10.6, 10.32]. A steady state will develop when the net flux of the neutrals to the surface is zero, or equivalently when the rate of byproduct formation equals the rate of byproduct removal. The idea is that the number of neutral species absorbed and reacted on the surface per time, according to simple Langmuir adsorption behavior, is proportional to how many sites are available: one minus the surface coverage. And the number of sites available depends on the neutral flux and on the ion bombardment which removes the byproducts and increases the sites for reactive neutral species adsorption. At steady state, the etch rate is then just proportional to the removal rate of byproducts, or equivalently to the neutral species adsorption rate, and depends on both the neutral and ion fluxes in a synergistic manner.

According to Langmuir adsorption theory, the number of reactive neutral species that adsorb (per unit time per area) on the surface to react with the surface material is

$$\#\text{ reactive neutrals adsorbed per time per area} = S_c(1 - \Theta)F_c \qquad (10.16)$$

where S_c is the sticking coefficient of the available area, Θ is the fraction of sites covered by the byproducts, so that $(1 - \Theta)$ is the fraction of sites available, and F_c is the flux of neutral species onto the surface. A chemical reaction constant, K, can be included, but it is just assumed to equal one here. We assume in this derivation that all neutral atoms that adsorb and stick on the surface will react quickly with the surface and form etch byproducts.

The reactive neutrals (in the etch byproducts) that are removed by ion bombardment per unit time per area from the surface is proportional to the byproduct coverage and equals

$$\#\text{ reactive neutrals (contained in byproducts) removed per time per area} = K_i\Theta F_i \qquad (10.17)$$

Micron Ex. 1022, p. 70
Micron v. YMTC
IPR2025-00294

F_i is the incoming flux of ions and K_i is the ion-induced etch yield, or the effective sputtering yield (in general, a measure of how many atoms or molecules are removed per incident ion in a given process). K_i can be much larger than the normal sputtering yield of surface atoms—removing reaction products by ion bombardment may be much easier than removing film atoms by direct physical sputtering of the surface.

We assume a steady-state condition will develop in which the number of neutrals adsorbed equals the number removed. Thus equating Eqs. (10.16) and (10.17) gives

$$S_c(1 - \Theta)F_c = K_i\Theta F_i \tag{10.18}$$

$$\therefore \Theta = \frac{1}{1 + \dfrac{K_iF_i}{S_cF_c}} \tag{10.19}$$

The etch rate is then just the flux of removed species, equal to Eq. (10.17) [or equivalently, the flux of adsorbed and reacted species given by Eq. (10.16)], divided by the density of the film being etched, N. (Any stoichiometric coefficients needed to relate the ratio of film atoms to the neutral species in the reactant or byproduct molecules can be added or just included in S_c or K_i). Therefore by using Eq. (10.19) for Θ we obtain

$$\text{Etch Rate} = \frac{1}{N}\frac{1}{\left(\dfrac{1}{K_iF_i} + \dfrac{1}{S_cF_c}\right)} \tag{10.20}$$

By writing the etch rate expression in this form, the two components (analogous to electrical conductances) are seen to be acting in series rather than in parallel.

We plot Eq. (10.20) in Figure 10–30. For simplicity we assume the density, N, is unity. Here the x-axis is ion flux times the ion yield, or F_iK_i, and the equation is plotted for various values of the chemical flux times the sticking coefficient, F_cS_c. However, due to the symmetry, we could interchange F_cS_c and F_iK_i and obtain the same results. One sees that for no ion flux, the etch rate is zero, no matter what the chemical flux is. Similarly, for no chemical flux, the etch rate is zero, no matter what the ion flux is. One also sees that as the ion flux is increased for a given chemical flux, the etch rate initially increases linearly but eventually saturates. The value it saturates at, or approaches, is equal to F_cS_c/density. Similarly, when increasing the chemical flux at a constant ion flux, the etch rate increases linearly and then saturates. The process is limited by the slower of the two component processes.

The same type of saturation behavior is seen with respect to the effective sputtering yield term, K_i. Increasing the effective sputtering yield by increasing the ion energy will result in an increase in etch rate, which will then saturate as the ion energy is further increased.

The initial linear behavior is made clear by noting that when F_iK_i is small and F_cS_c is large, then by Eq. (10.20) the etch rate becomes approximately equal to just F_iK_i/density. This is the same as the physical term in the linear etch model and shows why the simple linear etch model can be used in some cases for ion-enhanced etching, as discussed earlier.

Since both ion bombardment and chemical reaction by the reactive neutral species are required in the saturation model, this ion-enhanced etching mechanism results in

Micron Ex. 1022, p. 71
Micron v. YMTC
IPR2025-00294

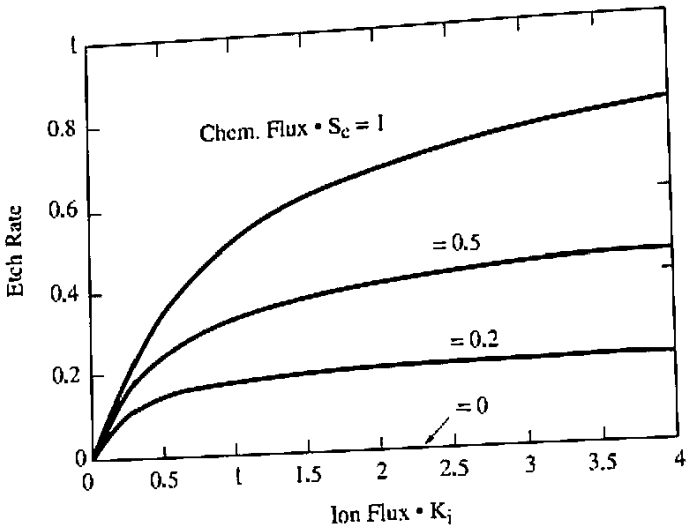


Figure 10–30 Etch rate versus ion flux for various values of the chemical flux, as calculated by Eq. (10.20). An identical plot can be obtained by interchanging $F_c S_c$ and $F_i K_i$.

mostly vertical etching. This is because the ion bombardment occurs mostly in the vertical direction, with no reemission. On sidewalls (vertical surfaces), F_i is close to zero, and hence the etch rate according to Eq. (10.20) would be close to zero in lateral directions.

Example Silicon is plasma etched for 5 minutes using a photoresist mask and this time the process follows the saturation/adsorption, or ion-assisted, etch model. The flux of chemical species, F_c, on an unobstructed flat surface is equal to 2×10^{18} atoms cm^{-2} sec^{-1} and the sticking coefficient is 0.01. The flux of ionic species, F_i, on an unobstructed flat surface is equal to 2×10^{16} atoms cm^{-2} sec^{-1} and K_i is 1. There is no etching of the photoresist, and no spontaneous chemical etching of the Si. How far is the Si etched in the vertical direction (away from the mask edge), and how far is the Si etched in the lateral direction right under the mask?

Answer In the vertical direction, away from the mask edge, there are both chemical and ion fluxes, and the total etch rate would be given by Eq. (10.20). The density of Si is 5.0×10^{22} atoms cm^{-3}. Therefore

$$\text{Etch Rate (vert)} = \frac{1}{5 \times 10^{22}\ \text{cm}^{-3}} \frac{1}{\left(\dfrac{1}{1 * 2 \times 10^{16}\ \text{cm}^{-2}\text{sec}^{-1}} + \dfrac{1}{0.01 * 2 \times 10^{18}\ \text{cm}^{-2}\text{sec}^{-1}}\right)}$$

$$= 2.0 \times 10^{-7}\ \text{cm sec}^{-1}$$

Micron Ex. 1022, p. 72
Micron v. YMTC
IPR2025-00294

For a 5-minute etch, the Si etched in the vertical direction is

$$\text{Etch depth(vert)} = 2.0 \times 10^{-7}\text{cm sec}^{-1} \times 300 \text{ sec} = 0.6\ \mu\text{m}$$

In the lateral direction, right under the mask edge, there is virtually no ion flux ($F_i \approx 0$), only chemical flux. Therefore the etch rate expression goes to zero. (And there is no spontaneous chemical etching.) Thus the Si etched in the lateral direction, right under the mask edge is virtually zero. A very anisotropic etch profile results.

The absence of lateral etching in this type of etching assumes that there is no spontaneous chemical etching, that is, no chemical etching without any ion bombardment. However, there may in fact be a degree of either spontaneous chemical or physical etching occurring in some systems. If the ion-enhanced etching occurs because the ion bombardment transfers energy to the surface atoms which speeds up the chemical reactions, there still may be appreciable etching without the enhancement. Or if the ion-enhanced etching is due to the presence of a byproduct layer whose removal is enhanced by ion bombardment, there may be significant spontaneous desorption of the byproduct layer. Likewise, there may be a finite component of spontaneous etching by ionic species for which neutral chemical species are not required, such as purely physical sputtering.

To account for any spontaneous etching, terms corresponding to pure chemical or pure physical etching can be included in the expression for ion-enhanced etching. In the simplest such model, terms the same as those used in the linear etch model are added to the ion-enhanced etching rate, with those terms scaled by some factor relative to the enhanced rate. For example, a ($S_C K_f F_c$/density) term can be added to Eq. (10.20) to provide for a spontaneous chemical etch component. Adding spontaneous terms would allow for some etching even if one of the two components were absent and could result in etch profiles that show some lateral etching in addition to the vertical etching [as in Figure 10–3(b)]. In more advanced models the spontaneous etch terms may be coupled with other terms, such as the surface coverage [10.26, 10.28, 10.30, 10.31, 10.32].

While Eq. (10.20) is a rather simple expression, and other more detailed versions of it have been developed, it captures the main features observed in ion-enhanced etching for many different mechanisms. Expressions the same as or very similar to this, most based on surface coverage or site considerations, have been used for a variety of ion-enhanced mechanisms. These include etching mechanisms where ion bombardment enhances the chemical etching by damaging the surface, where the sputtering yield of the surface is increased by the chemical reaction between the reactive neutral species and the surface atoms, as well as different byproduct removal mechanisms. (And it is often difficult to distinguish between the different mechanisms, both experimentally and conceptually.) In each of these cases, the analysis generally follows that as outlined above, with the ion bombardment term [Eq. (10.17)] corresponding to different ion-induced etch processes (damage creation, byproduct removal, etc.). But the end result is an expression for etch rate very similar to that given in Eq. (10.20), with the two components

Micron Ex. 1022, p. 73
Micron v. YMTC
IPR2025-00294

acting in series and in a synergistic manner. The saturation/adsorption model, or variations of it, has been used to model a variety of etch systems, including Si, SiO_2, and W thin films, under a variety of conditions and chemistries [10.26, 10.27, 10.28, 10.29, 10.30, 10.32, and 10.33].

Something that this expression does not account for is an inhibitor mechanism in which an inhibitor/byproduct forms or deposits independently of the main etch species and reaction, such as when etching Al with Cl_2 and a separate inhibitor component. Nor does it model thick or excess inhibitor formation and the highly sloped etch profiles that can result. Modeling which explicitly includes these processes will be described later.

We now describe some SPEEDIE plasma etch simulations using the saturation/adsorption etch model, as described by Eq. (10.20). Here the chemical components (neutral reactive species, such as free radicals) and physical components (ions) work together. Only when and where both are present does etching occur. In the first simulation, approximately equal contributions from the chemical and ionic etching are specified by having the K_iF_i and S_cF_c products equal. Figure 10–31 shows the simulation, with each etch contour representing a time increment of 30 seconds in the 240-second total etch time. As expected in this model, very anisotropic etching is achieved even with a strong chemical component. This is because ion bombardment is necessary in this ion-enhanced mechanism, and the ions only strike in a near-vertical direction. Etch chemistries are often chosen that produce this synergy between chemical and ionic components.

The shape of the etched sidewall can be changed in the saturation/adsorption model by changing the n factor for the ion arrival angle distribution. A smaller value for n (closer to 1), corresponding to a less directed flux, gives a more bowed sidewall. A less directed flux can occur for a higher pressure or a lower wafer bias.

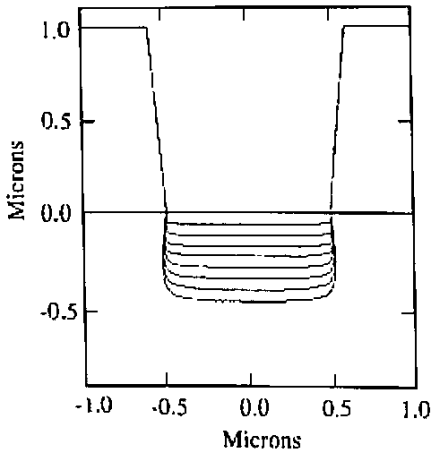


Figure 10–31 SPEEDIE simulations for etching of Si with saturation/adsorption etch model. Approximately equal components of chemical and physical etching are used.

Micron Ex. 1022, p. 74
Micron v. YMTC
IPR2025-00294

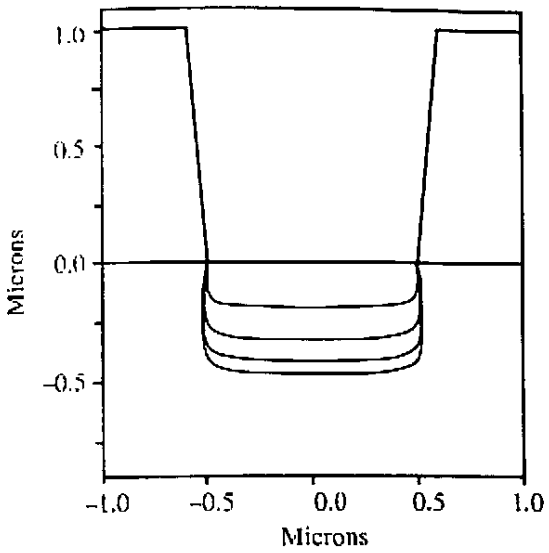


Figure 10–32 SPEEDIE simulations for etching of Si with saturation/adsorption etch model. The chemical flux is kept constant (at 2×10^{18} cm^{-2} sec^{-1}) while the ion flux is linearly increased from 0 to 1×10^{16} cm^{-2} sec^{-1} in equal increments. Each contour here corresponds to the final etch profile for the different ion fluxes. The etch rate is initially linear with ion flux but then starts to saturate.

Next we do a series of simulations with this same model in which the chemical flux is kept constant, but the ion flux is increased. Figure 10–32 shows the simulation profiles. The maximum chemical flux is kept at 2×10^{18} cm^{-2} sec^{-1} while the maximum ion flux is varied from 0 to 2×10^{16} cm^{-2} sec^{-1} in equal increments. S_c and K_i equal 0.01 and 2, respectively. Unlike the plots in the previous simulation figures which showed the different time interval profiles, only the final 240-second etch profile is shown for each simulation in this figure. In this case the different profiles correspond to the different maximum ion flux values used. One can see that for zero ion flux, no etching at all takes place. As the ion flux increases, the etching increases. At first the etch rate is nearly linear with ion flux, but as the ion flux is increased more, the etch rate starts to saturate and the increase in the etch rate slows down. Eventually the etch rate will not perceivably increase at all with an increase in ion flux. This illustrates the saturation effect we discussed previously for this model and illustrated in Figure 10–30.

A result very similar to Figure 10–32 would be produced if the chemical flux were increased while the ion flux remains constant. With no chemical flux, no etching at all occurs. As the chemical flux increases, the net etch rate increases linearly at first, then not as fast, and eventually saturates. The etching of silicon and silicon dioxide is often done with a high chemical flux, operating in or near the ion-limited, chemical species saturated regime. However at the bottom of high aspect ratio features, chemical-limited etching may occur due to inadequate transport of the neutrals in some cases [10.25].

10.5.4 Etching Models — More Advanced Models

There are other models used in topography simulators—some of them variations of the saturation/adsorption model and some of them quite complex—which attempt to

Micron Ex. 1022, p. 75
Micron v. YMTC
IPR2025-00294

capture details of specific etch processes. Some of these more advanced models also try to directly address issues such as the sidewall inhibitor mechanism in ion-enhanced etching, and physical sputtering in sputter etch systems. We will not discuss these in detail but will briefly describe a few of them.

One such model in SPEEDIE attempts to separate the sidewall inhibitor effect from other ion-enhanced etch mechanisms in case two different effects may be dominating in different regions. For instance, there may be an ion-enhanced chemical reaction occurring at the bottom of the structure being etched where there is little inhibitor remaining, while the sidewall inhibitor may be affecting things on or near the sidewalls. This is implemented in the Sidewallpass model in SPEEDIE [10.17, 10.34] by modifying the saturation/adsorption model. The result is that the etch rate versus ion flux curve in Figure 10–30 is changed so that the left-hand portion, below some threshold level, drops faster than normal. The idea is that on or near the sidewalls, where the ion flux is low to begin with, it may be even lower due to the ions being consumed by the sputtering of a thin sidewall inhibitor layer. Zheng and McVittie [10.34] showed that in the case of etching polysilicon with a SF_6/Cl_2ClF_5 chemistry this model better matches the actual etch profile, with even less etching and bowing on the sidewalls where the ion flux is low. (However, this model does not explicitly account for thick or excess inhibitor formation, as we shall discuss below.) Other models have been developed which similarly consider multiple ion-enhancement mechanisms.

In other more advanced models, the formation and sputtering of a thick sidewall inhibitor layer are explicitly included. In these the sloped etch profiles due to excess inhibitor formation (as illustrated in Figure 10–14) are modeled, something that the simpler saturation models do not do. Examples are SPEEDIE's "Simuletchdepo Thick Sidewall Etch" model [10.17, 10.35] and Avant!'s TAURUS-TOPOGRAPHY's dry etch model [10.18], which include simultaneous deposition and etching of a polymer inhibitor layer. In SPEEDIE's model the polymer deposition is controlled by a CVD-like process with the inhibitor flux (the "deposited flux" in Figure 10–26) coming from the gas phase above the wafer, separate from the flux of reactive neutral etching species. Ion sputtering of the inhibitor layer then allows for etching of the substrate or film in the vertical direction. Such models can include ion-enhanced deposition and sputtering of the deposited material [like Eq. (9.58) in Chapter 9 for high-density plasma CVD deposition], as well as purely chemical etching of the inhibitor-free surfaces (for chlorine etching of Al, for example) or ion-enhanced chemical etching of the inhibitor-free surfaces (for etching of SiO_2 or Si, for example). Han and colleagues [10.35] have shown that this approach can model high-density plasma etching of silicon dioxide, using an ICP plasma source and C_2F_6 etchant gas. Ion-enhanced deposition and sputtering of the polymer with an ion-flux-dependent sticking coefficient, along with ion-enhanced etching of the SiO_2 (utilizing the saturation/adsorption expression), are used in this modeling.

Another advanced model similar to these was developed by Tuda and colleagues [10.36] for plasma etching of Si with Cl_2/O_2. This model includes passivation layer formation from surface oxidation and from etch byproducts arriving from the plasma as well as being directly redeposited from the bottom surface onto sidewalls. Other models include ion reflection, trenching, and localized surface charging. For HDP systems, a contribution from ionized chemical species to the chemical component of etching

Micron Ex. 1022, p. 76
Micron v. YMTC
IPR2025-00294

might also be included. All these advanced models can obviously be quite complicated, with many parameters.

Finally, advanced simulators may also include a separate model for pure physical etching, or ion sputtering, which includes redeposition of the sputtered material [10.37]. The expression used for this in SPEEDIE [10.17] is

$$\text{Etch rate} = \frac{K_{sp}Y(\theta)F_i - K_{rd}S_{rd}F_{rd} - S_{cd}F_d}{N} \tag{10.21}$$

The first term is due to the sputtering, and the sputtering yield can be angle dependent. The second and third terms are due to redeposition of sputtered material. In particular the second term is due to the direct redeposition from every other point on the structure where sputtering occurs. The third term is from material that is sputtered off the surface but goes into the plasma and then drops back down to the wafer surface. The third term can be very difficult to calibrate. N is the density of the film being etched.

10.5.5 Other Etching Simulations

As we mentioned in Chapter 9, commercial suppliers of integrated circuit simulation tools offer both empirical and more physically based models. Here we present examples of both types. The first is from Avant!'s TAURUS-TOPOGRAPHY simulator [10.18], utilizing the dry etch model with polymer deposition. This model is similar to SPEEDIE's physically based Simuletchdepo model described above. Using direct and indirect flux calculations similar to those in SPEEDIE, TAURUS-TOPOGRAPHY simulates the deposition, reemission, and sputtering of polymer material that occurs in the formation of a sidewall inhibitor layer. In the example described here, SiO_2 is plasma etched over Si using a photoresist mask.

Figure 10–33 shows the simulated results of the sidewall polymer etch model. Figure 10–33(a) shows the simulated results after 0.9 minutes of etching. One can see the sidewall polymer that has formed. This layer inhibits lateral etching of the oxide. No polymer layer is present on the trench bottom because of strong ion bombardment and sputtering there, and also because of less polymer deposition due to shadowing. Figure 10–33(b) shows the simulation after 1.8 minutes of etching. The sidewall layer is now thicker, affecting the etch profile as described earlier and illustrated in Figure 10–14. A sloped etch profile, with no etch bias, results due to the high-polymer deposition-to-etch ratio.

Finally, some commercially available simulation tools provide simpler, more empirical models. Silvaco's ATHENA simulator (using the ELITE topography tool) [10.19] is an example and we will use it here to simulate etching of silicon through a photoresist mask. In these simpler models, the user specifies the etch rates of the different components and various parameters to obtain the shape of the etch profile, rather than specifying fluxes. There is both a "wet etch model" and a "RIE model" in ATHENA. The wet etch model is completely isotropic, while the RIE model contains elements of both the linear etch and saturation/adsorption models. We will briefly describe the RIE model here and provide some examples.

In the RIE model in ATHENA, the etching process is separated into three adjustable etch rate components: the isotropic, the directional, and the chemical. Using the

Micron Ex. 1022, p. 77
Micron v. YMTC
IPR2025-00294

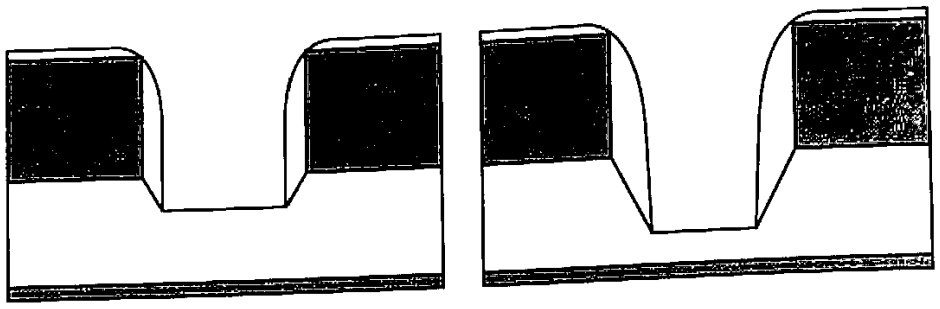


Figure 10–33 Avant!'s TAURUS-TOPOGRAPHY [10.18] simulation using their dry etch model with simultaneous polymer deposition. (a) shows the result of etching silicon dioxide over silicon with a photoresist mask after 0.9 minutes. Notice the sidewall polymer layer that has formed, inhibiting lateral etching. (b) shows the etch profile after 1.8 minutes. The sidewall layer is thicker and the etch profile in the oxide is sloped due to the high deposition-to-etch ratio.

first two is similar to using the linear etch model. The isotropic component, designated by r_{iso}, etches equally in all directions. The directional component, designated by r_{dir}, etches only in the vertical direction. For a sloped surface, where the etch rate normal to the surface is important, the etching due to r_{dir} is $r_{dir} * \cos\alpha$. Here α is the angle between the surface normal and the vertical direction. By using one or both of these two components, one can simulate purely chemical/isotropic etching, purely physical/directional etching, or a linear combination of the two. (As with the linear etch model, the physical component here may indeed be due to an ion-enhanced etching mechanism, but for which the chemical component is not limiting the process.) One can control the degree of etch anisotropy by changing the relative values of these two parameters, such that the degree of anisotropy is

$$A_f = \frac{r_{dir}}{r_{iso} + r_{dir}} \tag{10.22}$$

[One can show that this is equivalent to our definition of anisotropy in Eq. (10.5) if one observes that $r_{lat} = r_{iso}$ and $r_{vert} = r_{iso} + r_{dir}$).] No sticking coefficient is used, nor are arrival angle distributions. For these components, it is assumed that the etching is purely isotropic for the one component, and purely vertical for the other. One just specifies the etch rates for each component. The Taurus topography simulator from Avant! has a similar etch model in which one simply specifies the degree of anisotropy desired.

The third component of the ATHENA RIE model is called the chemical component. This implicitly assumes an ion-enhanced etch mechanism. When one specifies the chemical component etch rate in the RIE model, one must also specify the "divergence" parameter. The divergence parameter determines the standard deviation of the ion's Gaussian angular distribution function. It is assumed that this chemical etching only occurs where an ion strikes. In this simple way both the chemical and ionic components of the ion-enhanced mechanism are taken into account in this model; however saturation

Micron Ex. 1022, p. 78
Micron v. YMTC
IPR2025-00294

effects are not accounted for. By varying the divergence, different shaped sidewalls are obtained, very similar to changing the n factor in the $\cos^n\theta$ ion arrival angle distribution used earlier. In ATHENA, all three components—the isotropic, the directional, and the chemical—can be specified, resulting in almost any shaped profile imaginable.

In the first series of ATHENA etch examples, silicon is etched through a photoresist mask using each of the three RIE model components. Figure 10–34(a) shows the initial structure. For the first example the silicon is etched with a purely isotropic component. An isotropic etch rate, r_{iso}, of 5 nm per second is specified. The time of the etch is set at 2 minutes, which should etch the silicon 600 nm deep. The resulting profile is shown in Figure 10–34(b). In the next simulation, pure physical or directed etching is done. This is done by specifying r_{dir} to be 5 nm per second and r_{iso} to be zero. The simulated profile is shown in Figure 10–34(c). In the final simulation, the ion-enhanced chemical etching component is used. This is done by designating the chemical component to be 50 and the divergence to be 5. The resulting profile is in Figure 10–34(d). Changing the divergence parameter is similar to changing the arrival angle distribution (the n value) of ions in the earlier models, due to changes in gas pressure, for example.

The final series of ATHENA simulations are shown in Figure 10–35. Here different combinations of isotropic, directional, and chemical (ion-enhanced) components are

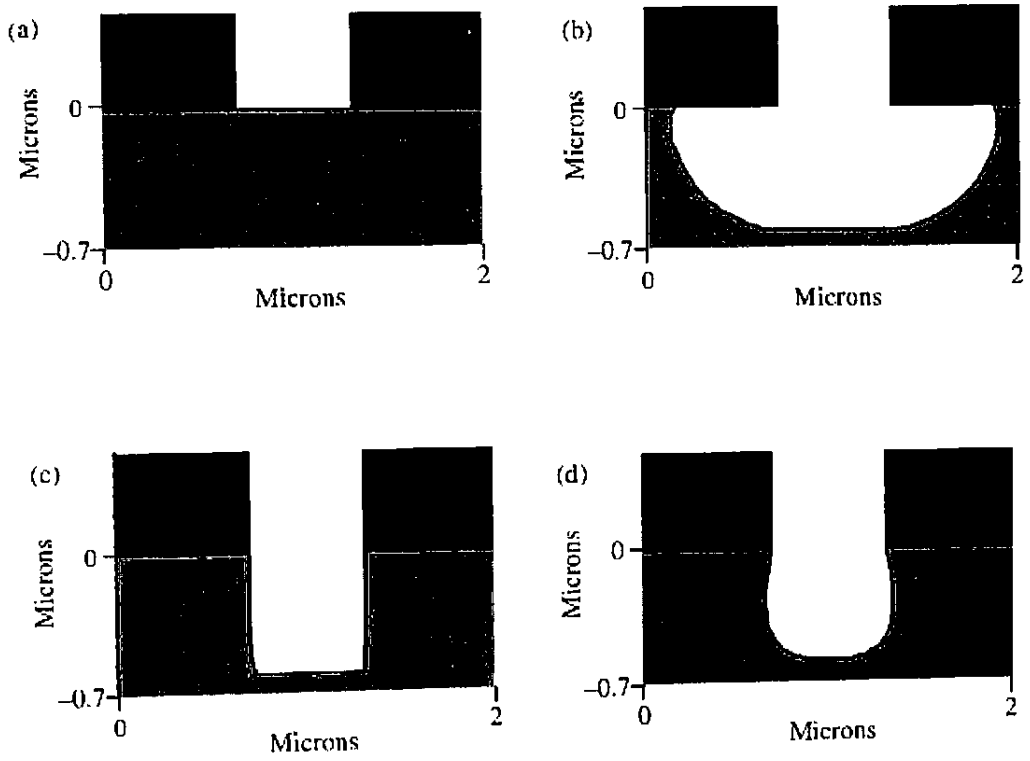


Figure 10–34 Silvaco's ATHENA [10.19] topography simulation of silicon etching using different etching components in the RIE model: (a) initial structure with photoresist mask over Si substrate; (b) purely isotropic etching; (c) purely directional; (d) ion-enhanced etching.

Micron Ex. 1022, p. 79
Micron v. YMTC
IPR2025-00294

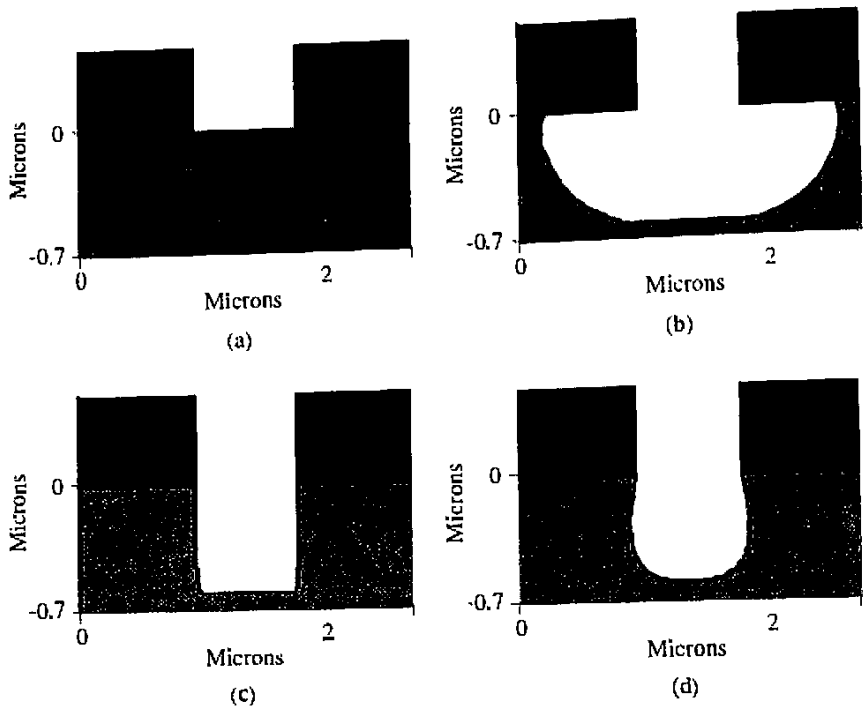


Figure 10–35 Silvaco's ATHENA [10.19] etch simulation using different etching component combinations in the RIE model: (a) chem = 50, div = 10, iso = 0, dir = 0; (b) chem = 30, div = 10, iso = 0, dir = 20; (c) chem = 30, div = 10, iso = 20, dir = 0; (d) chem = 30, div = 10, iso = 10, dir = 10. These illustrate the variety of etch profiles that are obtainable with this easy-to-use tool.

used to obtain a wide variety of etch profiles. These simulations demonstrate the usefulness of such simulation models. It is relatively simple to use them and calibrate them against actual etch profiles. These types of models are often used to characterize a particular etch system and etch chemistry used to plasma etch a particular film. One can build up a library of etch equipment, materials, etch chemistry, and plasma conditions to use in future simulations. This is sometimes done by commercial suppliers of these simulation tools and a model parameter library for various commonly used pieces of deposition and etch equipment with model parameters for various films and normal operating conditions is included with the simulator. One can then use these models and parameters to optimize an etch or deposition process without being involved with all the details. These types of simulations also run very quickly.

Of course the main advantage of the more physically based models is that they try to be more closely linked to actual physical processes. This is especially true for the models currently being developed which actually model the etch-enhancement mechanism, such as inhibitor layer formation and removal. As a result, these types of models are more apt to be valid for conditions outside those for which they are calibrated and tested, but both types of models are useful for different applications.

Micron Ex. 1022, p. 80
Micron v. YMTC
IPR2025-00294

10.6 Limits and Future Trends in Technologies and Models

With the ever-decreasing feature sizes in future generations of integrated circuit technology, the challenges in etching will certainly continue. Etching features with smaller and smaller dimensions will obviously pose problems. Damage to the underlying films and active regions will also be issues as the dimensions decrease and plasma processing is used. High-density plasma etch systems will surely help in these regards. A high-density plasma at low gas pressures and the decoupling of the plasma density and ion energy mean that fast, anisotropic etching can be achieved while minimizing the ion-induced damage. Development of this type of etch technology will surely continue.

With ever-increasing wafer sizes in the future, uniformity and loading problems will be harder to control. Improvements in equipment design will have to continue to overcome these issues. More *in situ* control will be required. In addition to endpoint detection, automatic feedback will be needed to control equipment and process parameters such as gas flow, pressure, and power to the plasma sources.

As with deposition equipment, a trend in etch equipment will be the use of cluster tools. By connecting to multiple etch (and deposition) chambers and passing the wafers from one chamber to another, one can perform several processing steps sequentially without breaking vacuum. This minimizes exposure of the wafers to atmosphere, reducing particulate contamination and surface oxidation between steps. For example, one can have chambers to etch TiN and Al, do a fluorine passivation, and strip the photoresist. This becomes more important as the trend continues toward multilevel stack structures. One can also combine deposition and etch chambers in such a tool. Most of these tools are single wafer, as opposed to batch systems. More control over each wafer is possible, but the etch rates must be high since each wafer must be processed individually.

There will be more challenges in etching specific films as the dimensions decrease and aspect ratios increase. For example, in Al metal etching the issues of corrosion, resist and residue removal, Cu byproduct removal, loading effects (both macro and micro), and of course profile control and selectivity will have to be addressed each time the structure dimensions are decreased. As we have seen, there are many issues and considerations involved in developing an etch process for each film, and it will be harder and harder to satisfy all the requirements.

New plasma etching techniques may be used to meet the increasing demands as the technology progresses. Recently a new plasma etch process, called the Bosch process, has been developed in the MEMS (Micro-Electro-Mechanical Systems) industry for etching very deep Si trenches. This uses fluorine chemistry in a high-density plasma, and both excellent anisotropy and selectivity with respect to SiO_2 masks are reported [10.38]. In this process, polymer deposition and etching steps are sequentially alternated in an HDP etch system. Whether this can be adapted in the future for etching isolation structures or polysilicon gates in VLSI structures is unclear, but new plasma etching methods along these lines may be developed and used.

Etching and patterning processes other than plasma etching may be used more in the future. Chemical-Mechanical Polishing (CMP) has found widespread use in the past few years and is now a mainstream process. As described in the next chapter, this uses a combination of wet chemicals and mechanical grinding to polish or etch the top surface

Micron Ex. 1022, p. 81
Micron v. YMTC
IPR2025-00294

of a film, leaving a very planar surface. Dielectric films and W plugs are now often planarized by this technique. When CMP is combined with the "damascene" fill and etchback process, also described in the next chapter, materials such as copper that are difficult to plasma etch can be patterned to integrated circuit specifications.

New materials will be added in the future. As we discuss in the next chapter, new metal interconnect materials such as copper and new dielectrics such as low-k dielectrics will soon be required. There has already been extensive development on integrating these types of materials into the fabrication process, including the patterning of these films. Etching some of these films, especially Cu, has been found to be very difficult, so much so that other methods for patterning these films such as CMP are more attractive.

The models and simulation tools for etching processes will also undergo changes and improvements. As we mentioned earlier in the chapter, we need to model the actual processes more deeply, such as explicitly modeling the sidewall inhibitor formation and removal and phenomena such as ion reflection and charging. Work in these directions has begun. And as with the deposition models, physically based models and simulation tools need to be combined with user-friendly and efficient software tools.

10.7 Summary of Key Ideas

We have seen in this chapter how etching is used to pattern films by selectively removing material with the use of mask layers, usually photoresist but sometimes other thin films. Etching can be either wet or dry, the former using liquid chemical etchants and the latter using gas-phase, plasma-produced etch species. Some of the issues that are important in etching are selectivity with respect to masks and underlying films, directionality (anisotropic versus isotropic etching) for profile control, mask erosion, etch bias or undercutting, etch uniformity, residue removal, and damage in the underlying layers caused by etching.

In wet etching, chemical reactions dominate the etch process. This leads to very selective but isotropic etching. In dry or plasma etching, two types of species are present that are important in the etch process: reactive neutral chemical species (such as free radicals) and ionic species. The first etches by chemical processes and is isotropic or nearly isotropic and can be very selective, while the second etches by more physical processes and is very directional, or very anisotropic, but not very selective. The three main types of etch mechanisms that occur in plasma etching are chemical etching (involving the neutral chemical species), physical etching or sputtering (involving the ion species), and ion-enhanced etching (involving both in a synergistic way). Ion-enhanced etching can occur by the ions enhancing the chemical etch process or by removing inhibitor layers. Directional etching can be achieved in this manner, as well as selectivity, a combination usually desired in an etch process. Many types of plasma etching equipment have been developed that utilize the different etching mechanisms, including barrel etchers, plasma mode etchers, Reactive Ion Etching (RIE) systems, High-Density Plasma (HDP) systems, and sputter etching equipment. These systems range from purely chemical to purely physical etching, with many systems operating in between these two. Where both chemical and physical components are present, as in RIE and HDP systems, plasma conditions and etch chemistries are usually selected so that the

Micron Ex. 1022, p. 82
Micron v. YMTC
IPR2025-00294

two etch components act synergistcally, and ion-enhanced etching occurs giving directional etching and good selectivity.

Most simulation models focus on the two components of etching, the chemical and physical. Advanced simulators model the etch process based on the fluxes and surface processes of the chemical and ion species. As in deposition modeling, the ion species have a narrow arrival angle distribution (being very vertical to the wafer) and a high sticking coefficient. The chemical species have a wide arrival angle distribution and low sticking coefficient. The two components can act independently or synergistically. In the linear etch model, the chemical and physical components of etching are combined in an independent linear fashion, and a wide range of etch profiles can be produced for different plasma etch systems and for certain conditions. In the saturation/adsorption model for ion-enhanced etching, the two species act synergistically, as described by the expression for two processes acting in series. Very directional anisotropic etching results, along with saturation effects. Variations can occur, such as when some spontaneous, non-ion-assisted chemical etching occurs in parallel, multiple ion-enhanced mechanisms are present, or when excess inhibitor material forms, and modifications or additional models can be utilized to capture these features.

In the future, structures will get even smaller and new materials will be used. New etching tools and processes will also evolve. The models and simulation tools will evolve as well. As with deposition models, they will become based even more on the actual physical processes.

10.8 References

[10.1]. C. J. Mogab, "Dry Etching," in *VLSI Technology*, ed. by S.M. Sze, McGraw-Hill, 1983, p.307.

[10.2]. W. S. Ruska, *Microelectronic Processing*, McGraw-Hill, 1987, p. 206.

[10.3]. C. Chang, "Experiments and Simulation of Plasma Deposition and Sputter Etching Processes," Ph.D. thesis, Stanford University, 1996, p. 93.

[10.4]. J. P. McVittie, private communication.

[10.5]. J. W. Coburn and H.F. Winters, "Ion and Electron Assisted Gas-Surface Chemistry—An Important Effect in Plasma Etching," *J. App. Phys.*, vol. 50, p. 3189, 1979.

[10.6]. J. W. Coburn, "Surface-science Aspects of Plasma-assisted Etching," *Appl. Phys. A*, vol. A59, p. 451, 1994.

[10.7]. R. A. Morgan, *Plasma Etching in Semiconductor Fabrication*, Elsevier Science, 1985.

[10.8]. M. Kimizuka, Y. Watanbe, and Y. Ozaki, "Pattern Profile Control in Magnetron Reactive Ion Etching of Poly-Si," *J. Vac. Sci. Tech. B.*, vol. 10, p. 2192, 1992.

[10.9]. H. C. Jones, R. Bennett, and J.Singh, "Size Dependent Etching of Small Shapes" in *Proc. of the Eighth Symp. on Plasma Prcoessing*, G. S. Mathad and D.W. Hess, eds. the Electrochem. Soc., 1990, p. 45.

[10.10]. J. P. McVittie, unpublished data.

[10.11]. M. A. Leiberman and A.J. Lichtenberg, *Principles of Plasma Discharges and Materials Processing*, J. Wiley & Sons, 1994.

[10.12]. B. Gorowitz and R. J. Saia, "Reactive Ion Etching," in *Plasma Processing for VLSI*, N. G. Einspruch and D. M. Brown, eds., Academic Press, 1984, p. 307.

[10.13]. W. R. Runyan and K. E. Bean, *Semiconductor Integrated Circuit Processing Technology*, Addison-Wesley, 1990, p. 276.

Micron Ex. 1022, p. 83
Micron v. YMTC
IPR2025-00294

[10.14]. D.L. Flamm, in *Plasma Etching, an Introduction*, D.M. Manos and D. L. Flamm, eds., Academic Press, 1989.

[10.15]. L. M Ephrath and E.J. Petrillo, "Parameter and Reactor Dependence of Selective Oxide RIE in CF_4 + H_2," *J. Electrochem. Soc.*, vol. 129, p. 2282, 1982.

[10.16]. P. Singer, "Plasma Etch: a Matter of Fine Tuning," *Semiconductor International*, December 1995, p. 65.

[10.17]. SPEEDIE is a 2D etch and deposition simulator developed at Stanford University.

[10.18]. TAURUS-TOPOGRAPHY is a commercially available topography simulator developed by Avant! Inc.

[10.19]. ATHENA and its ELITE topography simulator are commercially available from Silvaco Inc.

[10.20]. V. I. Singh, E. S. G. Shaqfeh, and J. McVittie, "Study of Si Etching in CF_4/O_2 Plasmas to Establish Surface Re-Emission as the Dominant Transport Mechanism," *J. Vac. Sci. Tech. B*, vol. B12, p. 2952, 1994.

[10.21]. V. I. Singh. E. S. G. Shaqfeh, and J. McVittie, "Simulation of Profile Evolution in Si Reactive Ion Etching with Re-Emission and Surface Diffusion," *J. Vac. Sci. Tech. B*, vol. B10, p. 1091, 1992.

[10.22]. D. L. Flamm, D. M. Donnelly and J. A. Mucha, "The Reaction of Flourine Atoms with Silicon," *J. Appl. Phys.*, vol. 52, p. 3633, 1981.

[10.23]. B. A. Heath, "Selective Reactive Ion Beam Etching of SiO_2 over Polycrystalline Si," *J. Electrochem. Soc.*, vol. 129, p. 396, 1982.

[10.24]. J. I. Ulacia and J. P. McVittie, "A Two-Dimensional Computer Simulator for Dry Etching Using Monte-Carlo," *J. Appl. Phys.*, vol. 65, p. 1484, 1989.

[10.25]. J. S. Han and J. P. McVittie, "Modeling of Aspect Ratio Dependent Etching in an Inductively Coupled Plasma," *Mat. Res. Soc. Symp. Proc.*, vol. 389, p. 197, 1995.

[10.26]. V. M. Donnelly, D. L. Flamm, W. C. Dautremont-Smith, and D. J. Weber, "Anisotropic Etching of SiO_2 in Low-frequency CF_4/O_2 and NF_3/Ar Plasmas," *J. Appl. Phys.*, vol. 55, p. 242, 1984.

[10.27]. R. Petri and D. Henry, "Tungsten Etching Mechanisms in Low-Pressure SF_6 Plasma," *J. Appl. Phys.*, vol. 72, p. 2644, 1992.

[10.28]. T. M. Mayer and R. A. Barker, "Simulation of Plasma-Assisted Etching Processes by Ion-Beam Techniques." *J. Vac. Sci. Tech.*, vol. 21, p. 757, 1982.

[10.29]. J. Pelletier and M. J. Cooke, "Microwave Plasma Etching of Si and SiO_2 in Halogen Mixtures: Interpretation of Modeling Mechanisms," *J. Vac. Sci. Tech.*, vol. B7, p. 59, 1989.

[10.30]. E. Zawaideh and N. S. Kim, "Plasma Etching Model Based on a Generalized Transport Approach," *J. Appl. Phys.*, vol. 62, p. 2498, 1987.

[10.31]. M. A. Lieberman and A. J. Lichtenberg, *Principles of Plasma Discharges and Materials Processing*, John Wiley & Sons, 1994.

[10.32]. D. C. Gray, I. Tepermeister, and H. H. Sawin, "Phenomenological Modeling of Ion-Enhanced Kinetics in Flourine-Based Plasma Etching," *J. Vac. Sci. Tech. B*, vol. 11, p. 1243, 1993.

[10.33]. J. P. Chang, A. P. Mahorowala, and H. H. Sawin, "Plasma-Surface Kinetics and Feature Profile Evolution in Chlorine Etching of Polysilicon," *J. Vac. Sci. Tech. A*, vol. 16, p. 217, 1998.

[10.34]. J. Zheng and J. P. McVittie. "Modeling of Side Wall Passivation and Ion Saturation Effects on Etching Profiles," *Proc. of IEEE Int'l. Mtg. Numerical Modeling of Process and Device for I.C.: NUPAD-V*, p. 37, 1994.

Micron Ex. 1022, p. 84
Micron v. YMTC
IPR2025-00294

[10.35]. J. S. Han, J. P. McVittie, and J. Zheng, "Profile Modeling in High Density Plasma Oxide Etching," *J. Vac. Sci. Tech.* vol. 13, p. 1893, 1995.

[10.36] M. Tuda, K. Ono, and K. Nishikawa, "Effects of Etch Products and Surface Oxidation on Profile Evolution During Electron Cyclotron Resonance Plasma Etching of Poly-Si," *J. Vac. Sci. Technol. B*, vol. 14, p. 3291, 1996.

[10.37]. C. Y. Chang, J. P. McVittie, and K. C. Saraswat, "Backscattering in Ar Sputtering of Oxide," *Appl. Phys. Lett.*, vol. 63, p. 2294, 1994.

[10.38]. J. Bhardwaj, H. Ashara, and A. McQuarrie, "Dry Silicon Etching for MEMS," *Proc. of Symp. on Microstructures and Microfab. Sys.*, Electrochem. Soc., 1997.

10.9 Problems

10.1. Why might pure chemical etching, such as in wet etching, be adequate for patterning the silicon nitride layer used to define the field oxidation area in the CMOS process flow given in Chapter 2?

10.2. If the etch anisotropy is 0, what is the undercut or etch bias when etching a 0.5-μm thick film? What is the undercut when the anisotropy is 0.75? Assume no overetch in each case.

10.3. In a certain process, it is desired that the pitch of metal lines be equal to or less than 1.0 μm (the pitch equals one metal linewidth plus one spacing between metal lines, measured at top of features). Assume that the metal linewidth and spacing are equal (that is, 0.5 μm each). The height of such structures is also 0.5 μm, and the minimum lithographic dimension is 0.25 μm.

a. What minimum degree of anisotropy is needed in an etch process in order to produce such a structure?

b. What minimum pitch could be obtained for such a structure with *wet* etching? (Again with minimum lithograph dimension of 0.25 μm, thickness of 0.5 μm, and equal metal width and spacing.)

10.4. What are the advantages and disadvantages of reactive ion etching versus sputter etching? Cite a hypothetical example of when you might want to use sputter etching rather than RIE.

10.5. Explain how loading effects can affect endpoint detection.

10.6. It is found that a certain plasma etch chemistry in a certain RIE etch system produces vertical sidewalls with zero etch bias when etching a particular film. Adding chemical A to the etch chemistry results in nonvertical sidewalls, and an etch bias. Adding chemical B to the original etch chemistry results in nonvertical sidewalls, but with zero etch bias. Explain what may be going on.

10.7. a. In a particular etch process, if selectivity is the biggest concern, which type(s) of etch equipment should be used?

Micron Ex. 1022, p. 85
Micron v. YMTC
IPR2025-00294

b. If the biggest concern is ion bombardment damage, which type(s) of etch equipment should be used?

c. If the biggest concern is obtaining vertical sidewalls, which type(s) of etch equipment should be used?

d. If the biggest concerns are selectivity *and* vertical sidewalls, which type(s) of etch equipment should be used?

e. What about selectivity *and* vertical sidewalls *and* damage, while maintaining reasonable etch rate?

10.8. It is observed that the sidewall slope in an etch process becomes more sloped as the temperature is reduced. Why?

10.9. If the anisotropy of an etch process is 0.45, sketch the etch profile. What percentage of the etch rate in the vertical direction is due to the spontaneous chemical etching and what percentage is ionic/physical, assuming a linear etch mechanism? State all assumptions.

10.10. For a particular plasma etch process in which the linear etch model is applicable, a degree of anisotropy of 0.8 or better is desired. If the unobstructed ionic flux on a flat surface is 1×10^{16} atoms $cm^{-2}\,sec^{-1}$ (with K_i equal to 1), what unobstructed chemical flux would result in an anisotropy of 0.8? For this process S_c is 0.01 and K_f is 0.1.

10.11. We want to see how the etch rate in the vertical direction might depend on pressure assuming that the etch follows the saturation/adsorption model. Assume that for a particular etch system that the chemical flux is directly proportional to the pressure, while the ion flux is inversely proportional to the pressure. That is $F_c = F_c'{*}P$ and $F_i = F_i'/P$. (P is normalized to 1 atm and unitless.) Also assume that density = 1 atom nm^{-3}, and that $K_iF_i' = S_cF_c' = 1$ atom $nm^{-2}\,sec^{-1}$.

a. Plot the vertical etch rate versus pressure, P, from $P = 0$ to 10.

b. Repeat with $K_iF_i' = 40$ atoms $nm^{-2}\,sec^{-1}$ and $S_cF_c' = 1$ atom $nm^{-2}\,sec^{-1}$.

10.12. In an etch process, there is a finite amount of purely chemical etching without any ion bombardment (i.e., spontaneous chemical etching). In addition, ion bombardment greatly increases the etch rate by facilitating the breaking up of the etch precursor. At high ion flux the etch rate saturates. No etching occurs when there is only ion bombardment with no chemical component.

a. Write a generalized etch rate equation that can describe this behavior.

b. Sketch an etch rate versus ion flux curve for this process for some nonzero chemical flux.

c. Sketch what the etch profile might look like for this process (i.e., etching through a window in a mask as in Figure 10–3).

Micron Ex. 1022, p. 86
Micron v. YMTC
IPR2025-00294